Department of Molecular and Cell Biology
Faculty of Science
University of Cape Town

RESEARCH REPORT

Prion-like properties of the N-terminal domains of the rat and human FoxG1 transcription factors.

Jessica Learmont
LRMJES001

Submitted in fulfillment for the degree of Master of Science
(Molecular and Cell Biology)
December 2006

Table of contents

Abstract

Prion proteins are proteins capable of infectious amyloid formation. The conformational switch from the soluble form of the protein to the amyloid form is self-perpetuating. The N-terminal domains of these proteins are often low complexity regions, rich in glutamine amino acid residues and amino acid repeat sequences. Forkhead box G1 (FoxG1) belongs to the family of HNF-3/ fork head genes, encoding winged-helix transcription factors. Expression is restricted to the olfactory neuroepithelium and the telencephalon of the developing forebrain, in vertebrate embryos. It has been suggested that FoxG1 regulates the proliferation of progenitor cells and prevents premature differentiation of neurons in a dosage dependent manner, leading to the expansion of the cerebral cortex. The N-terminal domains (NFoxG1 domains) of mammalian FoxG1 orthologues are low complexity regions, rich in histidine, proline and glutamine amino acid residues. As these low complexity domains are typical of the N-terminal domains of prion proteins, I have tested the hypothesis that the NFoxG1 domains act as a prion-like switch.

The N-terminal domains of the human and rat orthologues were fused to a constitutively active rat glucocorticoid receptor (GR^{526}). When present in the active conformation, the NFoxG1:GR^{526} protein was able to regulate a β-galactosidase reporter plasmid, resulting in a characteristic blue colour accumulating in the colonies when cultured on X-gal media. When NFoxG1:GR^{526} was inactive, it failed to activate the β-galactosidase reporter and colonies remained white. 25.29% of the human NFoxG1:GR^{526} fusion proteins switched into an inactive prion-like state, whereas 1.06% of the rat switched states, typical of other prion proteins. The inactive form of the GR protein reverted back

to the active state, although at a lower percentage than the initial conversion percentage. In an alternative assay, these domains were fused to green fluorescent protein (GFP) and the solubility of the protein in yeast was observed using fluorescent microscopy. The human and rat NFoxG1:GFP constructs resulted in both soluble and aggregated GFP *in vivo*.

Western blot analysis confirmed that the GR^{526} protein was expressed at similar levels in both blue and white colonies. The inactive state of the GR^{526} protein was found to be cured by growth on a protein denaturant, suggesting a prion-like mechanism. The NFoxG1:GR^{526} protein extracted from blue colonies was found to sediment at the same rate as a control soluble protein on a sucrose gradient, while the protein extracted from the white yeast colonies was found to sediment at a much faster rate, typical of aggregated proteins. A yeast mating experiment was used to determine whether the inactive state of the GR^{526} protein was transmissible, therefore displaying a prion-like mechanism. White and blue yeast colonies transformed with the NFoxG1:GR^{526} constructs were mated, to determine whether the inactive state of the NFoxG1:GR^{526} fusion protein was transmissible. The inactive states of the NFoxG1:GR^{526} constructs converted active NFoxG1:GR^{526} to an inactive state, demonstrating that the mechanism by which the domain forms aggregates is prion-based.

Acknowledgements

I would like to thank Assoc. Professor Nicola Illing for her supervision and guidance, and Faezah Davids for her advice and technical help. I would also like to thank Nicholas Bredenkamp, Sally Anne Walford, Inonge Mulako and Zac McDonald, as well as the rest of the laboratory, for their technical help and suggestions for troubleshooting, during my research. Special thanks to the members of my family and Marcel for their support and encouragement throughout this research project.

Abbreviations

AD	Alzheimer disease
ApCPEB	*Aplysia* cytoplasmic polyadenylation element binding protein
BF-1	Brain factor-1
BMP	Bone morphogenetic protein
Bp	Base pair
BrdU	Bromodeoxyuridine
BSA	Bovine serum albumin
BSE	Bovine spongiform encephalopathy
Cdk	Cyclin-dependent kinase
CJD	Creutzfeld-Jakob disease
CP	Cortical plate
CR	Cajal-Retzius neurons
C-terminal	Carboxy-terminal
DTT	Dithiothreitol
EDTA	Ethylenediaminetetraacetic acid
FGF-8	Fibroblast growth factor-8
Fox	Forkhead box
FSI	Fatal sporadic insomnia
G/A	Glycine and alanine amino acid residues
GAPDH	Glyceraldehyde 3 phosphate dehydrogenase
GFP	Green fluorescent protein
GR^{526}	Glucocorticoid receptor protein
Gro/TLE	Groucho/Transducin-like enhancer of split
GSS	Gerstmann-Straussler-Scheinker syndrome
GuHCl	Guanidinium hydrochloride
HDAC	Histone deacetylase
Hes	Hairy/Enhancer of Split
hFoxG1	Human FoxG1
HNF	Hepatocyte nuclear factor
H/P/Q	Histidine, proline and glutamine rich region
HRP	Horse radish peroxidase
IPTG	Isopropyl-β-D-thiogalactopyranoside
-leu/trp/ura	Leucine/tryptophan/uracil deficient media
MAP2	Microtubule-associated protein 2
NFoxG1	N-terminal domain of FoxG1
NM	Sup35 N-terminal domain (prion determinant)
PBS	Phosphate buffered saline
PCR	Polymerase chain reaction
PD	Parkinson disease
PMCA	Protein misfolding cyclic amplification
PPL	Primordial plexiform layer
Q/N	glutamine/asparagine amino acid residues
SAP	Shrimp alkaline phosphatase
SDS-PAGE	Sodium dodecyl sulfate-polyacrylamide gel electrophoresis

SP	Subplate
SVZ	Subventricular zone
TGF-β	Transforming growth factor-β
U	Enzyme unit
*X*FoxG1	*Xenopus* FoxG1
X-gal	5-bromo-4-chloro-3-indolyl-β-D-galactosidase

List of figures

List of tables

CHAPTER 1

Introduction

1. 1. FoxG1 in early neural development

Forkhead box G1 (FoxG1), previously named Brain factor 1 (BF-1) (Kaestner *et al.*, 2000), belongs to the family of HNF-3/ fork head genes, which encode winged-helix transcription factors (Lai *et al.*, 1993 and Xuan *et al.*, 1995). This family of transcription factors includes *fork head*, a Drosophila nervous system gene (Weigel *et al.*, 1989), mammalian hepatocyte nuclear factors (HNF) 3α, 3β and 3γ (Lai *et al.*, 1991), and to date at least 43 members of the human FOX gene family (Katoh and Katoh, 2004). This class of transcription factors is characterized by the DNA binding domain, containing a conserved 100-amino acid region, which folds into three α-helices and two large "wings" (Kaestner *et al.*, 2000), hence the name winged-helix. Irregular expression of these genes results in chronic disorders and disease.

1.1.1. Development of the telencephalon

FoxG1 is expressed in the olfactory neuroepithelium and the telencephalon of the developing forebrain, where it is required for normal development of these structures (Tao and Lai, 1992 and Xuan *et al.*, 1995). During the development of the central nervous system the caudal section of the neural tube gives rise to the spinal cord, while the rostral gives rise to the brain. The brain is initially subdivided into the forebrain, midbrain, and hindbrain. The telencephalon arises from the forebrain, and develops from approximately embryonic day 10.5 to 17.5 (E10.5-E17.5) in mice (Caviness *et al.*, 1995). The telencephalon develops into

the cerebral hemispheres, including the cerebral cortex, hippocampus, olfactory bulbs and the basal ganglia (Tao and Li, 1992 and Martynoga *et al.*, 2005). The cerebral neocortex is a six-layered structure unique to mammalian brains, and absent throughout other vertebrates (Clark *et al.*, 2001). The six layered structure is composed of the ventricular, subventricular, intermediate, subplate, cortical plate, and marginal zones, forming the deep to more superficial layers respectively (Rakic, 1995). There is huge variation in the surface area of the neocortex between mammals, with the human structure displaying an approximate 1000-fold increase in comparison to that of the mouse and a ten-fold increase in comparison to that of the monkey, while the relative thickness of the structures varies by a factor of two (Fig. 1.1, Rakic, 1995, Sultan, 2002).

The expansion of the surface area of the neocortex is a significant element in the evolution of mammals, with advanced cognitive functions evident in those with larger cerebral hemispheres (Hill and Walsh, 2005). Expansion of the neocortex relies on the proliferation of cortical progenitor cells. These cells undergo symmetrical cell division, thereby increasing the number of progenitor cells prior to dividing asymmetrically, giving rise to differentiated neurons (Rakic, 1995). The progenitors of cortical neurons are present in the ventricular and subventricular zones, and form a pseudostratified epithelial layer. Cajal-Retzius (CR) neurons are the earliest born neurons in the development of the cerebral cortex, and are present in the outermost layer of the structure. CR neurons originate in the subventricular zone, and form the preplate. The preplate is later divided into the marginal zone and the subplate, by the neurons forming the cortical plate (Fig. 1.1). Radial glial cells are present throughout the layers of the cortex, and it is along these cells that differentiated neurons migrate radially, reaching the cortical plate layer of the cortex. Migrating cells originating from the same area

of the subventricular zone form ontogenetic columns in the cortical plate, in which they are arranged radially, one above the other. Within the ontogenetic columns the cells are arranged according to their arrival date, older cells are present closer to the ventricular zone, and the newly arrived cells are present closer to the surface of the structure. The thickness and the surface area of the neocortex rely on the length of the columns, and the number of columns respectively, both of which are affected by the number of cortical progenitor cells (Molnar *et al.*, 2006, Rakic, 1995).

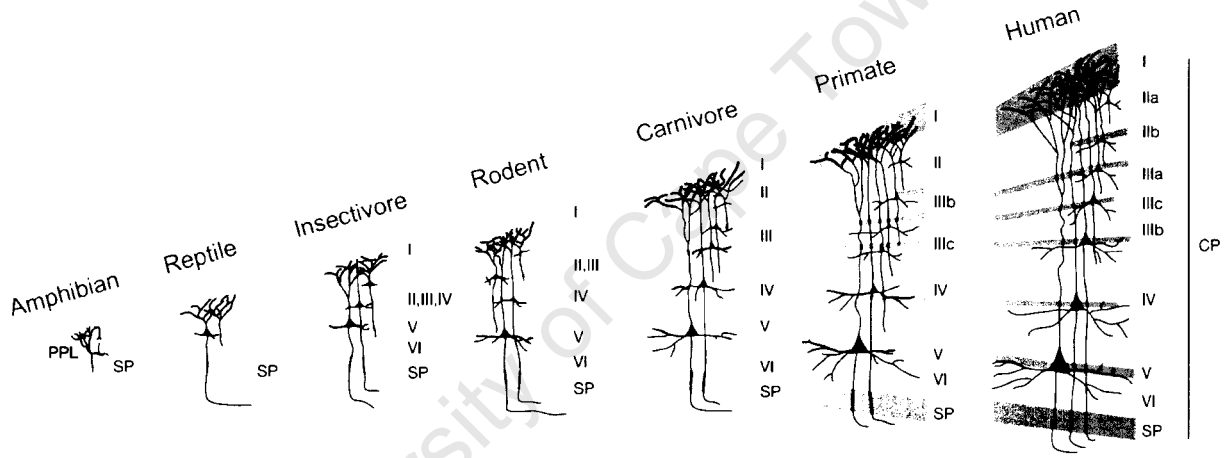

Figure 1.1. Differences in the cerebral cortex size are associated with differences in cortex circuitry. The cerebral cortex is derived from two developmental cell populations, namely the primordial plexiform layer (PPL) or preplate, and those of the cortical plate (CP). The preplate is homologous to the simple cortical structures seen in amphibians and reptiles, and develops first in mammalian brain development. As the cortical plate develops, the preplate layer is split into layer I (marginal zone) and the subplate (SP). Cortical plate layers develop from the deeper layers first, to the superficial last. In mammalian brains, the cortical plate layers are elaborated in those with increased cognitive function, the human cortical plate layers II and III are subdivided into IIa, IIb, and IIIa-IIIc respectively, while in rodents the layers II and III make up a single layer. Taken from Hill and Walsh, 2005.

1.1.2. Characterization of FoxG1

FoxG1 was originally identified in the screening of a rat adult brain cDNA library with a HNF-3α probe (Tao and Lai, 1992). FoxG1 was shown to be expressed in both the adult and

fetal rat brain, with a four fold increase in E17 in comparison to the adult tissue. *In situ* hybridization studies revealed the transcription factor was expressed in the ventricular zone of the cortex, hippocampus and olfactory bulb, as well as the olfactory epithelium. FoxG1 was later shown to be expressed in the optic chiasm (Pratt *et al.*, 2004). The human and mouse homologues was consequently cloned using a rat derived probe in the same manner (Li *et al.*, 1996, Murphy *et al.*, 1994). FoxG1 orthologues were subsequently identified in zebrafish and the chordate, amphioxus. FoxG1 was expressed in the anterior neural tube of these organisms, a similar pattern seen in other vertebrates (Toresson *et al.*, 1998).

In order to investigate the role of FoxG1 in brain development, transgenic mice were produced in which the FoxG1 gene was deleted through a null mutation (Xuan *et al.*, 1995). At E9.5, when compared to wildtype embryos, homozygous null mutants displayed minimal differences in the size of the telencephalon. However, by E10.5 and E12.5 a vast reduction in the size of the telencephalon was apparent, and at birth the cerebral hemispheres of the mutants were reduced by 95% in mass. Bromodeoxyuridine (BrdU), used to label proliferating cells, revealed that the reduction in size of the telencephalon was a result of the early depletion of the progenitor cell population. Premature onset of neuronal differentiation, assayed by the expression of microtubule-associated protein 2 (MAP2) in postmitotic neurons, was also apparent. In wildtype embryos (E12.5) MAP2 positive cells were restricted to a thin layer of cells on the outer layer of the ventricular zone, made up of the earliest born neurons. Mutant embryos however displayed a thickening of this layer as a consequence of an increase in the number of neural progenitor cells exiting the cell cycle and differentiating into MAP2 positive neurons. These results suggest that FoxG1 plays a role in regulating the

proliferation of progenitor cells in the telencephalon, and preventing their premature differentiation into neurons.

Hanashima *et al.* (2004) confirmed these results by examining the effect of FoxG1 on Cajal-Retzius neurons in mice. In the E18.5 cortex of FoxG1 mutants CR neurons were found to be in excess when compared to wildtype embryos. The cells were visualized with the use of *reelin*, a CR marker. These results suggest that FoxG1 functions to suppress the excess production of CR neurons after their normal birthdate, and thus plays an important role in the regulation of differentiation, and the development of the six-layered cerebral cortex.

1.1.2.1. The function of FoxG1 differs in the dorsal and ventral telencephalon

Xuan *et al.* (1995) showed that in FoxG1 mutant embryos the dorsal telencephalon was not affected as severely as the ventral region at E12.5. The dorsal telencephalon gives rise to the cerebral cortex, while the ventral develops into the ganglionic eminences, the primordia of the basal ganglia. The ganglionic eminences, present in wildtype embryos at E12.5, were absent in the mutants at the same embryonic stage, and the ventral region did not display any markers typical of the region. At E12.5 the dorsal telencephalon was present more ventrally in the mutant embryos, and was reduced in size. They suggested that the absence of the ventral structures was a result of the lack of proliferating precursor cells in the region after E9.5, and that role of FoxG1 in proliferation was uniform across the telencephalon. The authors did not however reject the possibility that the role of the transcription factor in the ventral region of the telencephalon differed to that in the dorsal region.

Martynoga *et al.* (2005) established that the role of FoxG1 differs in the ventral telencephalon, by studying cell cycle kinetics in the telencephalon of mutant embryos. At E10.5 there is a more severe slowing of the proliferation rate of progenitor cells in the dorsal region of the mutant embryos in comparison to the wildtype, in agreement with Xuan *et al.* (1995). The cells in the ventral region, however, were seen to proliferate at the same rate as those cells in the wildtype embryos. The authors were also unable to visualize any gene markers characteristic of the ventral region, confirming results originally described in Xuan *et al.* (1995). Martynoga *et al.* (2005) concluded that FoxG1 is required for specification of the ventral telencephalon, as in the absence of the transcription factor it fails to develop. These results suggest that while FoxG1 controls proliferation and differentiation in the dorsal telencephalon, it is required for correct patterning of the ventral telencephalon.

The hypothesis that FoxG1 temporally regulates differentiation and proliferation in the dorsal region of the telencephalon has been criticized by other researchers. Muzio and Mallamaci (2005) have argued that FoxG1 regulates patterning in the dorsal telencephalon, as well as the ventral. The authors interpret the excess number of CR neurons in FoxG1 mutant mouse embryos (Hanashima *et al.* 2004) as a repatterning of the region, opposed to a lack of repression of differentiation by FoxG1. It is suggested that the neocortical plate in FoxG1 mutants is absent, and is replaced by the more caudal hippocampal plate. The authors believe that FoxG1 is required for the repression of the development of the hippocampus, and is an important repressor in dorso-medial patterning. It was noted that in FoxG1 mutant embryos a true hippocampal plate failed to develop and thus further research is required to determine the role of FoxG1 in such patterning.

1.1.2.2. FoxG1 acts in a dosage dependent manner

Ectopic expression of *X*FoxG1 (*Xenopus laevis* FoxG1 mRNA) in the posterior neural plate of *Xenopus* embryos provided further insight into the role of FoxG1 in the development of the telencephalon (Bourguignon *et al.*, 1998). When injected with high concentrations (0.5 ng) of synthetic *XFoxG1* RNA, proliferation of the neural progenitor cells in the injected area was evident, with a concomitant lack of expression of *N-tubulin*, a neuronal differentiation marker. These embryos did however; exhibit signs of differentiation in the adjacent tissue. Interestingly, when injected with low concentrations (90 pg) of the *Xenopus* mRNA, neural progenitor cells in the injected area were seen to differentiate, and were no longer in a state of division. The results suggest that FoxG1 acts as both a repressor and activator of neurogenesis, in a dosage-dependent manner: stimulating proliferation at high concentrations and inhibiting neuronal differentiation, and promoting differentiation when present in low concentrations. These results make possible the idea that FoxG1 acts in a gradient-related manner during the development of the telencephalon, an idea also expressed by Muzio and Mallamaci (2005).

1.1.3. FoxG1 acts as both a transcriptional repressor and activator

Qin, the chicken orthologue of FoxG1, was isolated from the avian sarcoma virus 31, found in spontaneous connective tissue tumours in adult chickens (Li and Vogt, 1993, Li *et al.*, 1995, Li *et al.*, 1997). *Qin* acts as a transcriptional repressor, suggesting that FoxG1 might have a similar function. In order to determine whether FoxG1 acts as a transcriptional repressor or activator Bourguignon *et al.* (1998) fused *X*FoxG1 to a strong repressor domain, EnR, derived from the *Drosophila* Engrailed protein. Independently, *X*FoxG1 was fused to a strong activator domain from the adenoviral protein, E1A. Embryos were injected with either

mRNA from the construct containing the activator, or repressor, and the results of the ectopic expression were compared to those obtained from injecting the wildtype *X*FoxG1. If FoxG1 acts as a transcriptional repressor, or activator, the authors anticipated that one of the experimental transcripts would mimic the wildtype mRNA, and the other would show the opposite affect. The development of the embryos injected with *XFoxG1-EnR* was almost identical to that of the embryos injected with the wildtype mRNA. Embryos injected with *XFoxG1-E1A* showed similar development to those injected with the wildtype mRNA, but were less similar than the *XFoxG1-EnR* injected samples. These results suggest that FoxG1 acts as both a repressor and activator of transcription.

Hardcastle and Papalopulu (2000) showed that *X*FoxG1 suppresses expression of $p27^{XIC1}$, a cyclin-dependent kinase (cdk) inhibitor, which is normally expressed in non-dividing cells and regulates cell cycle. It is through this inhibitor that the transcription factor seems to affect cell proliferation. The authors found that $p27^{XIC1}$ is suppressed by high FoxG1 concentrations at the mRNA level, and in the absence of protein synthesis, while low concentrations of FoxG1 were seen to induce expression. It was also found that injecting $p27^{XIC1}$ into *Xenopus* embryos blocked the cell cycle, but was not sufficient to induce expression of *N-tubulin,* a result of the injection of *XFoxG1.* These results imply that the regulation of cell proliferation by FoxG1 is mediated through $p27^{XIC1}$, while cell fate is regulated in a different manner.

1.1.3.1. In order to repress transcription, FoxG1 interacts with Groucho/TLE and Hes

The mammalian transcriptional co-repressor Transducin-like Enhancer (TLE) 1 is homologous to the *Drosophila* Groucho (Gro), which represses neuronal differentiation through the formation of transcription complexes (Yao *et al.*, 2000). In *Drosophila,* Groucho

interacts with Hairy/Enhancer of Split (Hes) to form complexes which inhibit the expression of proneural genes, positive regulators of neuronal differentiation. In these complexes the Hes proteins fulfill the DNA binding function, and Groucho acts as a transcriptional repressor. This mechanism of repression by Gro/TLE and Hes is conserved in invertebrates and vertebrates. In 2001 Yao *et al.* showed that FoxG1 interacts with Gro/TLE1 and Hes. The authors showed that FoxG1 was capable of forming complexes with Gro/TLE1, which both included, and excluded Hes. In the latter complex the FoxG1 protein itself provided the DNA binding domain. FoxG1 did not form complexes with Hes, independently of Gro/TLE1, suggesting that Gro/TLE1 is required as an adaptor for the interaction between the two. It is thought that through the formation of these complexes FoxG1 is able to repress neuronal differentiation. FoxG1 was found to recruit histone deacetylase (HDAC) 1, and when inhibited by trichostatin A, a decrease in repression of proneural genes by FoxG1 was noted. Histone deactylases have previously been shown to interact with Gro/TLE proteins. More recently Marçal *et al.* (2005) demonstrated that the newly identified Gro/TLE-related gene product 6 (Grg6) may be involved in the regulation of neurogenesis. Grg6 inhibits interactions between FoxG1 and Gro/TLE, therefore suppressing repression of proneural genes by the complex, and is required for neuronal differentiation.

1.1.3.2. FoxG1 disrupts the TGF-β signaling pathway

FoxG1 has also been shown to disrupt the β-type transforming growth factor (TGF-β) signaling pathway (Pelton *et al.*, 1991). TGF-β proteins are secreted growth factors that are involved in organogenesis and morphogenesis in the developing embryo. Their functions include, amongst others: regulation of differentiation, extracellular matrix deposition and inhibition of proliferation. In mouse embryos, of the three TGF-β forms (1, 2 and 3) both

TGF- β2 and 3 were expressed strongly in the developing brain and central nervous system, where they are believed to regulate proliferation of neuronal progenitor cells. In the TGF-β signaling pathways the TGF-β ligand binds to the outer surface of the cell via a complex of type I and II receptor kinases. In response to ligand binding, type I receptor kinases are phosphorylated by the type II TGF-β receptors, which in turn phosphorylate specific Smad proteins (2 and 3). The phosphorylated Smad protein associates with Smad4 forming a complex which is translocated into the nucleus. In the nucleus the Smad complex is able to regulate transcription of target genes, through the interaction with DNA-binding transcription factors (Smad binding partners) (Derynck and Zhang, 2003). In 2000, Dou *et al.* showed that FoxG1 associates with the Smad binding partner FoxH2, which is required by the Smad2/3/4 complex to bind DNA. Rodriguez *et al.* (2001) subsequently demonstrated that FoxG1 was also able to bind the Smad proteins themselves, preventing the formation of the Smad2/3/4 complex. The carboxyl-terminus of FoxG1 was found to be exclusively required for this means of disruption. Furthermore, Seoane *et al.* (2004) showed that FoxO proteins are key partners in the TGF- β pathway, resulting in transcriptional activation of *p21Cip1*, a cdk which represses growth-promoting transcription factors. FoxG1 was shown to associate with FoxO3 or Smad3/4 in this pathway, disrupting it. Thus, FoxG1 inhibits neuronal differentiation by associating with Gro/TLE and Hes, and promotes proliferation by disrupting the TGF- β pathways, which would ordinarily repress the cell cycle.

1.1.3.3. BMP4 and FGF-8 may be regulated by FoxG1

Bone morphogenic protein (BMP) 4 belongs to the TGF-β superfamily and has shown to be required for neuronal differentiation and the repression of progenitor cell proliferation (Li *et al.*, 1998). BMPs 1-4 use a similar signaling mechanism as other members of the TGF-β

superfamily, but make use of specific BMF-ligand transmembrane receptors, and activate Smads 1, 5 and 8 (Derynck and Zhang, 2003). In 1999, Dou *et al.* showed that by E10.5 in mice embryos, BMP4 is expressed in a pattern complementary to that of FoxG1, BMP4 is localized to the dorsomedial telencephalon and the roof of the telencephalon. The authors suggested that FoxG1 might repress BMP4 and hence examined the expression patterns of BMP4 in FoxG1 null mutant embryos. By E11.5 in mutant embryos, BMP4 was visualized in the entirety of the dorsal telencephalic neuroepithelium, indicating the expansion of the domain of expression. These results suggest that FoxG1 is required for the down-regulation of BMP4 in certain areas of the developing telencephalon. Similarly, Hanashima *et al.* (2002) showed that the regions of expression of BMP6, 7 and 2 are also expanded in the telencephalon of FoxG1 mutant mice. With the use of a FoxG1 DNA-binding domain mutant, the authors demonstrated that this domain is required for the down-regulation of BMPs, resulting in the repression of neuronal differentiation. It was also noted that stimulation of proliferation by FoxG1 was independent of the DNA-binding domain, indicating that control of proliferation and neuronal differentiation are mediated independently.

A second growth factor, fibroblast growth factor (FGF)-8, is also believed to be regulated by FoxG1. FGF8 is required for the continued proliferation of precursor cells, and is an inhibitor of neurogenesis in the midbrain, where it is expressed in the rostral metencephalon (Lee *et al.*, 1997). Fukuchi-Shimogori and Grove (2001) showed that FGF8 is required for rostro-caudal patterning of the telencephalon, where it displays similar functions. Martynoga *et al.* (2005) have demonstrated that there is a marked reduction in the expression of FGF8 in E10.5 FoxG1 mutant mice embryos, when compared to wildtype embryos. However at E9.5, *Fgf8* expression was detectable in the rostral telencephalon of both the mutant and wildtype

embryos. This reduction in expression at E10.5 coincided with the decreased rate of proliferation in the rostral telencephalon, indicating that FoxG1 might upregulate FGF8 expression and maintain progenitor cells in a proliferative state.

1.1.4. FoxG1 is comprised of three distinct domains: the N-terminus, the DNA-binding domain and the C-terminus

The cloning of various FoxG1 orthologues from vertebrates, including reptiles, fish, birds and mammals, has revealed that both the DNA-binding and the carboxy (C)-terminal domains are almost identical, while there is considerable variation evident in the N-terminal domain of the transcription factor (Bredenkamp *et al.*, 2006). The DNA-binding domains of the orthologues all contain the 100-amino acid region characteristic of the winged-helix family (Kaestner *et al.*, 2000), while the C-terminal domains contain a conserved 211 amino acid region. FoxG1 is grouped into class 1 of the FOX proteins, because of the basic C-terminal region typical of this class (Katoh and Katoh, 2004).

As previously discussed, Yao *et al.* (2001) showed that the DNA-binding domain of FoxG1 was required for the repression of proneural genes by the Gro/TLE1 complex. The domain was also shown to be necessary for the down-regulation of BMPs, and the subsequent repression of neuronal differentiation (Hanashima *et al.*, 2002). The C-terminal domain of FoxG1 was shown to be required for binding to the Smad proteins, or Smad binding partners, leading to the disruption of the TGF-β pathway, and promoting proliferation (Dou *et al.*, 2000, Rodriguez *et al.*, 2001, and Seoane *et al.*, 2004). The high levels of conservation in these regions may signify the conserved function amongst the orthologues.

The N-terminal domains of FoxG1 orthologues share a common sequence in the first 30 amino acid residues, including a predicted Casein kinase 1 phosphorylation site, which has been shown necessary for FoxG1 nuclear localization (Regad *et al.*, 2006), after which the domain is significantly different. The N-terminal domains of mammalian orthologues are of particular interest; these contain significant quantities of histidine (H), proline (P) and glutamine (Q) amino acid residues (Tao and Lai, 1992, and Bourguignon *et al.*, 1998), while these expanded domains are severely reduced in the FoxG1 orthologues of other vertebrate species, such as that of *Xenopus* and zebrafish (Fig. 1.2).


```
HUMAN       MLDMGDRKEVKMIPKSSFSINSLVPEAVQNDNHHASH.GHHNSHHPQHHHHHHHHHHPP     59
RAT         MLDMGDRKEVKMIPKSSFSINSLVPEAVQNDNHHASH.GHHNSHHPQHHHHHHHHHH.PP    58
MOUSE       MLDMGDRKEVKMIPKSSFSINSLVPEAVQNDNHHASH.GHHNSHHPQHHHHHHHHHH.PP    58
CHICKEN     MLDMGDRKEVKMLPKSSFSINSLVPEAVQSDNHS.GH.SHHNSHHPHHHHHHHHHH..PP    56
XENOPUS     MLDMGDRKEVKMIPKSSFSINSLMPEAVQNDNHPQPHHHHHHQQQPQHLQLPQQHHL.QP    59
ZEBRAFISH   MLDMGERKEVKMIPKSSFSINSLVPEAVQSDNHH....HHHHQQQ.Q.......HHH...    45

                                          xx xx       x               xxx

HUMAN       PPAPQPPPPPQQQQPPPPPPPPAPQPPQTRGAPAADD..DKGPQQLLLPPPPPPPPAAALD   117
RAT         PPAPQPPPPPPQQQQQ..PPPAPQPPQARGAPAADD..DKGPQPLLLPP......SAALD    108
MOUSE       PPAPQPPPPPPQQQQQQ.PPPAPQPPQARGAPAADD..DKGPQPLLLPP......STALD    109
CHICKEN     PP.........QQ.........PQ....RAAAAEEEDEEK..APLLLPPPAA....GALE     88
XENOPUS     HH.........................RPLQ.EEDELDK...SLL.............E     76
ZEBRAFISH   .........................RTVH.EEEE..K..TPLPAQVQ.........E     63

              xx x x x x x   xxx   x  x   x       xxxxxx     xxx  xx

HUMAN       .GAKADGLG.GKGEPGGG.PGELAPVGPDEKEKGAGAGGEEKKGAGEGGK             164
RAT         .GAKADALG.AKGEPGGG.PAELAPVGPDEKEKGAGAGGEEKKGAGEGGK             155
MOUSE       .GAKADALG.AKGEPGGG.PAELAPVGPDEKEKGAGAGGEEKKGAGEGGK             156
CHICKEN     .AAKAEALA.GKGEAGAA.AAEL.....EEKEK....AAEEKKGAAEGGK             126
XENOPUS     V..KTESLPPGKGDPAAS...ELP..G.EDKDK.....IDDKKVD...GK             110
ZEBRAFISH   Q..KSENT.CAKSDNSS....HDSSST.DEKEKQ.....EEKRDA....K              96
```

Figure 1.2. Amino acid alignment of the N-terminal domains of various FoxG1 orthologues. The mammalian orthologues contain the expanded H/P/Q rich domain (solid line below sequence), which is reduced in other orthologues such as chicken, and *Xenopus*. The excess proline residues present in the human and absent in the lower mammals, such as rat, are underlined in red. Large numbers of glycine and alanine amino acid residues are present downstream of this expanded region in the mammalian orthologues (x, above sequence). Sequence shading similarity is 65.7%.

While a stretch of histidine residues is present in all of the orthologues, the mammalian orthologues include a stretch of 17-21 proline amino acid residues (Bredenkamp *et al.*, 2006, Fig. 1.2). The N-terminal domains of the mammalian orthologues also contain large numbers of glycine (G) and alanine (A) amino acid residues.

The presence of the expanded H/P/Q-rich domain in mammalian orthologues, similar to the expanded domains and amino acid repeats seen frequently in the N-terminal domains of prion proteins (Lindquist, 1997 & Shorter and Lindquist, 2005), has raised an interesting question: does this domain act as a prion-like switch, inducing a conformational change and aggregation of the FoxG1 protein, thereby regulating its activity during neuronal development?

1.2. Prions: proteins capable of infectious amyloid formation

Prions are widely believed to be infectious proteins capable of self-perpetuating changes in conformation, with the prion form of the protein acting as a self-replicating agent (Shorter and Lindquist, 2005). The term "prion" is derived from "proteinaceous infectious particle", and the concept began with the study of various mammalian neurodegenerative diseases (Prusiner, 1982). These include: Creutzfeldt-Jakob disease (CJD), Gerstmann-Sträussler-Scheinker (GSS) syndrome, Fatal Sporadic Insomnia (FSI), and kuru in man, scrapie in sheep, and bovine spongiform encephalopathy (BSE) (Prusiner, 1982 and 1998). Prion particles are believed to form ordered aggregates under physiological conditions, and are devoid of nucleic acids. Prions are sensitive to protein denaturing agents, such as proteases and acidic sodium dodecyl sulfate (SDS), and are unaffected by exposure to UV radiation and other nucleic acid-altering substances (Alper *et al.*, 1967 and Peretz *et al.*, 2006).

1.2.1. Mammalian prion diseases

The abovementioned mammalian diseases all have in common a conversion of the prion protein PrP, which is normally expressed in mammalian cells. Spongiform encephalopathies result when the cellular form of the protein, PrP^{c}, is converted into the insoluble prion form, PrP^{sc}. PrP is a plasma membrane anchored glycoprotein, expressed in the developing and mature central nervous system, although not essential for normal development (Steele *et al.*, 2006). Steele *et al.* (2006) found that PrP^{c} expression was strongest in fully differentiated, mature neurons, and lowest in multipotent neuronal precursors. PrP^{c} increases cellular proliferation in the subventricular zone (SVZ) of the mammalian central nervous system, a region containing multipotent precursor cells. In humans, more than 20 different mutations of the PrP gene are known to cause inherited prion diseases, while how sporadic disease occurs is largely unknown (Prusiner, 1991 and 1998).

Brandner *et al.* (1996) demonstrated that the PrP^{c} protein is necessary for the development of scrapie. Embryonic telencephalic tissue from mice over-expressing PrP was grafted onto brain tissue of PrP null mutant mice (*Prn-p*$^{0/0}$), while simultaneously injecting the tissue with scrapie prion particles. Similarly, deficient brain tissue was engrafted with wildtype tissue and that of the mutants, and injected with the prion particles. The authors found that grafting the PrP over-expressing tissue to the brain resulted in the development of scrapie after 70 days, while grafting wildtype tissue resulted in the development of the disease at 160 days. The *Prn-p*$^{0/0}$ host, engrafted with the deficient telencephalic tissue, did not display any pathological signs of scrapie. Thus, in the development of prion diseases, PrP^{c} is necessary for infection by PrP^{sc}.

1.2.2. Yeast prions are non-pathogenic, heritable phenotypes

Three prions have been found in the yeast *Saccharomyces cerevisiae*. These prion states, namely [*URE3*], [PSI^+] and [*RNQ1*] are able to produce heritable changes in phenotype, without a change in nucleic acid sequence, and are a determined by the genes encoding Ure2p, Sup35 and Rnq1 respectively (Chernoff *et al.*, 1995, Sondheimer *et al.*, 2001, Ter-Avanesyan *et al.*, 1994 and Wickner, 1994). Yeast prions are non-pathogenic and are transmissible between mating cell types, displaying non-Mendelian patterns of inheritance when passed on to daughter cells.

Yeast prions generally share no sequence homology to other prions, or to each other, but do share a number of structural traits (Lindquist, 1997, and Sondheimer *et al.*, 2001). The N-terminal domains are usually dispensable for their cellular function, but are required for prion accumulation; these domains are also often rich in glutamine (Q), asparagine (N) and other polar amino acid residues, including oligopeptide repeat sequences, and often display conformational flexibility (Derkatch *et al.*, 2004). Interestingly, it is the C-terminal domain of the yeast prion Rnq1 which is intrinsically unstructured. Similarly, the N-terminal domain of the mammalian PrP protein contains regions (amino acid residues 1-103) of conformational flexibility, and while the amino acid sequence is not Q/N-rich, it does contain oligopeptide repeats (Shorter and Lindquist, 2005).

1.2.3. Formation of amyloid fibres

A feature shared by both mammalian and yeast prion proteins is the ability to form amyloid fibres *in vitro* and *in vivo* (Govaerts *et al.*, 2004, Krishnan and Lindquist, 2005, and Scheibel *et al.*, 2004). Amyloids are described as protein aggregates which form fibres 5-10 nm in

diameter, with β-pleated sheet conformation. They display a greater resistance to proteases and detergents than soluble proteins and bind the dyes Congo Red and Thioflavin T and S (Shorter and Lindquist, 2005). Different prion strains of the same protein have been identified, which differ in the structure and size of the prion fibres. In yeast, the Sup35 protein forms β-rich amyloid fibres. Fibres formed by the N-terminal domain (NM) have been extensively studied to further understand the formation of amyloids in general (Krishnan and Lindquist, 2005). The authors found two regions within the NM domain that formed intermolecular contacts during fibre formation, the "head" region (residues 25-38), and the "tail" region (residues 91-106). The residues (43-85) between these regions were referred to as the "central core", and did not contribute to intermolecular contacts. They demonstrated that the contacts between individual NM proteins occurred in a "head-to-head" and "tail-to-tail" manner, and that the residues forming the amyloid core rapidly entered an unstructured molten form, prior to fibre formation.

Krishnan and Lindquist (2005) suggested that in this molten state the "head" regions initially come into contact, in what seems to be a lag phase in fibre formation. Following formation of this nucleus, the "tail" regions form intermolecular contacts. These contacts result in the formation of fibrils, which form bi-directionally by recruiting additional proteins; fibrils are then connected in some manner to form prion fibres (Fig. 1.3). The C-terminus of the NM protein was found to be excluded from the fibril formation, and remains unstructured. The authors also noted that a change in the intermolecular contacts produced different prion strains, and thus the manner in which the amyloid core is formed, determines the fibre structure.

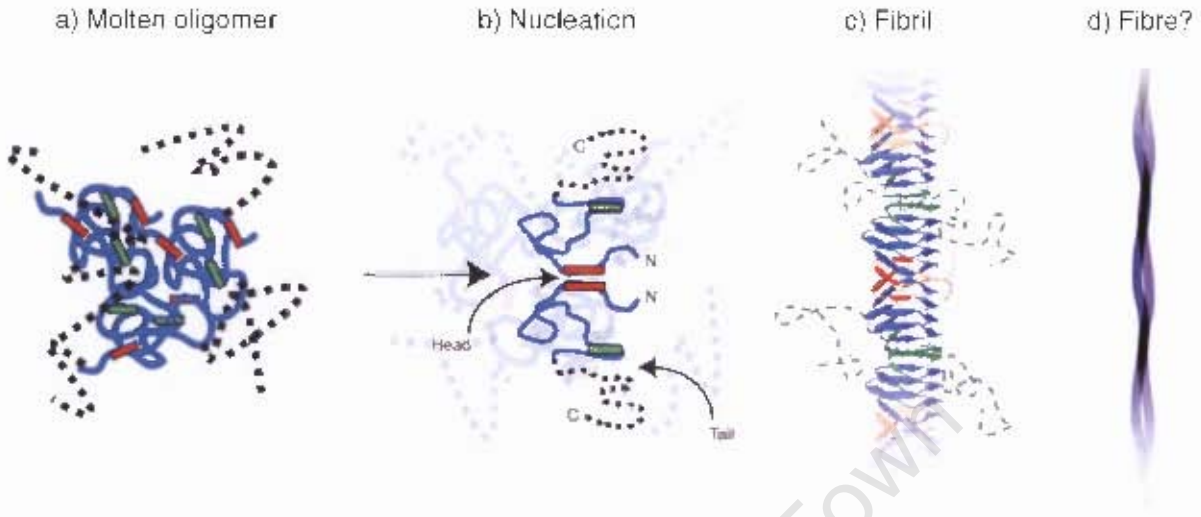

Figure 1.3. Suggested events in the formation of the prion fibre. Initially the conformation of proteins is altered to a molten state (a), in which "head" regions (red) are able to form intermolecular contacts (b), followed by the "tail" regions (green). This is followed by the bi-directional formation of fibrils (c), in which the C-terminus of the protein is not included (dotted line). Fibres are later formed from multiple fibrils (d). Taken from Krishnan and Lindquist, 2005.

1.2.4. Evidence for the prion hypothesis

Although accumulation of these fibres *in vivo* has revealed a possible mechanism whereby they are formed (Krishnan and Lindquist, 2005), and it is accepted that the prion and non-prion form of the protein are necessary for propagation of the fibres (Brandner *et al.*, 1996, Shorter and Lindquist, 2005), the ultimate evidence for the prion hypothesis is the formation of fibres *in vitro*, using recombinant protein, and propagation of the prion once introduced into cells in which it is absent. It has been shown that transforming [*psi*$^-$] yeast cells with recombinant protein fibres formed *in vitro*, composed only of the prion domain of Sup35 induces [*PSI*$^+$], while soluble recombinant protein has no effect (King and Diaz-Avalos, 2004, and Tanaka *et al.*, 2004). Recently, synthetic mammalian prion fibres have been produced which are able to induce prion disease in mice. When transgenic mice, over-expressing PrP comprising residues 89-231, are injected with synthetic PrP (89-230) amyloid fibres,

produced in *Escherichia coli,* disease is induced (Legname *et al.*, 2004). Injection with soluble proteins had no such effect. Similarly, when transgenic mice over-expressing the GSS syndrome-associated PrP P101L mutation, were injected with synthetic PrP P101L folded into a β-rich conformation, GSS syndrome was induced (Tremblay *et al.*, 2004). Saa *et al.* (2006), recently developed Protein Misfolding Cyclic Amplification (PMCA) technology, a technique used *in vitro* to amplify PrP^{sc} aggregates in a cyclic manner similar to PCR. Small quantities of PrP^{sc} aggregates are incubated with PrP^{c}, resulting in the formation of large aggregates which can be broken into smaller fragments by sonication, and are self-perpetuating. When injected into wildtype hamsters, these aggregates induced disease in the same manner as prions purified from scrapie infected brain tissue.

1.2.5. Regulation of yeast prions

In yeast, the conformational switching seen in prions is a novel method of post-translational control, and is not a disease state. Prion aggregation is regulated by chaperone proteins. It has been shown that expression of the chaperone Hsp104 is necessary for all three prion states to exist (Chernoff *et al.*, 1995, Moriyama *et al.*, 2000, and Sondheimer *et al.*, 2001), and determines inheritance of the prion state. Chaperones are proteins which assist in the folding of other proteins, by preventing aggregation of unfolded forms. Over-expression or inactivation of Hsp104 causes curing of the [PSI^{+}] phenotype, thus an intermediate level of the chaperone is required for prion formation and maintenance (Chernoff *et al.*, 1995). Another yeast chaperone has been identified, which specifically regulates [RNQ^{+}] (Sondheimer *et al.*, 2001). Sis1, a member of the Hsp40 family, co-immunoprecipitates with Rnq1 and contains a glycine/phenylalanine (G/F) rich domain, which has been shown to be

essential for the formation of the prion fibres. Similar chaperones have not been identified in mammals.

1.2.6. Prions in memory formation

Prion fibre formation is not restricted to proteins involved in disease, or to yeast; a neuronal isoform of the *Aplysia* cytoplasmic polyadenylation element binding (CPEB) protein has been found to have prion-like properties (Si *et al,* 2003). CPEB acts as both an activator and repressor of dormant mRNA translation. In order to activate dormant mRNA, CPEB elongates the poly(A) tails of target molecules. The neuronal isoform of the *Aplysia* CPEB protein lacks phosphorylation sites. The authors noted the similarities between the N-terminal domain and the same region of the known yeast prions; the *Ap*CPEB N-terminus contains a high number of glutamine amino acid residues, including six repeats, and shows conformational flexibility. The authors demonstrated that not only did the *Ap*CPEB protein contain prion-like properties, but that the self-perpetuating prion form of the protein is the active form, able to bind to and activate dormant mRNAs. CPEB is translated at particular synapses in response to neurotransmitters (serotonin in *Aplysia*) and it is suggested that the prion form of the protein accumulates as a result of this trigger, to facilitate long-term memories at these specific synapses. As the turn-over of the prion form of proteins is reduced in comparison to the soluble form, the active form of *Ap*CPEB might be able to maintain long-term changes in mRNA translation at specific synapses, in response to serotonin as a physiological signal. It is suggested by the authors that this mode of action may be used by proteins involved in other biological processes, possibly including neuronal development.

1.2.7. Prions vs. amyloids: when is an amyloid a prion?

Although prions are proteins capable of forming self-perpetuating amyloid fibres, not all naturally occurring protein amyloid fibres are a result of prions. The formation of amyloid fibres is seen in various non-prion diseases, including Alzheimer disease (AD), Parkinson disease (PD), Huntington disease and type II diabetes (Dobson, 2003). In *E. coli*, the extracellular Curli protein forms amyloid fibres that are involved in colonization of inert surfaces, biofilm formation and binding to host proteins, but it is not considered a prion (Chapman *et al.*, 2002). These amyloid fibres, like those of prions, are β-rich, with the β-strands running perpendicular to the fibril axis. What distinguishes prions from non-prion amyloids is their transmissibility (or infectivity) to uninfected cells and tissue. The absence of transmissibility may result from many factors. In the case of PrP^{sc} (a mammalian prion) infectivity can occur via the food chain, as the prion aggregates are resistant to proteases in the mammalian gut the disease is transmitted between species (Shorter and Lindquist, 2005). It is possible that the non-transmissibility of non-prion amyloids is a result of the lack of a similarly successful mechanism. It is also possible that in non-transmissible amyloids a difference in amino-acid residue use prevents cross-species transmission, a barrier not restricting prions. Work on yeast prions has revealed that the accumulation of short amyloid fibres is more successful at both changing the phenotype of the host, and in transmitting the prion. It seems that a greater number of short fibres release more self-replicating fibre ends, which are transmitted between mating cells and to offspring. It is possible that non-prion amyloid fibres have increased fibre length, decreasing the rate of possible transmissibility. The infectivity of a protein displaying prion-like properties can easily be investigated, allowing researchers to determine whether the protein is able to form non-prion amyloids, or whether it is a prion.

1.2.8. Investigating possible prion-like properties of proteins

Two assays have been developed to investigate whether proteins display prion-like properties. Originally designed to study yeast prions, these assays have been used successfully to investigate other proteins, such as the *Aplysia* CPEB protein (Si *et al,* 2003). The assays rely on the ability of prions to confer upon other proteins a change in conformational state. Suspected prion domains can be fused to a glucocorticoid receptor (GR^{526}) construct, and the functionality of the construct in yeast cells determined (Li and Lindquist, 2000). Similarly, suspected prions can be visualized when fused to green fluorescent protein (GFP), and the ability of the protein to aggregate can be investigated via fluorescent microscopy (Patino et al., 1996).

1.3. Research aims

In this research dissertation, I have used these assays to investigate whether the N-terminal domain of FoxG1 has prion-like properties. I have compared the prion-like properties of the human and rat orthologues. These orthologues have been specifically chosen to determine whether any prion-like properties are dependent on the length of the expanded H/P/Q-rich domain present in the N-terminus of the transcription factor, and whether prion-like properties are functionally different between mammals with large (human) and small (rat) cerebral hemispheres. The ability of the N-terminal domains to form aggregates with GFP, and confer upon the GR protein an ability to change conformation was examined. In order to determine whether the prion-like state was a result of a prion, or a non-prion amyloid, heritability of the prion-like state to daughter cells and transmissibility to uninfected mating cell types was also investigated.

CHAPTER 2

The N-terminal domains of rat and human FoxG1 can confer upon other proteins a change in conformation

---

2.1. Introduction

The N-terminal domains (NFoxG1) of mammalian FoxG1 (or BF-1) orthologues are of particular interest, due to the expanded H/P/Q-rich domain. Similar tracts of amino acid residues are often present in prion proteins. In this research dissertation, I have tested the hypothesis that the N-termini of FoxG1 orthologues have prion-like properties, enabling the FoxG1 protein to change conformation, and exist in both ordered aggregates and in a soluble state. The prion-like properties of NFoxG1 of the rat and human orthologues were compared with the use of yeast assays.

The yeast prion determinant Sup35 has been used to establish whether prions are able to impose upon other proteins the ability to change their conformational state (Li and Lindquist, 2000). The N-terminal domain of Sup35 (NM domain), which is necessary for prion fibre formation, was fused to a constitutively active rat glucocorticoid receptor (GR^{526}). A GR^{526}-regulated β-galactosidase reporter plasmid was co-transformed into yeast cells and the colour of the colonies was used to determine the conformational state of the GR^{526} protein. When GR^{526} proteins were in their active, native conformation, yeast colonies plated on X-gal media acquired a blue colour. The Sup35 NM domain was able to confer upon the GR^{526} protein an alternative conformation, rendering it inactive. As the inactive protein was unable to activate the GRE promoter driving the β-galactosidase expression, yeast cells failed to produce the

characteristic blue colour. Upon restreaking of white colonies, the prion form was transmitted to daughter cells. However, a small percentage of the progeny were able to revert to the active state.

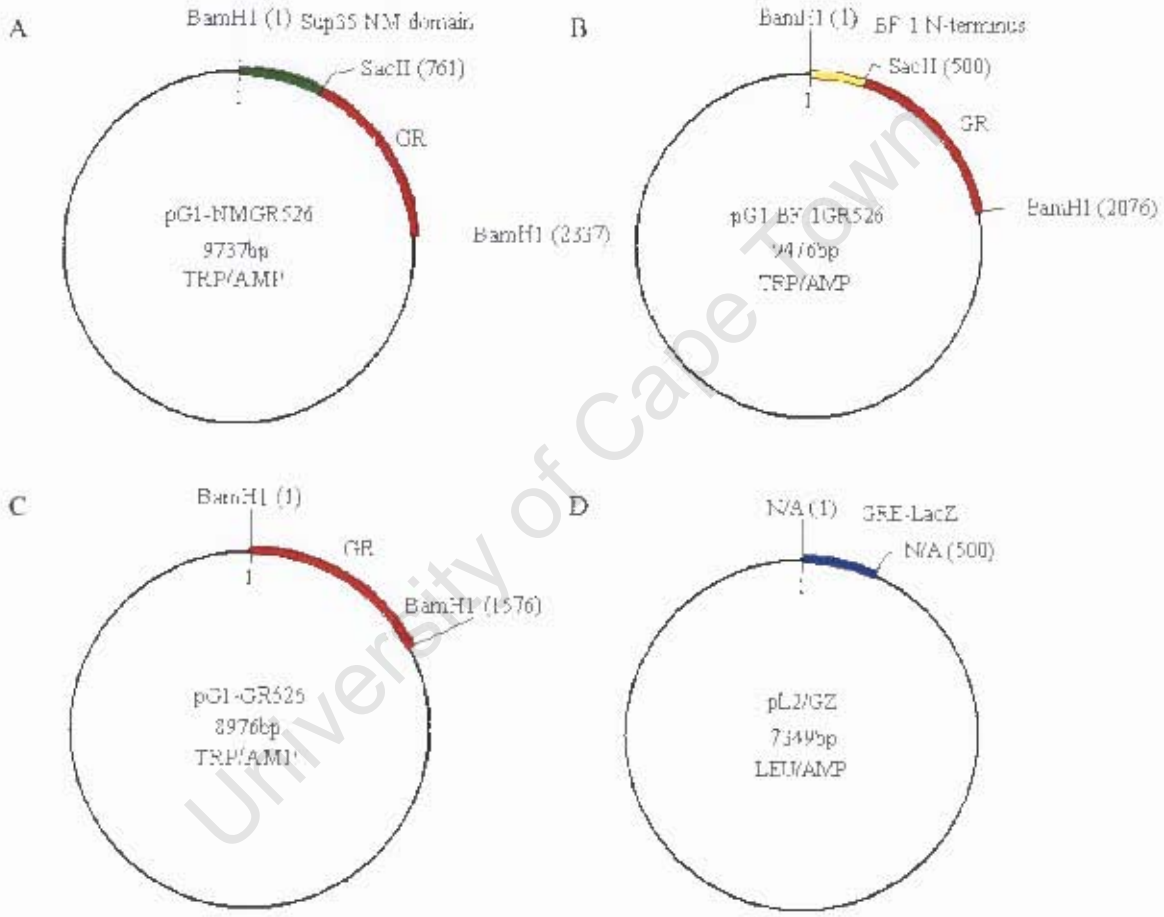

Figure 2.1. Plasmid maps of the constructs used in the yeast β-galactosidase assay for prion-like activity. (A) pG1-NMGR^{526} was used as a positive prion control. (B) The NM fragment was replaced by the rat and human NFoxG1 domains, producing the pG1-BF1GR^{526} constructs. (C) The plasmid pG1-GR^{526} was used as a GR^{526} positive control, as the GR^{526} was constitutively active and able to regulate GRE-lacZ in the pL2/GZ vector (D). The position of the restriction enzyme recognition sites are shown, as are the selectable markers specific to the plasmids.

In this study, the rat and human FoxG1 N-terminal domains were fused in frame to a constitutively active rat glucocorticoid receptor (GR^{526}), in the plasmid pG1-NMGR^{526} (Fig.

2.1). The NM fragment, encoding the N-terminal domain of Sup35, was replaced by the FoxG1 (BF-1) N-terminal domain (NFoxG1), resulting in the rat (pG1-rBF1GR^{526}) and human (pG1-hBF1GR^{526}) constructs. The constructs were co-transformed into yeast with a GR^{526} regulated β-galactosidase vector, pL2/GZ (Fig. 2.1, 2.2), and the colour of the yeast

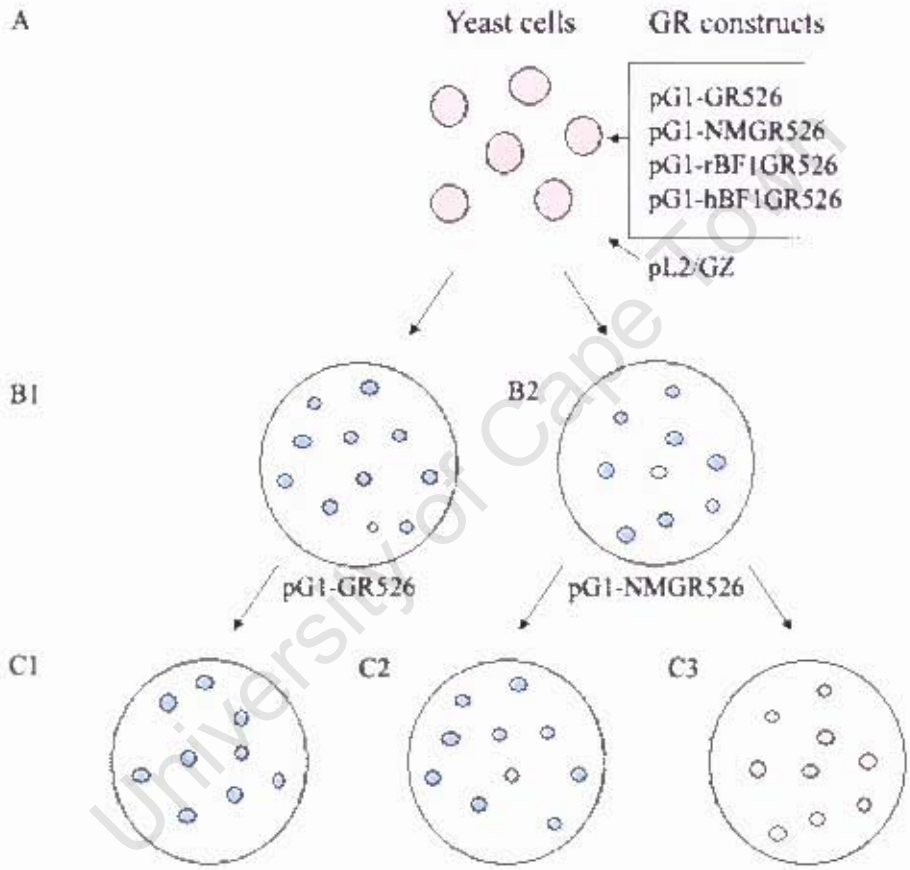

Figure 2.2. Yeast assay for prion activity. (A) Yeast cells were individually transformed with the GR^{526} constructs, and simultaneously with the GR^{526} regulated β-galactosidase (pL2/GZ). Yeast cells transformed with the various constructs were plated on X-gal media, and the colour of the colonies determined. The negative prion control (pG1-GR^{526}) yielded only blue colonies (B1), while the positive prion control (pG1-NMGR^{526}) yielded both blue and white (B2). (C) Upon replating, the blue pG1-GR^{526} colonies produced only blue colonies (C1), while the blue pG1-NMGR^{526} colonies continued producing blue colonies with a small percentage of white progeny (C2). Replating the white pG1-NMGR^{526} colonies resulted in white colonies, with a small percentage of the white colonies converting back to the active state (C3). The assay was used to determine whether the human and rat NFoxG1 constructs were also able to change the conformation of the GR^{526} protein, rendering it inactive.

cells when plated on X-gal media was recorded (Fig. 2.2). The pG1-NMGR^{526} construct was used as a positive prion control, while the pG1-GR^{526} plasmid was used a GR^{526} control (i.e. negative prion control), in the assay summarized in Fig. 2.2.

An additional assay used to investigate the ability of prion-like proteins to form aggregates, has been developed using the Sup35 NM domain and green fluorescent protein (GFP) (Patino *et al*, 1996). The Sup35 NM domain was fused to GFP and transformed into yeast cells. Fluorescent microscopy revealed that the Sup35 NM domain induced GFP to adopt either its native, soluble form, or an insoluble form. When Sup35 was present in the prion state, both small and large aggregates were visible.

This assay was used to determine whether the human and rat NFoxG1 domains were similarly able to form aggregates *in vivo*. The NFoxG1 domains were fused in frame to GFP, in the plasmid p2μGFP, producing rat (p2μ-rBF1GFP) and human (p2μ-hBF1GFP) constructs, which were transformed into yeast. Fluorescent microscopy was used to view the transformed yeast cells and to determine whether the presence of the NFoxG1 domains resulted in GFP aggregation. The plasmid p2μGFP was used as a GFP control, resulting in soluble GFP *in vivo*, and the human and rat NFoxG1 constructs were examined for signs of either small or large GFP aggregation.

2.2. Materials and methods

2.2.1. Analysis of secondary structure of FoxG1 orthologues

The amino acid composition of *Xenopus,* rat and human FoxG1 were used to determine whether the transcription factors contain intrinsically folded or unstructured domains typical

of prion proteins. The IUPred server (http://iupred.enzim.hu/) was used to estimate which regions in the amino acid content were unstructured, and those which are folded into predictable secondary structure (Dosztányi *et al.,* 2005).

2.2.2. PCR amplification of FoxG1 orthologues

The cloning strategy to subclone the N-terminal domains of the FoxG1 (BF-1) orthologues upstream of GR^{526} for the prion assay is summarized in Fig. 2.3. For cloning into the pG1-$NMGR^{526}$ plasmid (Table 2.1), the NFoxG1 domains of the human and rat orthologues were amplified by Polymerase Chain Reaction (PCR), from the plasmids pGEM-T easy:hBF1 and pC52:rBF1 respectively (Table 2.1). The region was amplified from each orthologue using FoxG1 specific primers: BF-1-BamH1 forward and BF-1-SacII reverse primers, BamH1 and SacII restriction enzyme sites were constructed on the 5' and 3' ends respectively (Table 2.2.). Approximately 100 ng of vector was used as a template in the following 20 ul reaction mix: 1.225 U Expand High Fidelity Enzyme Mix (Roche), 1 X Expand High Fidelity $MgCl_2$ Buffer, 0.25 mM dNTPs, 0.5 µM of each primer, and 1.2 M betaine. Betaine (N,N,N-trimethylglycine) was added to the reaction mix to destabilize secondary structure that results from the high GC content of the FoxG1 orthologues (Bredenkamp *et al.,* 2006, Henke *et al.*, 1997). Cycling conditions were as follows: 94 °C for 3 minutes (1 cycle), 94 °C for 30 seconds, 45 °C for 30 seconds, 72 °C for 1 minute (5 cycles), 94 °C for 30 seconds, 57.5 °C for 30 seconds, 72 °C for 1 minute (5 cycles), 94 °C for 30 seconds, 66.5 °C for 30 seconds, 72 °C for 1 minute (25 cycles) and 72 °C for 7 minutes (1 cycle).

For cloning into the p2µGFP plasmid (Table 2.1), the N-terminal domains of human and rat FoxG1 were similarly amplified, using the same reaction mix, with the addition of BamH1

Table 2.1. Plasmids used for the glucocorticoid receptor and GFP assays, including sources and references.

Plasmid name	Source	Reference
pG1-GR^{526}	Addgene plasmid 1124	Li *et al.*, 2000
pG1-NMGR^{526}	Addgene plasmid 1122	Li *et al.*, 2000
pL2/GZ	Addgene plasmid 1282	Kimura *et al.*, 1999
p2μGFP	Addgene plasmid 1195	Patino *et al.*, 1996
pGEM-T easy:hBF1	N. Illing Lab	Bredenkamp *et al.*, 2006
pCS2:rBF1	N. Papalopulu Lab (gift)	N/A

Table note: Addgene plasmids available from www.addgene.org.

Table 2.2. Primers used for amplification of the N-terminal domains of FoxG1 orthologues, and screening of the resulting constructs.

Primer name	Primer sequence (5' - 3')	T_m (°C)
BF-1-BamH1 fwd.	CGG ATC CTC GAT GCT GGA CAT GGG	66.9
BF-1-SacII rvs.	ATC CGC GGA TAC CCG TC(C/T) TTG CCG	70.2/68.6
BF-1-BamH1 rvs.	ATG GAT CCA TAC CCG TC(C/T) TTG CCG	66.1/64.6
GR^{526} specific rvs.	CAC ATT GCT TGT GGA GCC TTT CG	62.9
GFP specific rvs.	AAG TTC TTC TCC TTT ACT CAT ATG GG	58.4

Table notes: all primers used in the study were designed during the research project, using DNAman (Lynnon Corporation), and T_m (melting temperature) was calculated using nearest neighbour thermodynamic methods (Breslauer *et al.*, 1986). Restriction enzyme recognition sites are underlined. Degenerate bases are shown in brackets.

restriction enzyme sites on both the 3' and 5' ends. The following primers were used: BF-1-BamH1 forward and BF-1-BamH1 reverse (Table 2.2). Cycling conditions were as follows: 94 °C for 3 minutes (1 cycle), 94 °C for 30 seconds, 43 °C for 30 seconds, 72 °C for 1 minute (5 cycles), 94 °C for 30 seconds, 55 °C for 30 seconds, 72 °C for 1 minute (5 cycles), 94 °C for 30 seconds, 65.5 °C for 30 seconds, 72 °C for 1 minute (25 cycles) and 72 °C for 7

minutes (1 cycle). All PCRs were performed using a PE Biosystems GeneAmp PCR system 9700 machine.

2.2.3. Ligation of FoxG1 N-terminal domain fragments into p-drive and transformation into *E.coli*

Following amplification by PCR, the N-terminal domains were electrophoresed on a 1.2% Agarose gel, viewed and excised under longwave UV light, and purified using the QIAquick Gel Extraction Kit (Qiagen). Purified DNA was ligated into the p-drive vector (Qiagen PCR cloning kit), according to the manufacturer's instructions (Fig. 2.3). The resulting p-drive constructs included the NFoxG1 rat and human fragments with constructed BamH1 and SacII cloning sites for cloning into the GR^{526} plasmid, and the NFoxG1 rat and human fragments with constructed BamH1 sites on both 5' and 3' ends for cloning into the GFP plasmid. The ligation mix was transformed into *E.coli* DH-5α competent cells prepared by the method of Chung and Miller (1988). Transformed colonies were screened on Luria agar plates supplemented with 80 µg/ml X-Gal, 0.5 mM IPTG and 100 µg/ml Ampicillin, to screen for galactosidase insertional inactivation and ampicillin resistance.

Figure 2.3. pG1-rBF1GR^{526} and pG1-hBF1GR^{526} plasmid construction. (A) Rat and human FoxG1 N-terminal domains were amplified with the use of FoxG1 specific primers (yellow arrowheads), from the vectors pCS2:rBF1 and pGEM-T easy:hBF1 respectively. (B) The 492bp and 512bp PCR fragments were visualized by electrophoresis and purified. Constructed restriction enzyme sites are shown.

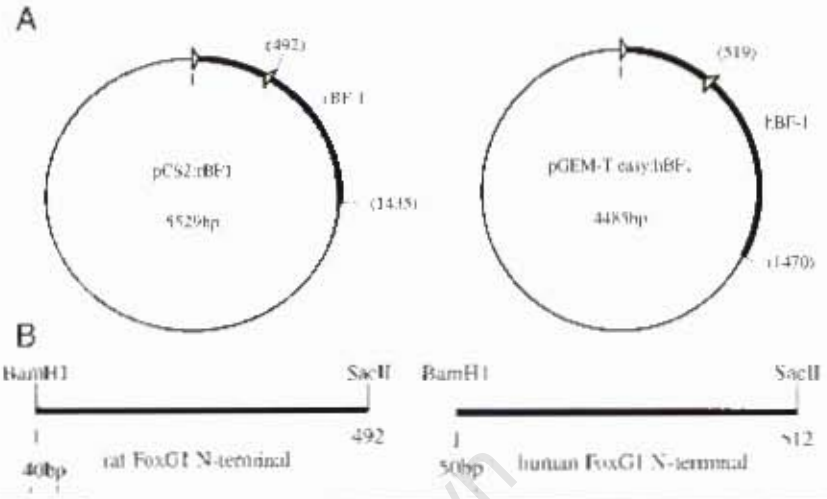

(C) The purified PCR fragments were ligated into the p-drive vector, and transformed into *E. Coli*. Sequencing was used to verify the inserts, the cloning forward and reverse primers (yellow arrowheads) were used. The FoxG1 N-terminal domains were digested from p-drive with BamH1 and SacII restriction enzymes.

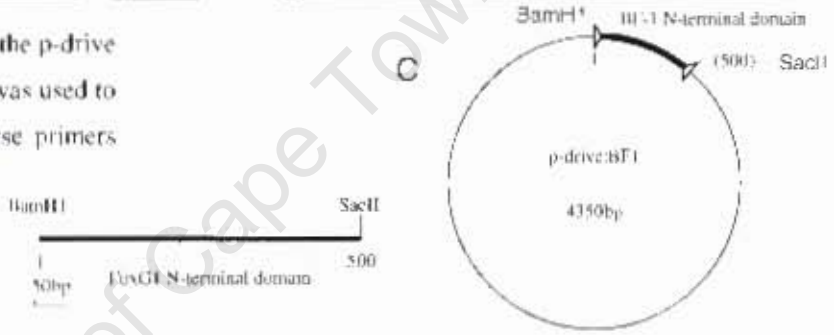

The plasmid pG1-NMGR^{526} (Fig. 2.1.A) was digested with SacII and partially digested with BamH1. Two plasmid species resulted, one in which the NM fragment was excised (D), and one in which the GR fragment was excised (E).

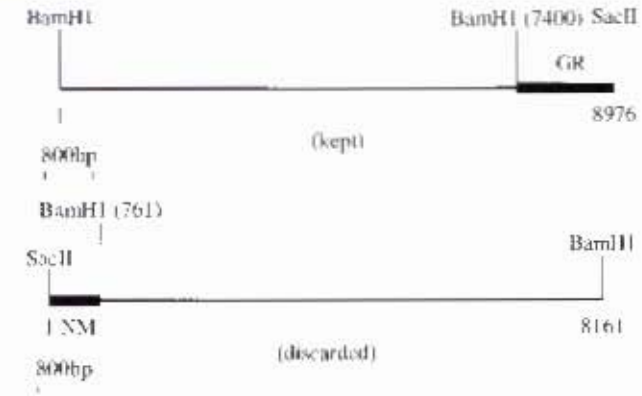

The purified FoxG1 N-terminal domains were ligated into the partially digested pG1-GR^{526} vector (D), and FoxG1 specific forward and GR^{526} specific reverse primers (F, yellow) were used to screen putative recombinant plasmids. (G) Constructs in which the FoxG1 N-terminal domains were fused to the NM fragment were selected against, as only the FoxG1 forward primer (yellow) would anneal to the vector.

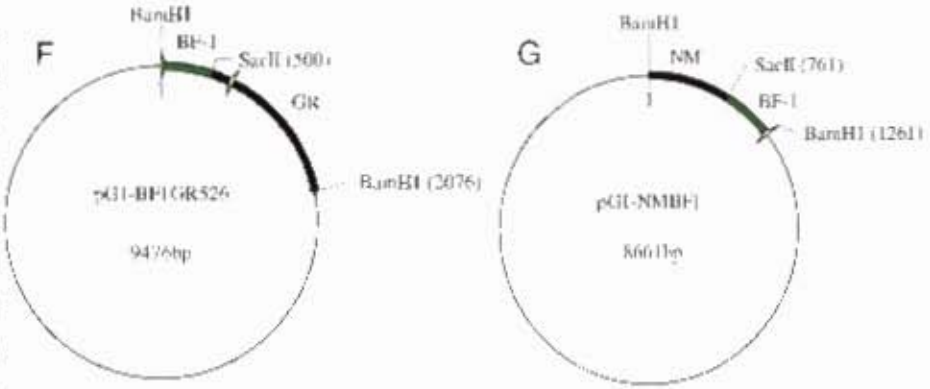

2.2.4. Screening transformants for correct inserts

Following transformation, white colonies were screened for the correct insert by colony PCR, using the same primers described previously (Table 2.2). 0.5 µl of overnight liquid cultures were used as template in the following 20 µl reaction mix: 1 X Supertherm Buffer, 2.25 mM $MgCl_2$, 0.25 mM dNTPs, 0.5 µM of each primer, 1.2 M betaine and 0.5 U Super-therm Taq DNA polymerase (Southern Cross Biotechnology). The cycling conditions were as follows: 94 °C for 3 minutes (1 cycle), 94 °C for 30 seconds, 68 °C for 30 seconds, 72 °C for 1 minute (30 cycles) and 72 °C for 7 minutes (1 cycle). PCR products were visualized by electrophoresis on a 1.2% Agarose gel. Plasmid DNA from selected positive colonies was purified using the High Pure Plasmid Isolation Kit (Roche), according to the manufacturer's instructions, quantified with the NanoDrop ND-1000 Spectrophotometer, and sequenced using the forward and reverse primers (Table 2.2). Sequencing was performed by Gene Care (Cape Town, South Africa).

2.2.5. Sub-cloning into plasmids pG1-NMGR^{526} and p2µGFP

For sub-cloning into pG1-NMGR^{526}, the FoxG1 N-terminal domain p-drive constructs were digested with restriction enzymes BamH1 and SacII (Fig. 2.3). 50 µl digests were performed using 0.1 U BamH1 and 0.06 U SacII per 1 µg DNA, including 1 X Buffer Green (Fermentas) and incubated overnight at 37 °C. Digested plasmid DNA was electrophoresed on a 1.2% Agarose gel, and the NFoxG1 domain fragments excised under longwave UV light. The excised fragment was purified using the QIAquick Gel Extraction Kit (Qiagen) according to the manufacturer's instructions. In order to remove the 761 bp yeast NM domain from the plasmid pG1-NMGR^{526}, it was necessary to first perform a complete SacII digest, followed by a partial BamH1 digest (Fig. 2.3). Plasmid DNA was digested with SacII, 0.1 U of the

enzyme was used per 1 µg DNA, with 1 X Buffer Blue (Fermentas), incubated overnight at 37 °C. Following SacII digestion, the plasmid was digested with 0.185 U per 1 µg DNA BamH1, with 1 X Buffer Blue. The reaction was incubated at 37 °C, for 15 min, before the addition of 1 X DNA tracking dye.

For cloning into the p2µGFP, the p-drive (BamH1-NFoxG1-BamH1) constructs were digested to completion with BamH1, 50 µl digests were performed using 0.1 U BamH1 per 1 µg DNA, with 1 X Buffer Green (Fermentas), and the digested inserts were purified as above. The p2µGFP plasmid DNA was digested with BamH1 in a similar reaction mix. Digested plasmid DNA was electrophoresed and purified in the same manner as the digested N-terminal domain inserts, and the 5' phosphates removed by Shrimp Alkaline Phosphatase (SAP), according to the manufacturer's instructions (Promega). Approximately equal concentrations of plasmid DNA and insert DNA were ligated in a 20 µl reaction, including 400 U T4 DNA Ligase (New England Biolabs) and 1 X Reaction Buffer. The ligation reactions were incubated at room temperature overnight and subsequently transformed into *E. coli* DH-5α competent cells.

2.2.6. PCR screening for correct constructs

In order to screen for inserts in the putative recombinant pG1-BF1GR^{526} plasmids, colony PCRs were performed following transformation, using a GR^{526} specific reverse primer and the BF-1-BamH1 forward primer (Table 2.2, Fig. 2.3). The reaction mix and the cycling parameters used were the same as those used for screening of inserts in the p-drive vector, with an annealing temperature of 55 °C. PCR products were visualized on a 1.2% Agarose gel and selected positive clones were sequenced as described earlier. Sequencing was performed

using both the BF-1-SacII and GR^{526} specific reverse primers, as well as the BF-1- BamH1 forward primer (Table 2.2).

Similarly, *E. coli* colonies transformed with the ligation mix of the plasmid p2μGFP, and the N-terminal domain inserts, were screened by PCR. A GFP specific reverse primer (Table 2.2), designed 24 bp from the start codon, and the BF-1-BamH1 forward primer were used to check the orientation of the inserts in the plasmid, as only one restriction enzyme was used for cloning. The same reaction mix and cycling parameters were used, as for the pG1-$BF1GR^{526}$ screening, with an annealing temperature of 58 °C. Following PCR, the products were visualized and the positive plasmids sequenced, using the GFP reverse, BF-1-BamH1 reverse and BF-1-BamH1 forward primers.

2.2.7. Yeast transformation

The following yeast strain was used for the assays: W303 (a/α, *ade2-1/ade2-1, trp1-1/trp1-1, leu2-3/leu2-112, his3-11/his3-15, ura3/ura3, canr1-100/CAN*). Yeast cells were transformed with either pG1-$hBF1GR^{526}$ or pG1-$rBF1GR^{526}$, and simultaneously with pL2/GZ by electrophoration (Table 2.1, Ausubel *et al.*, 2001). Yeast were also transformed with pG1-$NMGR^{526}$ and pL2/GZ, as a positive prion control, and pG1-GR^{526} with pL2/GZ, as a negative prion control (Table 2.1 and 2.3). p2μGFP, p2μ-hBF1GFP, and p2μ-rBF1GFP were all separately transformed into yeast cells. Following transformation, all yeast transformed with the GR^{526} based plasmids and pL2/GZ were plated on leucine and tryptophan deficient media, while GFP based plasmids were plated on uracil deficient media (Table 2.3) To confirm transformation, yeast cells were recovered from a stationary phase culture and were resuspended in 0.5 ml 1M sorbitol, 0.1M EDTA (pH 7.5), and incubated for 1 hour, at 37 °C

with 0.02 ml 2.5 mg/ml Zymolase solution (Sigma), to digest the cell wall. Following treatment the cells were recovered and plasmid DNA was purified using the High Pure Plasmid Isolation Kit, according to the manufacturer's instructions (Roche).

Table 2.3. Individual transformation of plasmids into yeast, selective media used, and purpose of transformation (control or experimental).

Plasmids transformed	Selective media	Control or experimental
pG1-hBF1GR^{526} and pL2/GZ	-leu -trp	Human N-terminal experimental
pG1-rBF1GR^{526} and pL2/GZ	-leu -trp	Rat N-terminal experimental
pG1-NMGR^{526} and pL2/GZ	-leu -trp	Positive prion control
pG1-GR^{526} and pL2/GZ	-leu -trp	Negative prion control
p2μ-hBF1GFP	-ura	Human N-terminal experimental
p2μ-rBF1GFP	-ura	Rat N-terminal experimental
p2μGFP	-ura	Negative prion control

2.2.8. Growth on X-gal media and β-galactosidase assay

For the β-galactosidase assay, yeast transformed with GR^{526} based plasmids and pL2/GZ were inoculated in 5 mls of –leu –trp dropout media, and grown to early stationary phase at 30 °C (OD_{600nm} = 1). Following growth in liquid media, approximately 300-600 cells were plated on dropout media agar plates and incubated for 4 days, or until colonies appeared. Colonies were velvet replica plated onto X-gal dropout media agar plates containing: 1 X BU salts (0.2611M Na_2HPO_4:$7H_2O$ and 0.25M NaH_2PO_4) and 80 mg/L of X-gal. Replica plates were grown for 4 days at 30 °C, or until colonies appeared. Blue and white colonies were counted. Blue and white colonies were picked and individually grown in 5 ml cultures to stationary phase, before being replated and screened for β-galactosidase activity. In this way, both the

percentage of blue colonies converting to white, and the percentage of white colonies reverting back to blue, was assayed. Three individual transformants, from each transformation, were plated in triplicate.

2.2.9. Fluorescent microscopy

Yeast cells transformed with the GFP constructs were viewed using fluorescent microscopy. Cells were grown in –ura dropout media to early stationary phase (OD_{600nm} = 0.8) at 30 °C. 20 µl of the cultures were viewed on glass slides (B&C, Germany) under the light microscope, using the (FITC) filter to measure GFP fluorescence. The Nikon Eclipse E600 fluorescent microscope fitted with a 100 X objective lens was used, and the images were captured with a Media Cybernetics CoolSNAP-Pro monochrome cooled CCD camera.

2.3. Results

2.3.1. The N-terminal domains of FoxG1 have no predicted secondary structure

The N-terminal domains of prion proteins are often rich in polar amino acid residues, amino acids repeats, and are devoid of predictable secondary structure (Lindquist, 1997). The amino acid sequences of the human, rat and *Xenopus* FoxG1 orthologues were analysed using the IUPred server, to determine whether the H/P/Q rich N-terminal domains show conformational flexibility. The application estimates the pairwise energy content of amino acid sequences, based on the likely interactions between the residues, and is able to distinguish between intrinsically folded and unfolded proteins (Dosztányi *et al.,* 2005).

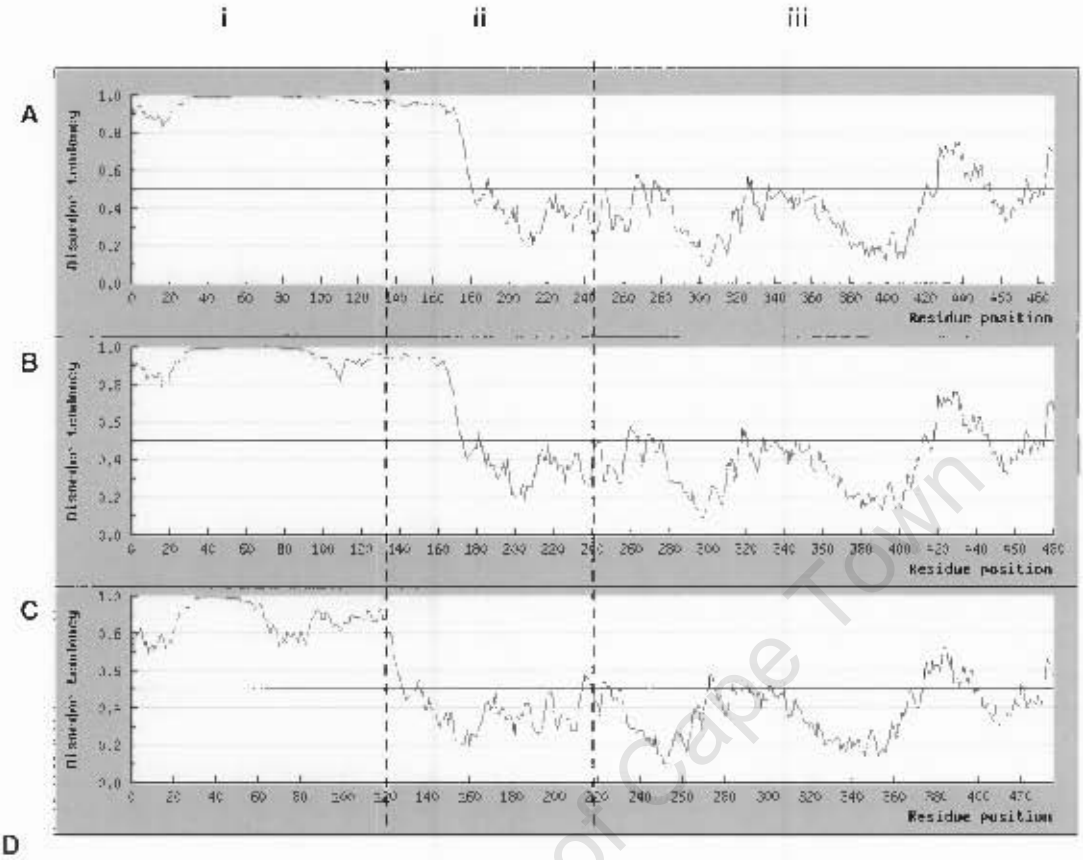

Figure 2.4. Disorder tendency of the amino acid residues of the human (A), rat (B) and *Xenopus* (C) FoxG1 orthologues. Values above 0.5 show high levels of disorder, and as a result prediction of secondary structure is impossible. Values below 0.5 represent those residues present in domains for which structure and intrinsic folding can be predicted. The N-terminal domains of the orthologues show conformational flexibility (i), while the conserved DNA binding (ii) and C-terminal (iii) domains display intrinsic folding properties. The amino acid sequence of the N-terminal domain of the human FoxG1 protein is shown below (D), with the H/P/Q rich region highlighted, and those residues unique to the human sequence (compared to the rat) underlined.

The N-terminal domains of the orthologues (residues 1 to approximately 164 in human, 1 to 155 in rat and 1 to 110 in *Xenopus*) displayed high levels of conformational flexibility (Fig. 2.4). The human orthologue, in comparison to the rat and *Xenopus*, showed a slightly higher sustained level of flexibility in the N-terminal domain, with a larger region of amino acids showing a maximum disorder tendency of 1.0, and when dipping slightly, reaching the 0.9

mark. The rat and *Xenopus* NFoxG1 domains reached the maximum level of 1.0, but showed dips in the disorder tendency of the amino acid residues at residue 110 and residues 60 to 85, respectively. These dips in disorder tendency can be correlated with the differences in the sequences; the dip shown by the rat sequence corresponds to the position of the six proline residues lacking in the sequence, but present in the human NFoxG1 domain (Fig. 1.2 and Fig. 2.4. D). The dip in the disorder tendency of the *Xenopus* NFoxG1 domain occurs at the position of the poly (Q) and poly (P) tracts lacking in the sequence, but present in the mammalian orthologues. Secondary structure is easily predicted in the conserved DNA binding and carboxy-terminal domains, adjacent to the N-terminal. The N-terminal domains of FoxG1 orthologues are therefore intrinsically unfolded regions, which include H/P/Q rich regions and many G/A amino acid residues.

2.3.2. Cloning of the N-terminal domains into the glucocorticoid receptor plasmid, pG1-NMGR^{526}

The N-terminal domains of rat and human FoxG1 were fused to a constitutively active rat glucocorticoid receptor (GR^{526}), to investigate whether the domain can induce a conformational switch in another protein. The N-terminal domains of rat (492 bp) and human (519 bp) FoxG1 were amplified by PCR with FoxG1 specific primers (Fig. 2.5). The primers were designed to construct BamH1 and SacII restriction enzyme sites, on the 5' and 3' ends respectively, to enable cloning into the plasmid pG1-$NMGR^{526}$. The PCR fragments were initially cloned into the p-drive vector, and sub-cloned into the pG1-$NMGR^{526}$ plasmid.

In order to sub-clone the FoxG1 N-terminal domain fragments into pG1-$NMGR^{526}$, the NM fragment within the vector, consisting of the N-terminal domain of the yeast Sup35 prion-

determinant, was removed via digestion with SacII and partial digestion with BamH1 and replaced with the FoxG1 N-terminal fragments digested out of the p-drive vector. A complete BamH1 digest of the pG1-NMGR^{526} vector was not possible due to a second BamH1 recognition site on the 3' end of the GR^{526} insert (Fig. 2.3). A GR^{526} specific reverse primer was used to confirm the sub-cloning of the N-terminal domains into the partially digested pG1-NMGR^{526}. The resulting constructs were screened by PCR, with the FoxG1 specific forward primer and a GR^{526} specific reverse primer (Table 2.2, Fig. 2.3). The FoxG1 and GR^{526}

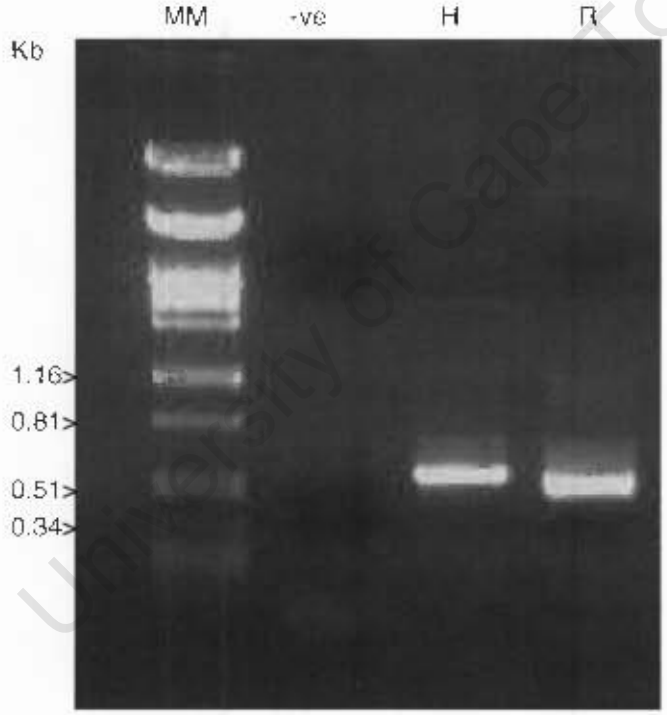

Figure 2.5. PCR amplification of the rat and human FoxG1 N-terminal domains. FoxG1 specific primers were used, which were designed to enable the addition of BamH1 and SacII restriction enzyme sites on the 5' and 3' ends respectively. MM: molecular weight marker (λDNA/PstI), applicable fragment sizes (Kb) are shown alongside. -ve: negative PCR control, including PCR grade water as the template. H: human N-terminal domain, 519 bp. R: rat N-terminal domain, 492 bp.

specific primers only produced a PCR product when the desired construct was present as a template, allowing selection of constructs in which the N-terminal domains of human and rat

FoxG1 were fused directly to GR^{526} (Fig. 2.6). The PCR screening allowed exclusion of constructs which did not produce PCR product, and therefore did not contain the FoxG1 N-terminal domain and the GR^{526} fragment in the correct orientation (Fig. 2.6).

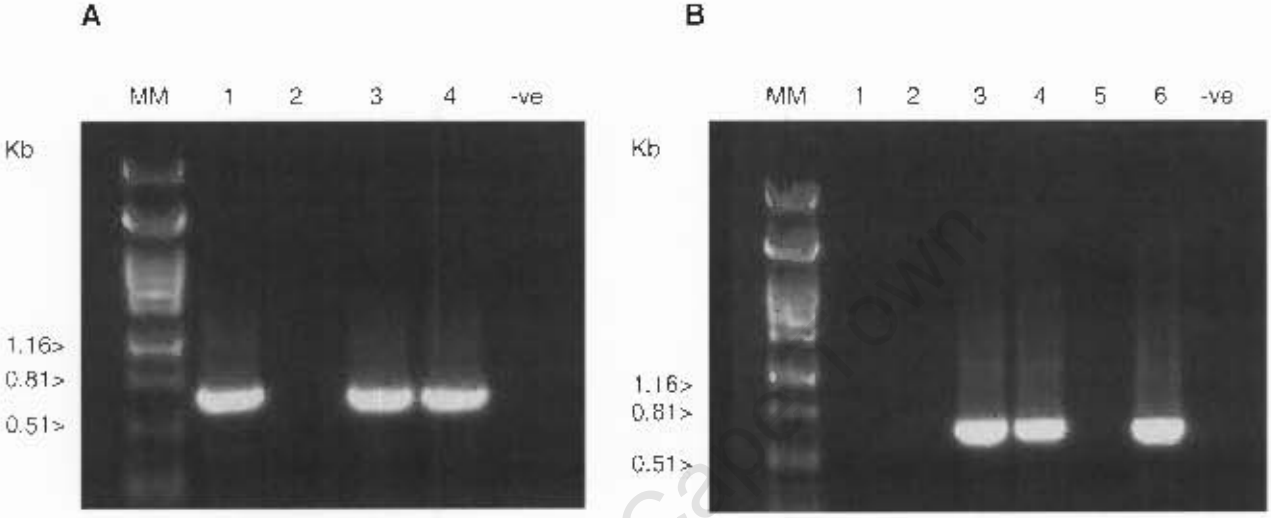

Figure 2.6. PCR screening of human and rat N-terminal GR^{526} constructs. FoxG1-BamH1 specific forward and GR^{526} specific reverse primers were used to screen constructs for pG1-hBF1GR^{526} (A), and pG1 rBF1GR^{526} (B). MM: molecular weight marker (λDNA/PstI), applicable fragment sizes (Kb) are shown alongside. -ve: negative PCR control, including PCR grade water as the template. (A) Samples 1, 3 and 4 show positive PCR products, and thus the desired human FoxG1 N-terminal GR^{526} construct. (B) Samples 3, 4 and 6 show positive PCR products, the desired rat FoxG1 N-terminal GR^{526} construct. Sample 2 (A) and samples 1, 2 and 5 (B) show no PCR product, and therefore do not include the FoxG1 N-terminus and GR^{526} in the correct orientation. The GR^{526} specific reverse primer was designed 222 bp downstream of the start codon, thus the human PCR product is 738 bp in size and the rat 711 bp.

2.3.3. β-galactosidase assay in yeast – the FoxG1 N-terminal domains are able to confer upon GR^{526} a change in conformation

Following plasmid construction and verification via sequencing (see supplementary data, Fig. S1 and Fig. S2), the rat and human NFoxG1:GR^{526} constructs were transformed into wildtype yeast cells, with the GR^{526} regulated β-galactosidase plasmid pL2/GZ to screen whether they could induce a conformational switch on β-galactosidase (Table 2.3). In the assay, pG1-GR^{526}

was used as a negative control and pG1-NMGR^{526} was used as a positive control for prion induced conformational change (Fig. 2.2). The transformed yeast colonies were replica plated onto X-gal media, following growth on –leu –trp dropout media, to determine the colour of the colonies.

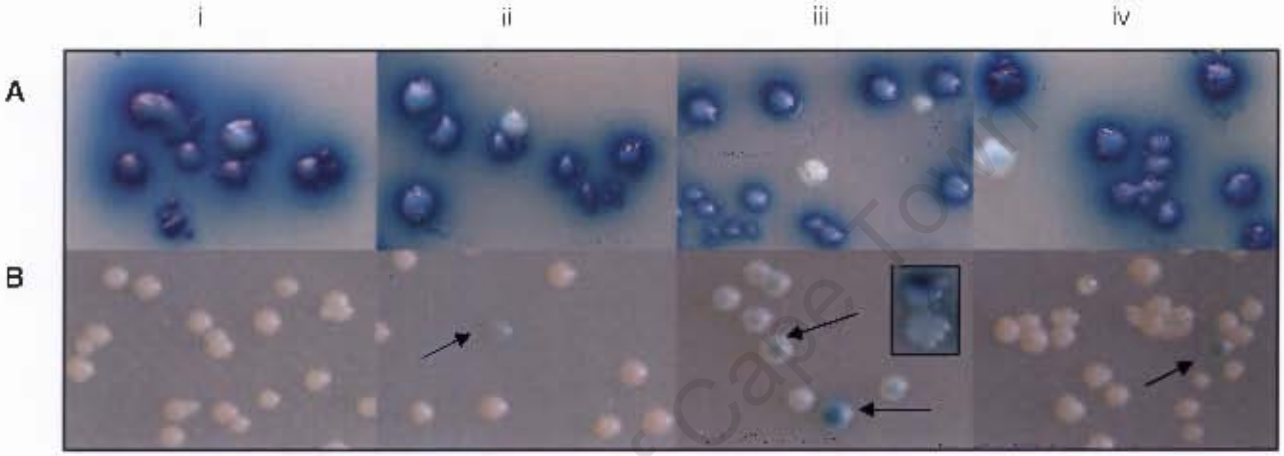

Figure 2.7. Analysis of colony colour when plated on X-gal media. (A) Colonies produced when first plated on X gal media. (B) Colonies produced following replating of white colonies on X-gal media. (i) pG1-GR^{526}, the GR^{526} control construct, produced blue yeast colonies and one white colony, which upon replating never reverted back to blue. (ii) pG1-NMGR^{526}, the positive prion control, produced white colonies, which were able to revert back to blue upon replating (arrow). (iii) pG1-hBF1GR^{526}, the human construct, produced both blue and white colonies, which reverted back to blue (arrows). Human mosaic colony shown as insert. Both the percentage of cells converting from blue to white, and white to blue, was much higher than those of the rat construct. (iv) pG1-rBF1GR^{526}, the rat construct, produced blue and white colonies and replating white colonies resulted in a small percentage of them reverting back to blue (arrow).

The control vectors produced the expected results. Yeast transformed with pG1-GR^{526} produced blue colonies and only one white colony (0.03%). This colony did not revert back to blue upon replating (Fig. 2.7. i and 2.8). The cells transformed with pG1-NMGR^{526} produced blue colonies, and white colonies (0.74%). 0.03% of white colonies reverted back to blue, when replated (Fig. 2.7. ii, Fig. 2.8). The human construct produced the most intriguing results, when transformed into yeast. 25.29% of the blue colonies converted to white colonies,

with 10.78% of the white colonies reverting back to blue, following replating (Fig. 2.7. iii and 2.8).

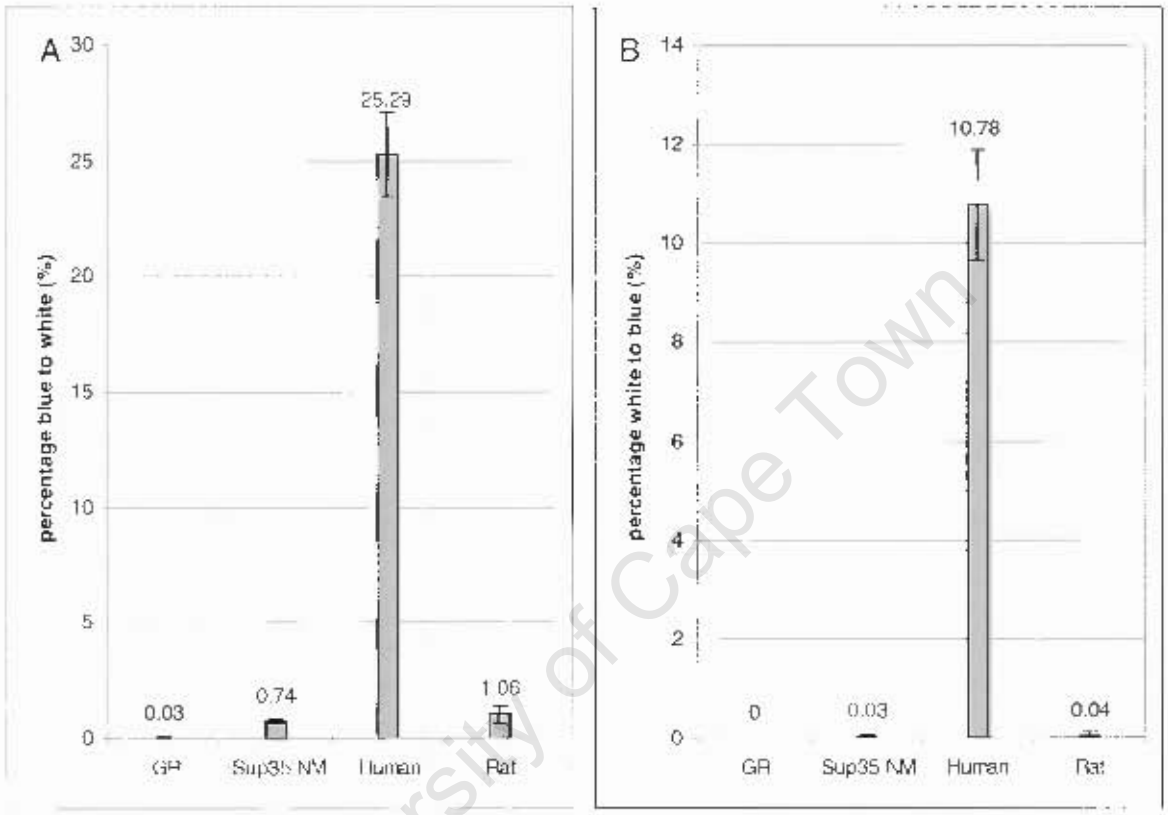

Figure 2.8. The percentage of cells converting from blue to white, and white back to blue, transformed with various GR^{526} constructs. (A) In the first plating, varying percentages of blue yeast colonies converted to white colonies, depending on the GR^{526} construct. The percentage of white cells produced by GR^{526} was negligible. The Sup35 NM and rat constructs behaved in the same manner, producing 0.74 and 1.06% white colonies respectively. The human construct produced the highest percentage of white colonies from blue colonies, at 25.29%. (B) Upon replating, fewer white colonies gave rise to blue colonies. The one white colony isolated from the GR^{526} transformed cells did not revert back to blue. The human construct produced 10.78% blue colonies, again far higher than the 0.04 and 0.03% observed for the rat and NM constructs respectively. Error bars show standard deviation of the samples. For each of the controls and the rat and human NHoxGI constructs, three individual transformants were plated in triplicate. Approximately 1000-1500 cells were counted per transformant.

A number of human colonies also appeared to be 'mosaic' colonies, which were made up of both blue and white cells, and thus displayed both colours (Fig. 2.7. iii). These results suggest

that the human construct changed conformation at a high rate, switching to and from the aggregated inactive GR^{526} state, to the soluble active state. The rat construct pG1-rBF1GR^{526}, produced similar results to the positive prion control, with 1.06% converting from blue to white, replating the white colonies produced fewer blue colonies (0.04%) (Fig. 2.7. iv and 2.8).

2.3.4. Cloning of the N-terminal domains into the GFP plasmid, p2µGFP

The N-terminal domains of the rat and human FoxG1 orthologues were cloned into the vector p2µGFP in order to determine whether the regions were able to form aggregates *in vivo*. The N-terminal domains of rat and human FoxG1 were amplified by PCR with FoxG1 specific

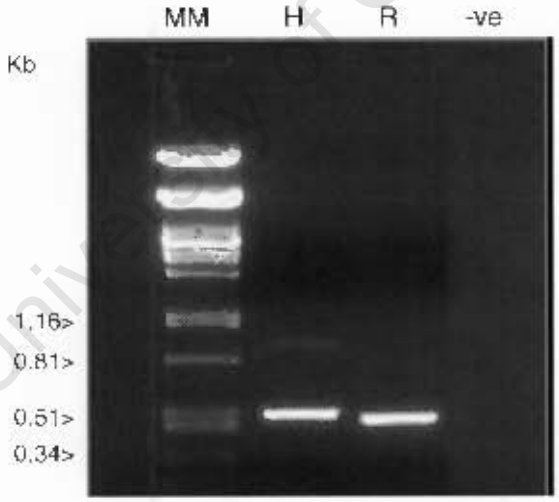

Figure 2.9. PCR amplification of the rat and human FoxG1 N-terminal domains. FoxG1 specific primers were used, which were designed to enable the addition of BamH1 restriction enzyme sites on the 5' and 3' ends. MM: molecular weight marker (λDNA/PstI), applicable fragment sizes (Kb) are shown alongside. H: human N-terminal domain, 519 bp. R: rat N-terminal domain, 492 bp. –ve: negative PCR control, including PCR grade water as the template.

primers (Table 2.2). The primers were designed to construct BamH1 restriction enzyme sites, on the 5' and 3' ends, to enable cloning into the plasmid p2µGFP. The amplified PCR

products (Fig. 2.9) were cloned into the p-drive vector, before being sub-cloned into the p2μGFP plasmid.

The N-terminal domain fragments were subcloned into the vector p2μGFP, via digestion with the restriction enzyme BamH1. Both the plasmid p2μGFP and the inserts were digested with BamH1 at the 5' and 3' ends, and colony PCRs were performed to identify clones in which the N-terminal domains were in the desired orientation, i.e. in the same orientation as GFP. A GFP specific reverse primer and the BF-1-BamH1 forward primer were used in the PCR screening (Table 2.2, Fig. 2.10). PCR products were detected when constructs included the NFoxG1 domains, and the region was fused in frame to GFP (Fig. 2.11). The plasmid p2μGFP was used as a soluble GFP control *in vivo*.

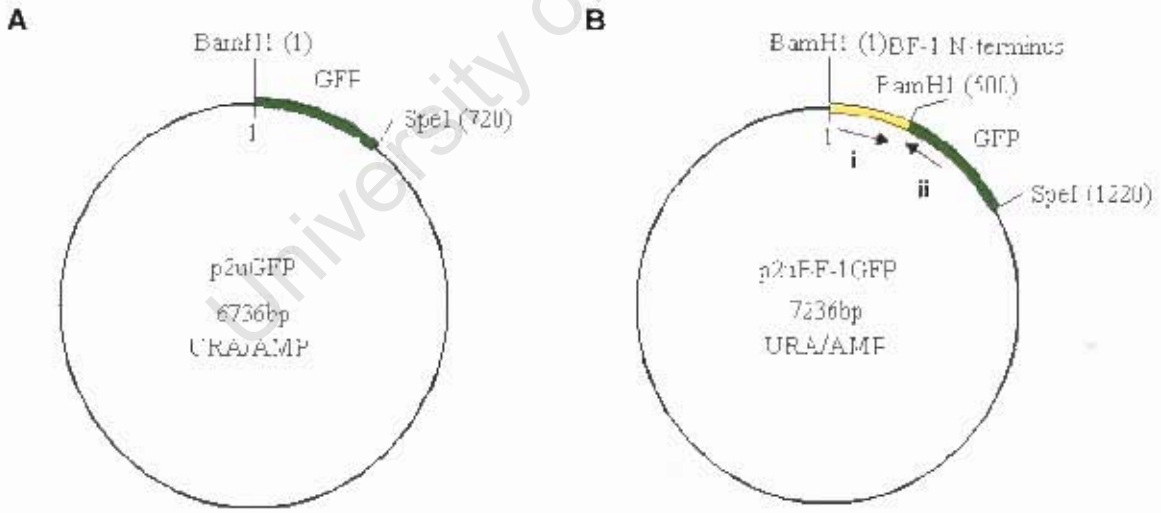

Figure 2.10. Plasmid maps of the constructs used in the GFP assay. (A) The plasmid p2μGFP was used as a soluble GFP control. (B) The rat and human FoxG1 N terminal domains were cloned into the GFP plasmid, producing the two p2μ-BF1GFP vectors. FoxG1 (i) and GFP (ii) specific primers (not to scale) were used to select the desired constructs. The position of the restriction enzyme recognition sites are shown, as are the selectable markers specific to the plasmid.

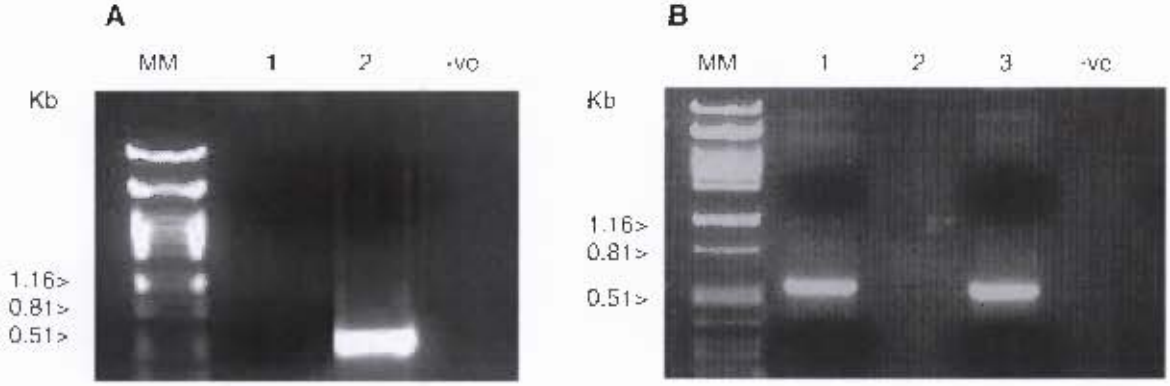

Figure 2.11. PCR screening of human and rat N-terminal GFP constructs. FoxG1 specific forward and GFP specific reverse primers were used to screen constructs for p2μ-rGFP (A), and p2μ-hGFP (B). MM: molecular weight marker (λDNA/PstI), applicable fragment sizes (Kb) are shown alongside. –ve: negative PCR control, including PCR grade water as the template. (A) Sample 2 shows a positive PCR product of 513 bp, matching the predicted size of the rat N-terminal GFP construct in correct orientation. (B) Samples 1 and 3 show positive PCR products of 540 bp, matching the predicted size of the human N-terminal GFP construct. Sample 1 (A) and sample 2 (B) show no PCR product and therefore do not include the FoxG1 N-terminal domains in the correct orientation.

2.3.5. GFP assay in yeast – the FoxG1 N-terminal domains aggregate *in vivo*

Sequencing of the constructs confirmed that the NFoxG1 domain inserts were in the correct orientation and that no mutations had occurred during the process of cloning (Fig. S3 and S4, supplementary data). The rat (p2μ-rGFP) and human (p2μ-hGFP) constructs were transformed into wildtype yeast, as was the control plasmid p2μGFP. Live yeast cells were viewed under the fluorescent light microscope. Untransformed wildtype yeast cells were also viewed to determine whether the yeast cells contained any intrinsic auto-fluorescence (Fig. 2.12-14).

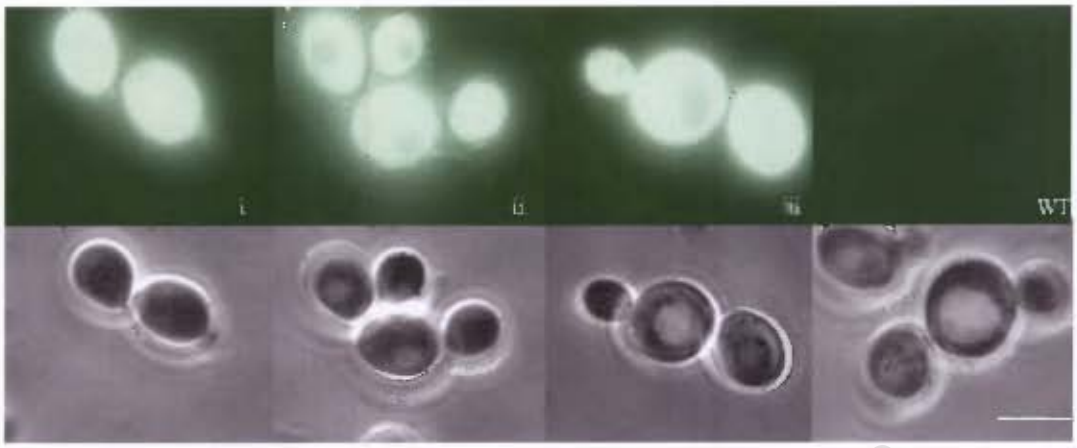

Figure 2.12. Fluorescent and light microscopy of GFP transformed yeast cells. Fluorescent microscopy images are displayed above light microscopy images of the same cells. GFP fluorescence in cells transformed with the control plasmid, p2μGFP, is soluble (i-iii). WT: untransformed wildtype yeast displays no intrinsic fluorescence. Scale bar shows 3 μm.

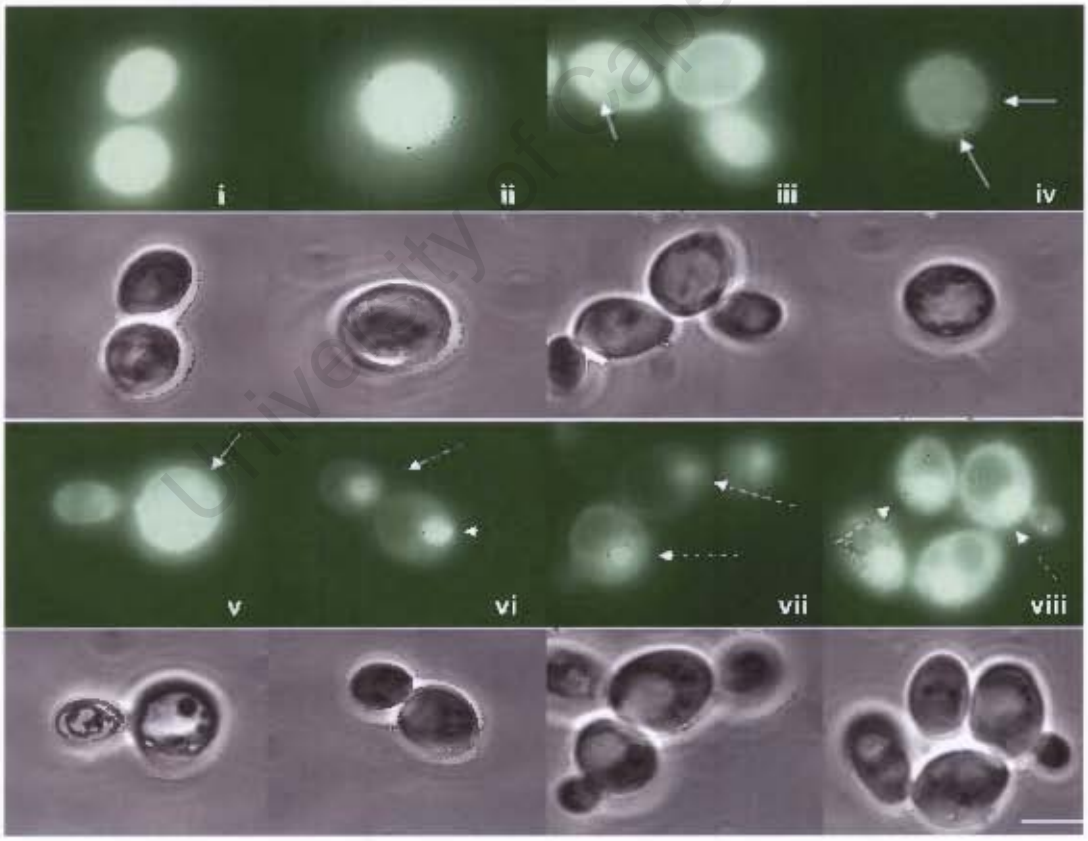

Figure 2.13. Fluorescent and light microscopy of yeast transformed with the human GFP construct. Yeast transformed with the human construct, p2μ-hBF1GFP, contained both soluble (i-ii) and aggregated GFP (iii-viii). Aggregated GFP was visible in both small (solid arrows) and large (broken arrows) aggregates, which were present in recently budded cells groups (vi-viii). In many of the cells containing aggregated GFP, the background soluble GFP was faint, relative to the soluble GFP seen in Fig 2.12. Scale bar shows 3 μm.

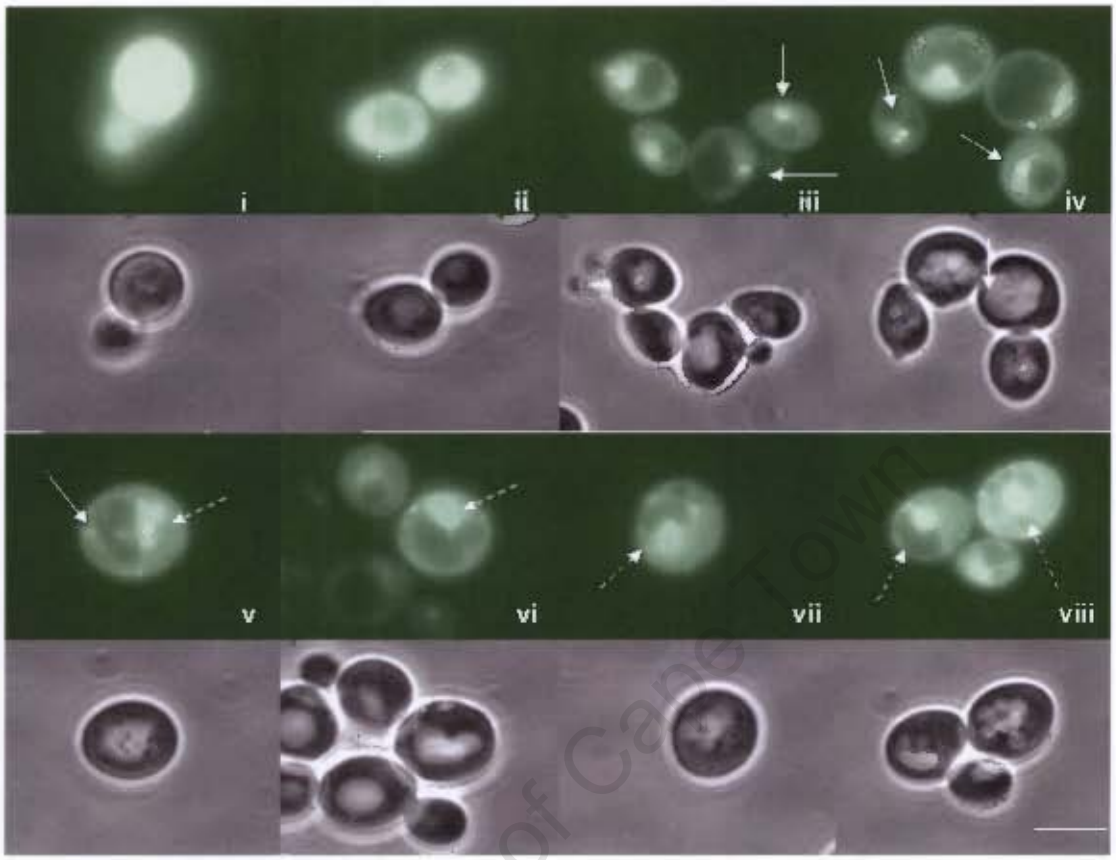

Figure 2.14. Fluorescent and light microscopy of yeast transformed with the rat GFP construct. Fluorescent microscopy images are displayed above the light microscopy images of the same cells. Yeast transformed with the rat construct, p2μrBFtGFP, contained both soluble (i-ii) and aggregated GFP (iii-viii). Aggregated GFP was visible in both small (solid arrows) and large (broken arrows) aggregates, which were present in recently budded cells groups (iii, iv and viii). In many of the cells containing aggregated GFP, the background soluble GFP was faint, relative to the soluble GFP seen in Fig 2.12. Scale bar shows 3 μm.

Fluorescent microscopy revealed that the yeast cells transformed with the control GFP plasmid p2μGFP contained soluble GFP (Fig. 2.12). The experimental plasmids on the other hand, seemed to contain both soluble and aggregated GFP (Fig. 2.13 and 2.14). The aggregates were present in various sizes, similar to those resulting from other prion domains, such as Sup35 NM domain (Patino *et al.*, 1996, Si *et al.* 2003). Aggregates of similar sizes were visible in recently budded cell groups, and in cells undergoing mitosis. Background

fluorescence was visible within the cells displaying aggregates; however the intensity of the fluorescence differed, from bright to relatively faint.

2.4. Discussion

Possible prion-like properties of the rat and human FoxG1 N-terminal domains were investigated, using two assays originally designed for yeast prions, and subsequently used to investigate the *Aplysia* CPEB protein (Li and Lindquist, 2000, Patino *et al.*, 1996, Si *et al.*, 2003). The N-terminal FoxG1 domains were of particular interest due to the unusual amino acid composition, including poly (H), poly (Q) and poly (P) tracts, which differed between the rat and human FoxG1 orthologues, as well as many glycine and alanine amino acid residues. Prion proteins frequently contain tracts of single amino acid residues, for example poly (Q) and poly (N), in their N-terminal sequences, as well as oligopepetide repeat sequences (Shorter and Lindquist, 2005 and Si *et al*, 2003). The rat and human orthologues were chosen for this study to investigate whether the differences in composition of their N-termini, namely the insertion of poly (P) tracts seen in the human sequence and absent in the rat, correlates with the differences in their prion-like properties.

In comparison to the remainder of the proteins, the N-terminal domains of prions often display high levels of conformational flexibility (Derkatch *et al.*, 2004, Shorter and Lindquist, 2005). The NFoxG1 domains of FoxG1 orthologues (human, rat and *Xenopus*) were found to be intrinsically unfolded protein sequences (Fig. 2.4). When compared to the DNA binding and C-terminal domains, conserved regions of the orthologues capable of folding into predictable secondary structures, the NFoxG1 domains showed high conformational flexibility. The human N-terminal sequence displayed the greatest level of conformational

flexibility, the amino acid sequence showed a sustained disorder tendency greater than 0.9, with a large domain of amino acids showing a maximum disorder tendency of 1.0. However, while reaching the maximum disorder tendency of 1.0, the rat and *Xenopus* NFoxG1 domains showed increasingly lower levels of disorder, with an even greater number of residues in the *Xenopus* sequence reaching only the 0.9 mark. A brief dip in the disorder tendency in the rat sequence and an expanded one in the *Xenopus* sequence corresponded to the differences in the sequences when compared to the human NFoxG1 domain. The position of the dips corresponded to those amino acids absent in the rat and *Xenopus* sequences consisting of poly (P) and poly (P/Q) tract insertions in the human sequence, respectively (Fig. 1.2, 2.4). These results show that the greater the number of proline and glutamine amino acid residues in the poly (P/Q) tracts, the greater the conformational flexibility of the NFoxG1 region, as seen in the brief dip in the rat sequence, when lacking six proline residues, and the larger dip in the *Xenopus*, when lacking a 27 residue tract present in the human sequence. This initial result provided further motivation to investigate possible prion-like properties of the N-terminal domains of FoxG1 orthologues and compare the possible differences between them, corresponding with the differences in their amino acid sequences.

Prion-like properties of the N-terminal domains of FoxG1 orthologues were investigated by fusing these domains to a constitutively active rat glucocorticoid receptor. The assay was used to determine whether the N-terminal domains are able to confer upon another protein a change in conformation. The rat NFoxG1:GR^{526} constructs behaved in a similar manner to the prion control plasmid, consisting of the N-terminal domain (NM) of the yeast prion determinant Sup35. Although the GR^{526} protein was in the active conformation in the majority of the colonies; a small percentage of the yeast transformed with the rat and NM

constructs showed a switch to an inactive GR^{526} conformation (Fig. 2.7, 2.8). Upon replating, the inactive conformation was seen to be inherited by daughter cells, but on occasion would revert back to the active state. The human NFoxG1:GR^{526} construct had different properties: the GR^{526} protein present in the yeast transformed with the human construct was also able to exist in both the active soluble state, as well as the inactive, aggregated state. However, the percentage of conversion between the two states was higher, in comparison to the rat and NM constructs. The presence of blue and white mosaic colonies implied that the percentage of cells converting was so high, that even in single colonies, the cells contained both active and inactive GR^{526} conformations. Cells transformed with the GR^{526} construct produced only one white colony, which did not revert to the active conformation. It is suggested that this white colony was a result of a spontaneous mutation in the GR^{526} protein, rather than spontaneous amyloid formation.

The N-terminal domains of rat and human FoxG1 orthologues were able to form aggregates *in vivo*. Cloning the NFoxG1 regions into a GFP plasmid allowed the visualization of these aggregates using fluorescent microscopy. GFP was soluble *in vivo* and was not seen to aggregate within the cells (Fig. 2.12). The rat and human FoxG1 N-terminal domains, were however able to induce aggregation of the GFP within the yeast (Fig. 2.13, 2.14). Both large and small aggregates were visible, as well as soluble protein. The presence of GFP aggregates of similar sizes in recently divided cell groups, and in budding daughter cells confirmed the heritability observed in the β-galactosidase assay. The percentage of yeast cells containing aggregated GFP was similar for the rat and human NFoxG1 constructs, although no actual quantification was performed. In a number of the cells containing aggregated GFP, the background soluble GFP was faint relative to other cells. Krishnan and Lindquist (2005)

investigated the formation of prion fibres by the Sup35 prion determinant and suggested that prior to prion fibre formation, protein conformation is lost and the protein is temporally present in a molten, unstructured form. It is suggested that these lower levels may also be a result of the accumulation of similarly unstructured or molten GFP, which was present in anticipation of adding to the already present aggregates, as the fluorescence of GFP depends on properly formed tertiary structure (Patino *et al.*, 1996). Alternatively, the lower levels of background soluble GFP, seen in cells with aggregated GFP, could be a result of the depletion of soluble protein due to aggregate formation.

Thus, the human and rat orthologues of FoxG1 share a number of traits with known prions: their N-terminal domains are unstructured, and contain tracts of amino acid residues, namely proline, glutamine and histidine, and the domains are able to confer a conformational change in other proteins, which is heritable. The human and rat NFoxG1 domains were also able to form aggregates *in vivo*. As previously discussed, not all proteins which are able to exist in distinct conformational states are prions: prions are proteins capable of infectious fibre formation (Shorter and Lindquist, 2005). Although the aggregates present in yeast cells in this chapter were seen to be heritable, the results are preliminary and do not confirm infectivity. In the next chapter, the physical properties of the conformational change in the GR^{526} protein are characterized, and the transmissibility of the aggregated form determined.

CHAPTER 3

Characterization of the prion-like properties of the N-terminal of FoxG1

3.1. Introduction

In the previous chapter, it was shown that the N-terminal domains of the rat and human FoxG1 transcription factors were able to confer upon the glucocorticoid receptor protein a change in conformation. In the β-galactosidase assay, the NFoxG1 domains were able to alter the conformation of the GR^{526} protein, rendering it inactive and resulting in white yeast colonies. It was hypothesized that the white colonies seen in the assay were a result of one of three distinct mechanisms, namely a reduction in GR^{526} expression levels, a mutation in the GR^{526} protein, or amyloid formation, whether prion or non-prion amyloid based. In this chapter, these possibilities were investigated using several diagnostic tests for prion proteins.

Western blot analysis was performed in order to determine whether the GR^{526} protein was expressed at similar levels in the blue and white colonies seen in the β-galactosidase assay. Previous research on the *Aplysia* CPEB protein has shown that the protein is able to alter the conformation of the GR^{526} protein in the β-galactosidase assay, resulting in white yeast colonies in which the GR^{526} protein is expressed at similar levels, when compared to protein extracted from blue colonies (Si *et al.*, 2003).

Subsequent investigation into whether the white yeast colonies seen in the β-galactosidase assay were due to a mutation in the GR^{526} protein was performed by growth on guanidinium hydrochloride. Guanidinium hydrochloride (GuHCl) is a non-mutagenic protein denaturant,

which has been shown to cure prion fibre formation (for example *Ap*CPEB, Sup35 NM domain and [URE3]) when present in low concentrations, while proteins in which a mutation has occurred are not cured (Chernoff *et al.*, 2002, Li and Lindquist, 2000, Si *et al.*, 2003, Wickner, 1994). The ability of GuHCl to cure a conformational change suggests a possible infectious prion-based mechanism, opposed to a non-prion amyloid mechanism (Chernoff *et al.*, 2002). Curing by GuHCl is not caused by denaturation of the prion proteins; as such low concentrations are used. Rather, curing results from the repression of prion fibre proliferation in dividing cells. Thus, several generations of growth on GuHCl are required to cure a prion state, as the preexisting prion aggregates are diluted sufficiently amongst progeny, but are unable to self propagate. In this study, white colonies transformed with the human and rat NFoxG1:GR^{526} constructs were grown on GuHCl supplemented media and the colour of the progeny determined.

Thirdly, evidence that the inactive state of the GR^{526} protein was a result of aggregate formation was obtained by examining the sedimentation rates of the protein when extracted from blue and white colonies. Previous studies have shown that the aggregated state of a prion protein sediments at a different rate than the soluble protein, being detectable in lower fractions on a sucrose gradient (Chernoff *et al.*, 2002, Si *et al.*, 2003). For example, the soluble state of the *Aplysia* CPEB protein was detected in fractions five and six, when an ultracentrifuged sucrose gradient was fractionated and numbered from the top downwards. The amyloid state of the protein was however detected in fractions nine and ten (Si et al., 2003). Thus, the sedimentation rates of the GR^{526} proteins in white and blue colonies were investigated in this study, providing further evidence to support the presence of the aggregates seen in the GFP assay (Chapter 2).

In the event that the inactive state of the GR^{526} protein was found to result from an alternative conformation, the mechanism of aggregate formation would be determined, whether prion or non-prion based. As previously discussed, prions are proteins capable of infectious, self-perpetuating amyloid formation (Prusiner, 1998). However, amyloid forming proteins do occur naturally, which are not infectious and are not considered prions (Shorter and Lindquist, 2005). For example, Alzheimer disease results from amyloid formation in brain tissue, resulting from poly-glutamine tract insertion in the β-amyloid precursor protein (βAPP), but the disease is not infectious (Checler and Vincent, 2002). Yeast mating experiments can be used to establish whether a suspected prion-like conformational change *in vivo* is transmissible (or infectious). Yeast cells can either be diploid or haploid, with haploid cells being either of two mating types, namely alpha (α) and a-types. An assay has been developed, in which blue and white α and a-type cells from the β-galactosidase assay are mated. If the inactive prion-like state of the protein is infectious, the progeny will be white in colour (Chernoff *et al.*, 2002). This assay has been used successfully to demonstrate the infectivity of the *Aplysia* CPEB protein (Si *et al.*, 2003) and the Sup35 NM domain (Li and Lindquist, 2000).

In order to perform the yeast mating experiment, the rat and human NFoxG1:GR^{526} domains were sub-cloned into the pYES2 yeast vector and transformed into the a-type yeast. The original plasmid constructs used in the β-galactosidase assay were transformed into an α-mating type yeast strain. In order to establish whether the change in conformation was transmissible to uninfected cells, white yeast colonies, containing the inactive GR^{526} conformation, were mated to blue colonies and the colour of the progeny determined (Fig. 3.1). The Sup35 NM domain provided a convenient prion control.

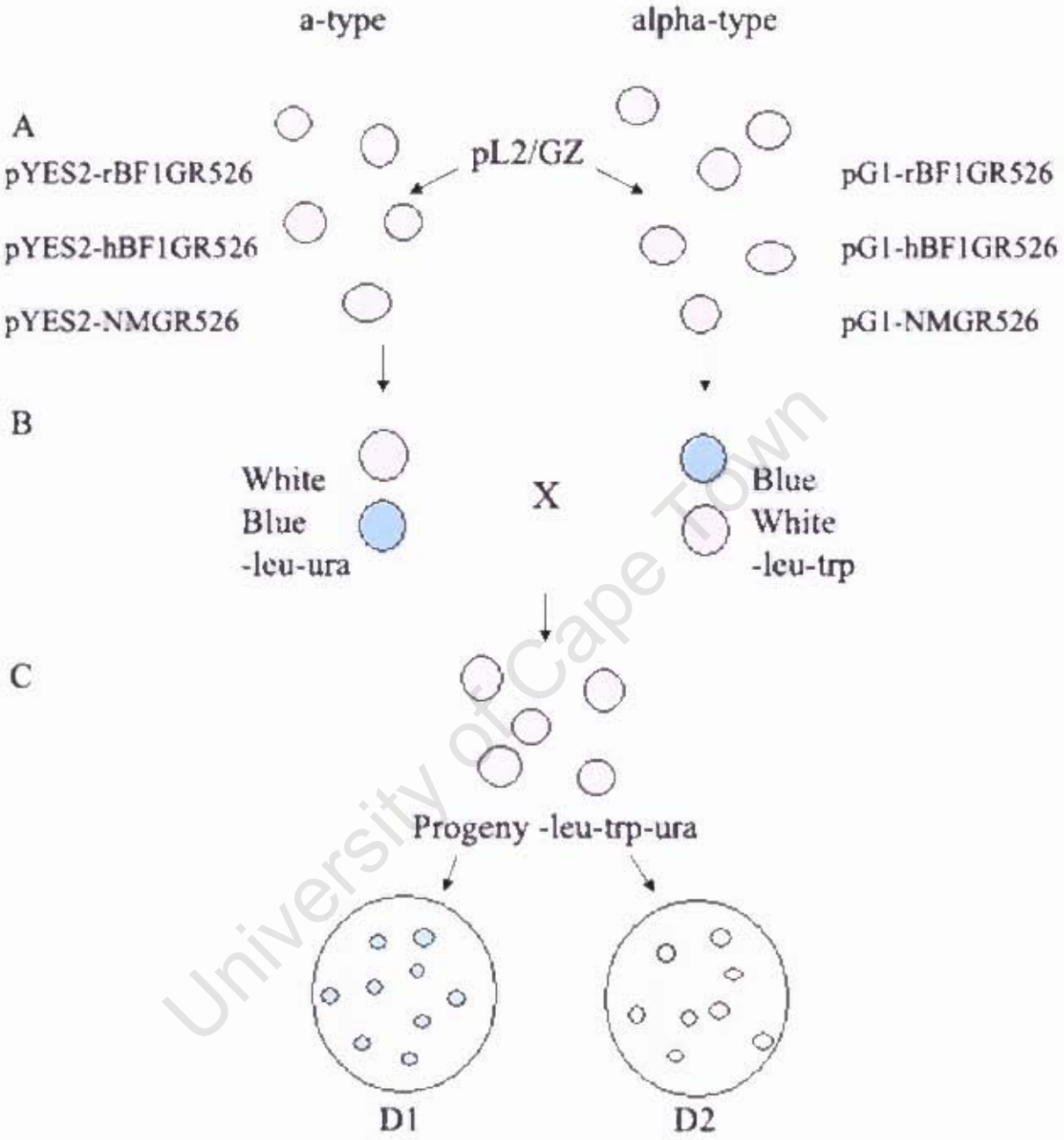

Figure 3.1. Yeast mating experiment to determine whether the inactive GR^{526} state is transmissible. (A) a-type yeast cells were transformed with the NFoxG1:GR^{526} and NM:GR^{526} pYES2 constructs and pL2/GZ (the GR regulated β-galactosidase reporter). α-type cells were transformed with the original GR^{526} based constructs, namely pG1-rBF1GR^{526}, pG1-hBF1GR^{526} and pG1-NMGR^{526}, and pL2/GZ. (B) The colours of the transformed cells were determined, and white and blue colonies from the corresponding human, rat, or NM plasmids were mated. (C) Diploid progeny were selected for on triple dropout media, and the colour of the colonies determined by growth on X-gal supplemented media (D). The diploid colonies could either be blue (D1) if the inactive GR^{526} conformation is not transmissible, or white (D2), if it is. The cells transformed with the NM plasmids, when mated, were expected to produce white colonies, as NM is the N-terminal domain of a known prion.

3.2. Materials and methods

3.2.1. Total protein extraction from yeast

Total cellular proteins were extracted from blue and white yeast cells transformed with either pG1-hBF1GR^{526} or pG1-rBF1GR^{526}, blue cells transformed with pG1-GR^{526}, used as a control for the active conformation, as well as untransformed wildtype cells, used as a negative control. Cells were harvested from overnight 50 ml YPD cell cultures, inoculated with either a blue or white colony (OD_{600nm} = 0.4-0.6), by centrifugation for 5 min, at 3000 rpm at 4 °C. Cells were washed once in ice cold sterile 1 X PBS, and harvested once again. Cell pellets were frozen in liquid nitrogen, and stored at -80 °C until proteins were extracted. Total cellular protein was extracted using the TCA method described in the Clonetech Yeast Protocols Handbook (2001), with the exception of the composition of the TCA buffer (20 mM tris-HCl pH8, 50 mM ammonium acetate, 2 mM EDTA). Protein concentrations were determined using the Bio-rad protein assay kit II (Bio-rad), according to manufacturer's instructions. The following standard concentrations of BSA were used as reference samples: 5, 10, 20, 30, 40 and 60 µg/ml.

3.2.2. Western blot analysis

Prior to SDS-PAGE, samples were boiled for 3 minutes in 1 X sample application buffer. 20 µg of each sample was electrophoresed on a 5% acrylamide stacking gel, and a 12% acrylamide separating gel, at 95 V. SDS-PAGE low range standards were used as molecular weight size markers (Bio-rad). Following electrophoresis, proteins were transferred in a tank transfer system overnight to a protran nitrocellulose transfer membrane (Schleicher & Schuell Bioscience), at 30 V. Membranes were subsequently stained with Ponceau S (Sigma), to confirm adequate transfer. The membranes were blocked by incubation in 5% skim milk in 1

X TBS, overnight at 4 °C. The membranes were incubated with primary antibodies in 2.5% skim milk in 1 X TBS, for four hours (Ausubel *et al.*, 2001). One membrane was hybridized with 0.5 µg/ml Rabbit polyclonal GR specific antibody (Abcam, ab3579), while the other was hybridized with 0.5 µg/ml Rabbit polyclonal GAPDH specific HRP conjugated antibody, used as a control (Abcam, ab9385). Following incubation with the primary antibodies, the membranes were washed in 1 X Wash Solution, provided with the LumiGLO Reserve Chemiluminescent Substrate Kit, according to the manufacturer's instructions (KPL). The membrane incubated with the GR specific primary antibody was subsequently incubated for one hour with 0.05 µg/ml goat anti-rabbit IgG secondary antibody (KPL), in 2.5% skim milk in 1 X TBS. All of the membranes were washed in 1 X Wash Solution, and exposed to the luminol-based chemiluminescent substrate, using the LumiGLO Reserve Chemiluminescent Substrate Kit, according to the manufacturer's instructions (KPL). Following exposure to the substrate, the membranes were exposed to Super RX medical X-ray film (Fuji) for 3-30 seconds, placed in developer (AGFA) for 1-2 minutes, rinsed in water and placed in rapid fixer (AGFA) for 2 minutes.

3.2.3. Growth of yeast on GuHCl supplemented media

White yeast cells transformed with either pG1-hBF1GR^{526}, pG1-rBF1GR^{526}, pG1-NMGR^{526} or pG1-GR^{526} and simultaneously with the pL2/GZ construct were grown on YPD media supplemented with 5 mM guanidinium-hydrochloride (GuHCl). Small amounts of overnight liquid cultures, inoculated with white yeast cells, were patched onto YPD GuHCl agar plates and incubated at 30 °C until the patch of colonies appeared. Following growth, the colonies were velvet replica plated onto fresh YPD GuHCl agar plates. This process was repeated three times, allowing the cells to have three consecutive passages on YPD with GuHCl (Chernoff *et*

al., 2002). Following growth on the YPD GuHCl agar plates, individual colonies were streaked out on YPD GuHCl agar, and subsequently patched onto solid X-gal supplemented dropout media to determine the state of the GR^{526} protein within the cells. Three individual transformants for each of the GR^{526} based constructs were assayed in triplicate.

3.2.4. Preparation of total cell lysates

Overnight YPD cultures were inoculated with yeast from either blue or white colonies transformed with the plasmids outlined in Table 3.1. Total cell lysates were prepared from the 100 ml cultures of the yeast, using the method outlined in Si *et al.* (2003). Cells were harvested by centrifugation at 3000 rpm, for 5 minutes at 4 °C. The yeast cells were washed once in 1 X PBS, and resuspended in 500 µl lysis buffer (Si *et al.*, 2003). Cells were broken with 500 µl glass beads (Sigma), by vortexing for 10 min at 4 °C. Samples were centrifuged for 20 minutes, 13 000 rpm at 4 °C, to eliminate cell debris. Protein concentration was determined as previously described (Chapter 3.2.1).

Table 3.1. Cell lysate preparations were collected from various transformed yeast cells.

Cell lysate preparations	Control or experimental
Blue pG1-hBF1GR^{526} & pL2/GZ	Human N-terminal experimental
White pG1-hBF1GR^{526} & pL2/GZ	Human N-terminal experimental
Blue pG1-rBF1GR^{526} & pL2/GZ	Rat N-terminal experimental
White pG1-rBF1GR^{526} & pL2/GZ	Rat N-terminal experimental
Blue pG1-NMGR^{526} & pL2/GZ	Positive prion control
White pG1-NMGR^{526} & pL2/GZ	Positive prion control
Blue pG1-GR^{526} & pL2/GZ	GR control

3.2.5. Sedimentation of proteins on sucrose gradients

Following preparation of cell lysates, approximately 1 mg of protein from each sample was loaded onto a 2 ml sucrose gradient. The sucrose gradients consisted of 1.5 ml 30% (weight/volume) sucrose in lysis buffer, layered above 0.5 ml 40% sucrose in lysis buffer (Si *et al.*, 2003). The sucrose gradients were centrifuged using the Beckman SW65i rotor for 1.5 hours, at a speed of 40 000 rpm at 4 °C. Following centrifugation, 200 µl fractions were collected from the top of the gradients, numbered from one to ten from the top downwards, and stored at -80 °C prior to western blot analysis.

3.2.6. Western blot analysis of sucrose gradient fractions

Following collection of the sucrose gradient fractions, 20 µl of the fractions numbered two to ten were electrophoresed via SDS-PAGE, as previously described. Each of the sucrose gradients (fractions two to ten) was electrophoresed on a separate 10% acrylamide gel. Western blots were performed as described in 3.2.2, with incubation of all of the membranes with the GR specific primary antibody. Detection of the GR^{526} protein was performed; the membranes were subsequently stripped (Ausubel *et al.*, 2001) and the western blots repeated with the GAPDH specific antibody.

3.2.7. pYES2 based plasmid construction and screening, for yeast mating experiments

In order to sub-clone the rat and human NFoxG1:GR^{526} and the NM:GR^{526} domain into the pYES2 vector (Invitrogen), the pYES2 plasmid, pG1-$NMGR^{526}$, pG1-$rBF1GR^{526}$ and pG1-$hBF1GR^{526}$ were digested overnight at 37 °C, with the restriction enzyme BamH1. 50 µl digests were performed using 0.1 U BamH1 per 1 µg DNA, including 1 X Buffer Green (Fermentas). Digested DNA was electrophoresed on a 1.2% Agarose gel, and the desired

fragments excised under longwave UV light. The excised fragments were purified using the QIAquick Gel Extraction Kit (Qiagen) according to the manufacturer's instructions. Approximately 150 ng insert DNA and 50 ng plasmid DNA were ligated in a 20 µl reaction, including 400 U T4 DNA Ligase (New England Biolabs) and 1 X Reaction Buffer. The ligation reactions were incubated at room temperature overnight and subsequently transformed into *E. coli* DH-5α competent cells (Chung and Miller, 1988). Following transformation, colonies were screened by PCR, to determine the orientation of the inserts within the pYES2 vector. 0.5 µl of overnight liquid cultures were used as template. The reaction mix and cycling parameters are the same as those described in 2.2.4, with an annealing temperature of 50 °C. A GR^{526} specific reverse primer was used (Table 2.1); with a T7 specific forward primer with the following sequence: 5' TAA TAC GAC TCA CTA TAG GG 3', T_m 46 °C. PCR products were visualized by electrophoresis on a 1.2% Agarose gel. Plasmid DNA from selected positive colonies was purified using the High Pure Plasmid Isolation Kit (Roche), according to the manufacturer's instructions and sequenced using the forward and reverse primers used for PCR screening.

3.2.8. Yeast transformation

The following yeast strains were used for this study: W303-1B (α, *leu2-3, leu2-112, trp1-1, ura3-1, his3-11, his3-15, ade2-1, can1-100*) and W303-1B/A (a, *ade2-1, ura3-1, his3-11, his3-15, leu2-3, leu2-112, trp1-1, can1-100*). Following sequencing and selection of plasmids, yeast cells were transformed with the plasmid constructs by electrophoration (Ausubel *et al.*, 2001). The a-mating type strain W303-1B/A was transformed with either pYES2-$hBF1GR^{526}$, pYES2-$rBF1GR^{526}$, or pYES2-$NMGR^{526}$ and simultaneously with pL2/GZ, and cultured on selective media (Table 3.2). While the α-type strain W303-1B was transformed with either

pG1-hBF1GR^{526}, pG1-rBF1GR^{526}, or pG1-NMGR^{526} and simultaneously with pL2/GZ, and cultured on selective media.

Table 3.2. Individual transformation of plasmids into yeast, selective media used, purpose of transformation (control or experimental), and yeast mating type.

Plasmids transformed	Selective media	α/a	Control or experimental
pG1-hBF1GR^{526} and pL2/GZ	-leu -trp	α	Human N-terminal experimental
pG1-rBF1GR^{526} and pL2/GZ	-leu -trp	α	Rat N-terminal experimental
pG1-NMGR^{526} and pL2/GZ	-leu -trp	α	Positive prion control
pYES2-hBF1GR^{526} and pL2/GZ	-leu -ura	a	Human N-terminal experimental
pYES2-rBF1GR^{526} and pL2/GZ	-leu -ura	a	Rat N-terminal experimental
pYES2-NMGR^{526} and pL2/GZ	-leu -ura	a	Positive prion control

3.2.9. Growth on X-gal media and β-galactosidase assay

To determine whether the GR^{526} protein within the yeast cells was in the active or inactive state, transformed yeast cells were inoculated in 5 mls of –leu –trp or –leu –ura dropout media, supplemented with galactose to activate the pYES2 *GAL1* promoter (Table 3.2), and grown to early stationary phase at 30 °C (OD_{600nm} = 1). Following growth in liquid media, approximately 300-500 cells were plated on dropout media agar plates and incubated for 4 days. Colonies were velvet replica plated onto X-gal dropout media agar plates (as described in 2.2.8). Replica plates were grown for 4 days at 30 °C, or until colonies appeared.

3.2.10. Yeast mating

Following identification of blue and white colonies from each transformation, the corresponding transformed α and a-mating types were mated on YPD agar plates (Table 3.3).

Blue α-type cells transformed with the rat and human NFoxG1:GR^{526} and NM:GR^{526} constructs were mated to white a-type cells transformed with the pYES2 based rat, human and NM constructs, respectively. White α type cells were similarly mated with blue a-type cells. All matings were performed in triplicate. Following growth overnight on YPD, yeast cells were cultured on triple dropout, -leu –trp –ura media, to screen for diploid cells. The state of the GR^{526} protein within the diploid cells was investigated by randomly selecting two diploid colonies from each mating, growing them in liquid media and plating them on galactose-supplemented X-gal dropout media, as previously described (3.2.9).

3.3. Results

3.3.1. Expression of the GR^{526} protein occurs in blue and white yeast cells

In order to confirm that the GR^{526} protein was expressed in equivalent levels in white yeast compared to blue yeast transformed with the rat and human NFoxG1:GR^{526} constructs, western blot analysis was performed, using a GR specific primary antibody. The western blot was incubated with both the GR specific antibody and a loading control antibody specific to glyceraldehyde 3 phosphate dehydrogenase (GAPDH). The western blot allowed detection of the 58 KDa GR^{526} protein in the cell extracts collected from blue pG1-GR^{526} transformed yeast, used as a positive control (Fig. 3.2). The GR^{526} protein was absent from untransformed, wildtype yeast, used as a negative control. The GR^{526} protein was expressed in both blue and white yeast transformed with the human and rat NFoxG1:GR^{526} constructs. The cell extracts collected from white yeast transformed with the human NFoxG1:GR^{526} construct showed lower levels of immuno-reactivity to the GR specific antibody, these reduced levels were however, maintained when the western blot was incubated with the GAPDH antibody. The GAPDH antibody detected the 38 KDa protein in all samples.

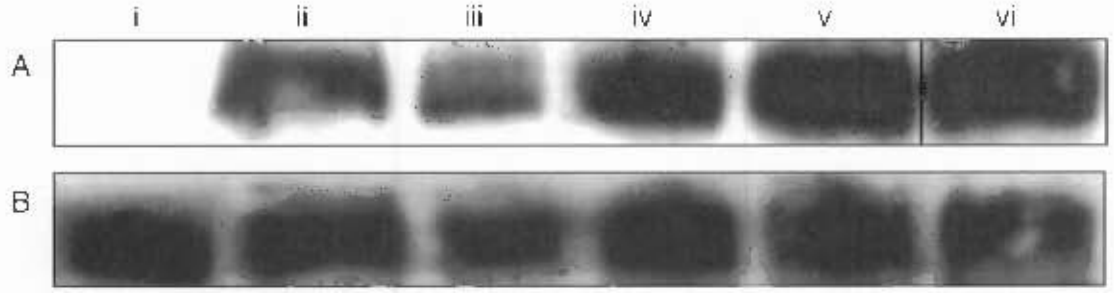

Figure 3.2. Western blot analysis of total protein extracts from blue and white cells transformed with the various GR^{526} based plasmids. (A) Western blot incubated with a GR specific antibody. (B) GAPDH specific antibody used as a loading control. (i) The GR^{526} protein was not detected in total proteins extracted from untransformed, wildtype yeast, but the GAPDH protein was. The GR^{526} protein was detected in blue (ii) and white (iii) yeast transformed with the human pG1-hBF1GR^{526} construct and blue (iv) and white (v) yeast transformed with the rat construct, pG1-rBF1GR^{526}. (vi) The GR^{526} protein was also detected in the blue yeast transformed with the control plasmid pG1-GR^{526}. When the membrane was incubated with a control antibody specific to the GAPDH protein, the protein was detected in all samples. The GAPDH antibody was used as a loading control, and levels of the protein were similar to the levels of the GR^{526} protein in the cell extracts. The size of the hNFoxG1:GR^{526} is approximately 76 KDa, the rNFoxG1:GR^{526} 75 KDa, the GR^{526} 58KDa, and yeast GAPDH 38 KDa.

3.3.2. The aggregated, inactive state of the GR protein is cured by a protein denaturant

Growth on guanidinium hydrochloride was used to determine whether the switch to the inactive conformation of the GR^{526} protein, seen in Chapter 2, could be cured by a protein denaturant. Previous studies have shown that low concentrations of GuHCl are able to cure prion aggregates, through repression of prion fibre proliferation in dividing cells, resulting in accumulation of the soluble form of the protein (Chernoff *et al.*, 2002). White yeast colonies transformed with the constructs pG1-hBF1GR^{526}, pG1-rBF1GR^{526} and pG1-NMGR^{526} were grown on GuHCl supplemented media, for three consecutive passages, and the colour of the progeny on X-gal media determined. Similarly, the one white yeast colony obtained from those cells transformed with the pG1 GR^{526} construct (Chapter 2) was grown on the GuHCl supplemented media. The Sup35 NM construct was used as a positive prion control. The

white yeast transformed with this construct were expected to revert to blue as a consequence of curing by GuHCl, and the GR^{526} transcription factor was once again able to activate the β-galactosidase reporter. The white cell obtained from the pG1-GR^{526} transformation was also grown on GuHCl to determine whether the inability of the GR^{526} protein to regulate the β-galactosidase construct within the cells was due to prion aggregation of the GR^{526} protein, or due to some other unknown cause, such as a random mutation. After three consecutive passages on GuHCl the colour of the progeny was determined: the white colonies derived from the strain transformed with the mutant $GR^{526(m)}$ construct, pG1-GR^{526}, remained white (Fig 3.3.i). The white colonies transformed with the NM construct, pG1-NMGR^{526}, produced the blue colour characteristic of the functional GR^{526} protein (Fig. 3.3.ii).

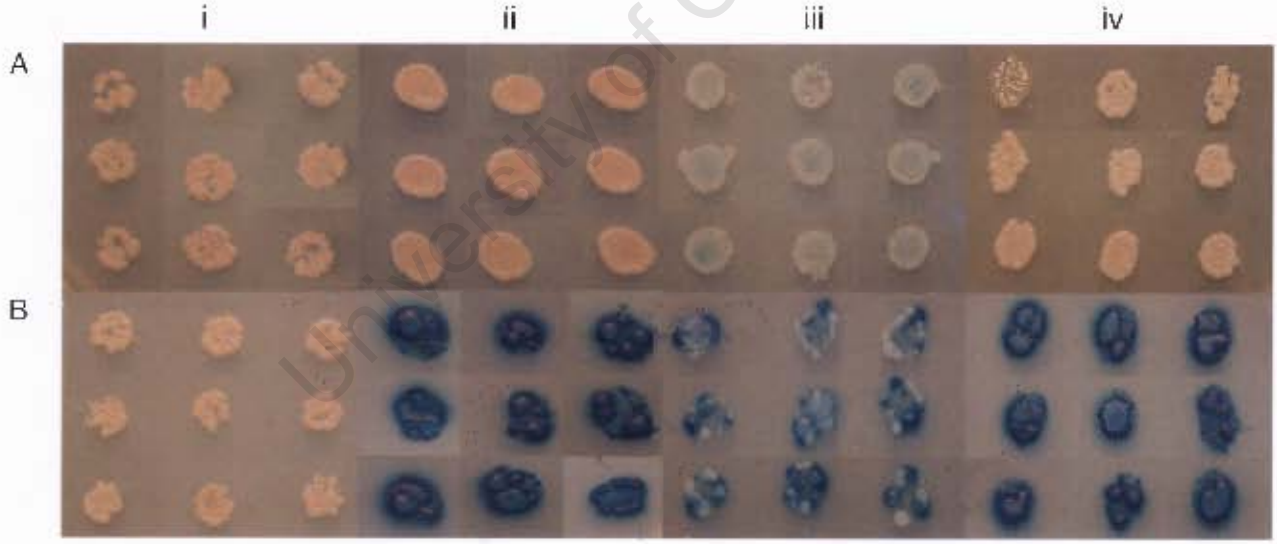

Figure 3.3. Growth on GuHCl cures the inactive protein conformation. (A) White colonies are grown on X-gal media to determine their colour prior to growth on GuHCl. (B) Following three consecutive passages on GuHCl, colonies are plated onto X-gal media to determine the colour of the progeny. (i) The one white mutant colony obtained from those transformed with pG1-$GR^{526(m)}$, was not cured by GuHCl and remained white. White colonies derived from the strain carrying the NM (ii), human (iii) and rat (iv) GR^{526} constructs were all cured by growth on GuHCl. The white colonies transformed with the NM construct, pG1-NMGR^{526}, were used as a positive prion control. Differences in background media colour are not due to differences in media composition.

The white cells transformed with the human and rat constructs, pG1-hBF1GR^{526} and pG1-rBF1GR^{526} respectively, were also cured by the protein denaturant, the progeny of the originally white colonies expressed soluble GR^{526} protein, which was able to regulate the β-galactosidase reporter plasmid (Fig 3.3.iii & iv). The percentage of colonies converting between the active and inactive GR^{526} conformations was high in the colonies transformed with the human NFoxG1:GR^{526} construct, in the β-galactosidase assay (Chapter 2), thus the patches of white cells on X-gal media included a number of blue yeast cells, resulting in a faint blue colour. These white cells, when cured, maintained a percentage of white cells, resulting in mosaic colonies (Fig. 3.3.iv).

3.3.3. GR^{526} proteins extracted from blue and white cells display different sedimentation rates

In order to determine whether the GR^{526} proteins extracted from blue and white yeast colonies had different physical properties, therefore confirming the aggregates seen in the GFP assay (Chapter 2), the rate of sedimentation for the proteins was investigated on sucrose gradients. Following ultracentrifugation, the gradients were fractionated from the top of the gradient downwards and numbered one to ten. Fractions numbered one were excluded from the blots due to spatial constraints; this was considered the safest selection based on previously published research (Si *et al.*, 2003). Western blot analysis was performed with both a GR specific antibody and a GAPDH antibody as a control. The GAPDH protein was found to have the same sedimentation rate in the blue and white cell extracts, with the greatest percentage of the protein detected in fractions three, four and five (when numbering from the top of the gradient downwards) of all samples (Fig 3.4.A). This result confirms that fractionation of proteins according to size was consistent for all gradients.

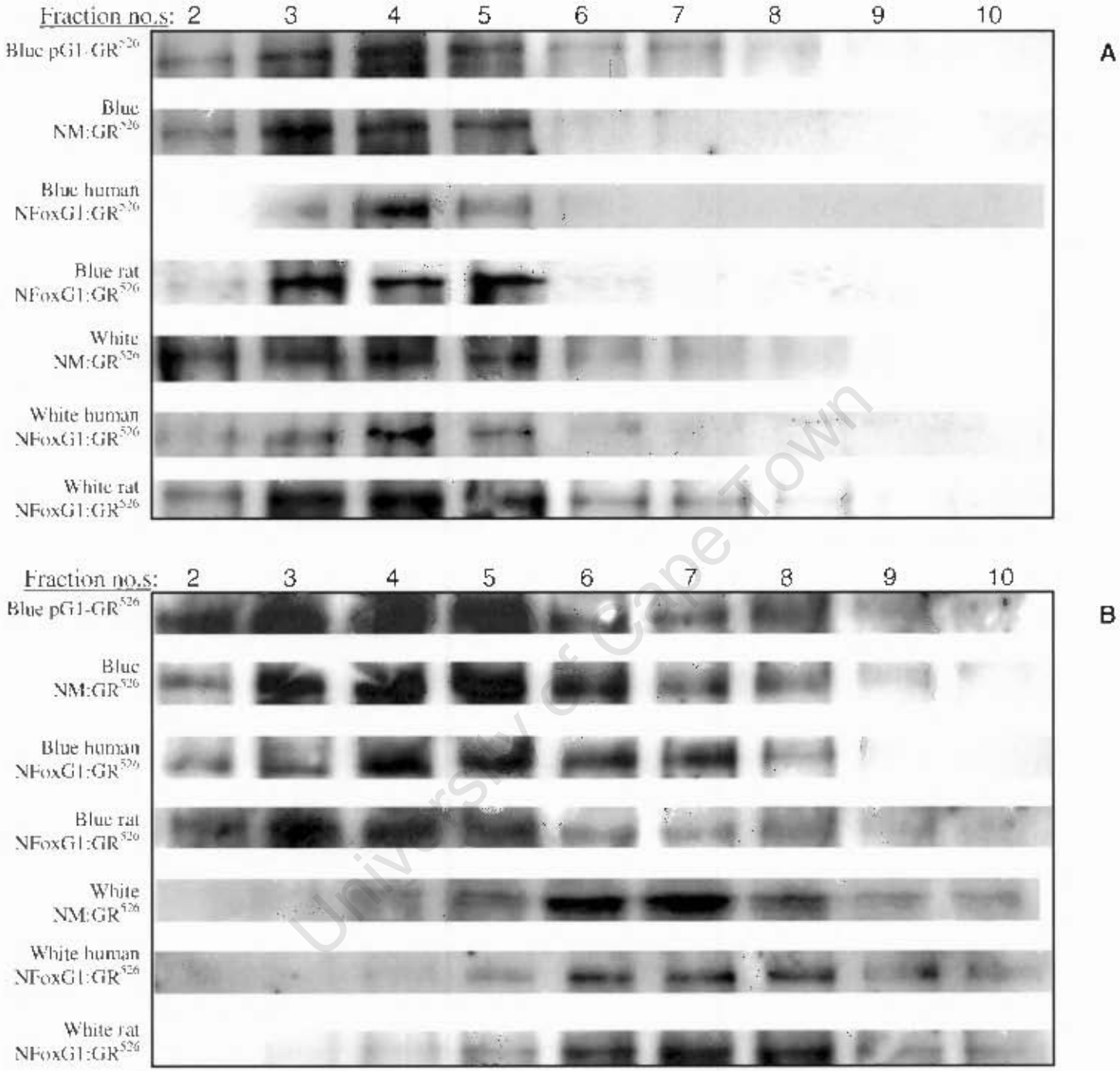

Figure 3.4. Western blot analysis of fractions 2-10 of the sucrose gradients. Following sucrose gradient ultracentrifugation equal volumes, irrespective of protein concentration, of each fraction were loaded onto the blots as indicated above the figures. The transformed yeast used in the gradients are indicated on the left of the blots. (A) The membrane probed with the anti-GAPDH antibody revealed that the 38 KDa GAPDH protein sedimented in fractions 3-5 in all the gradients. (B) Membranes probed with the anti-GR antibody showed that the GR^{526} protein from blue colonies sedimented predominantly to fractions 3-6, while those from white colonies sedimented predominantly to fractions 6-8.

Similarly, the gradient fractions were investigated by western blot analysis with a GR specific primary antibody. The western blots revealed that the GR^{526} proteins sedimented at a different rate when extracted from blue versus white yeast colonies. The soluble GR^{526} proteins extracted from blue colonies transformed with the control non-prion plasmid, pG1-GR^{526}, the prion control plasmid pG1-NMGR^{526}, pG1-hBF1GR^{526} and pG1-rBF1GR^{526} were all present predominately in fractions three, four and five (Fig. 3.4.B), like the soluble GAPDH protein (Fig. 3.4.A). The GR^{526} proteins extracted from white colonies transformed with the plasmids pG1-NMGR^{526}, pG1-hBF1GR^{526} and pG1-rBF1GR^{526} sedimented predominantly to fractions six, seven and eight (Fig. 3.4.B). These results suggest that while the functional GR^{526} proteins extracted from blue yeast colonies sediment at the same rate as a soluble yeast protein, namely GAPDH, the inactive GR^{526} proteins isolated from white yeast colonies sedimented at a higher rate and are in a denser, aggregated form.

3.3.4. Sub-cloning of the FoxG1 N-terminal domains and GR^{526} into the vector pYES2

In order to perform the yeast mating experiment, the NFoxG1 domains fused to GR^{526} and the Sup35 NM domain fused to GR^{526}, were sub-cloned into the yeast expression vector pYES2, with a uracil selectable marker. The NM:GR^{526}, hNFoxG1:GR^{526} and rNFoxG11:GR^{526} fragments were digested out of the original constructs, and ligated into the pYES2 vector in the multiple cloning site (Fig. 3.5).

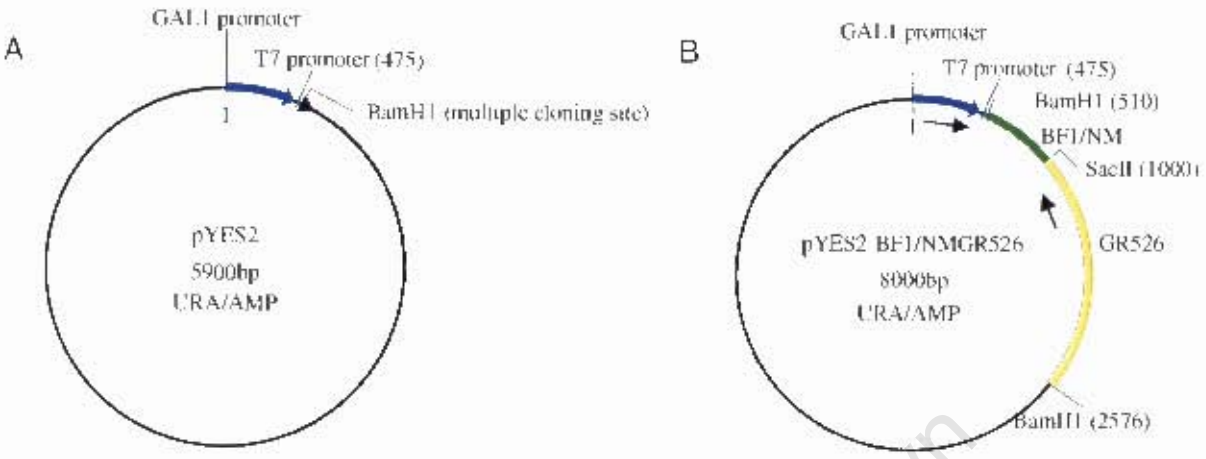

Figure 3.5. Plasmid maps for the pYES2 vector, and the resulting pYES2-BF1/NMGR^{526} constructs. (A) The pYES2 yeast expression vector was used as a backbone in the vectors constructed for the yeast mating experiment. Expression of the vector is inducible, requiring either raffinose or galactose to be expressed. The resulting NFoxG1/NM:GR^{526} constructs (B) were identified with the use of T7 and GR^{526} specific primers (arrows, not to scale). The position of the restriction enzyme recognition sites are shown, as are the selectable markers specific to the plasmids.

Pulative recombinant constructs were identified by colony PCR, with a T7 forward and GR^{526} specific reverse primer (Fig. 3.5 and 3.6). The GR^{526} and T7 specific primers produced a PCR product when the insert was in the same orientation as the *GAL1* promoter, allowing selection of the desired constructs (Fig. 3.6). The PCR screening allowed exclusion of constructs in which the NFoxG1/NM:GR^{526} inserts were in the opposite orientation to the promoter. Following PCR identification of the constructs, sequencing was performed to verify that no mutations had occurred during the sub-cloning procedure.

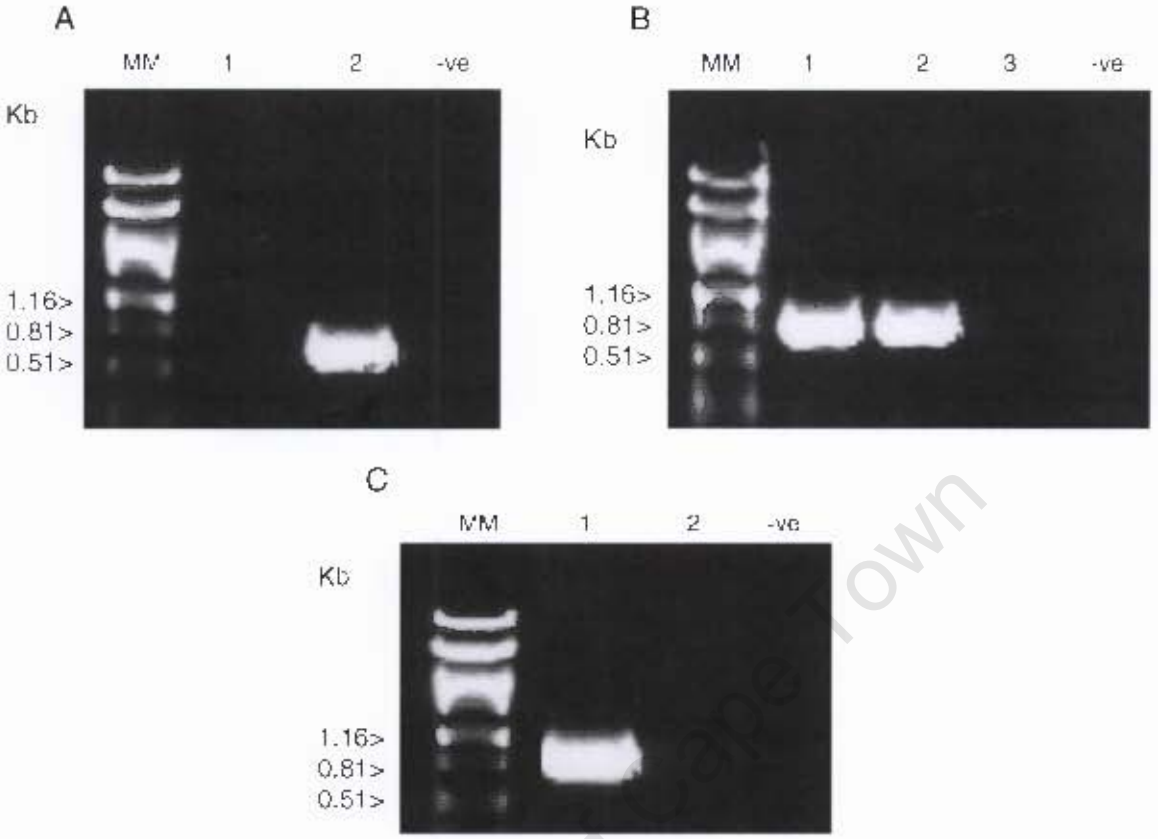

Figure 3.6. PCR screening of the pYES2-rBF1GR^{526}, pYES2-hBF1GR^{526} and pYES2-NMGR^{526} constructs. T7 and GR^{526} specific primers were used to screen constructs for pYES2-rBF1GR^{526} (A), pYES2-hBF1GR^{526} (B) and pYES2-NMGR^{526} (C). MM: Molecular weight marker (λDNA/PstI), applicable fragments sizes (Kb) are shown alongside. –ve: negative PCR control, including PCR grade water as the template. (A) Sample 2 shows a positive PCR product, and thus the desired pYES2-rBF1GR^{526} construct. (B) Samples 1 and 2 show the desired pYES2-hBF1GR^{526} construct. (C) Sample 1 shows the desired pYES2 NMGR^{526} construct. Samples 1 (A), 3 (B) and 2 (C) show no PCR product, therefore the insert was not in the correct orientation. The rat product was 756 bp, the human product 783 bp and the NM product 1028 bp.

3.3.5. The inactive state of the NFoxG1:GR^{526} proteins are transmissible

Following sequence verification, pYES2-rBF1GR^{526}, pYES2-hBF1GR^{526} and pYES2-NMGR^{526} were transformed into the a-mating type yeast cells with the pL2/GZ reporter construct, while the original GR^{526} based constructs, pG1-rBF1GR^{526}, pG1-hBF1GR^{526} and pG1-NMGR^{526} were transformed with the pL2/GZ construct into α-type yeast cells. The yeast mating experiment relies on the transmissible nature of prion aggregates, versus non-prion

amyloids, which are not transmissible when the amyloid form is exposed to tissue in which it is absent. White α-type colonies from each transformation were selected and mated with blue a-type colonies from the corresponding plasmid transformation (i.e. pYES2-hBF1GR^{526} in blue a-type cells mated with pG1-hBF1GR^{526} in white α-type cells, and so on, Fig. 3.7). The reverse was also performed; blue α-type colonies from each transformation were selected and mated with white a-type colonies from the corresponding plasmid transformation (Fig. 3.7). The NM constructs were used as a positive prion control, previous research has shown the prion form of the protein to be transmissible between mating cells, thus the mating was expected to result in white coloured progeny (Li and Lindquist, 2000).

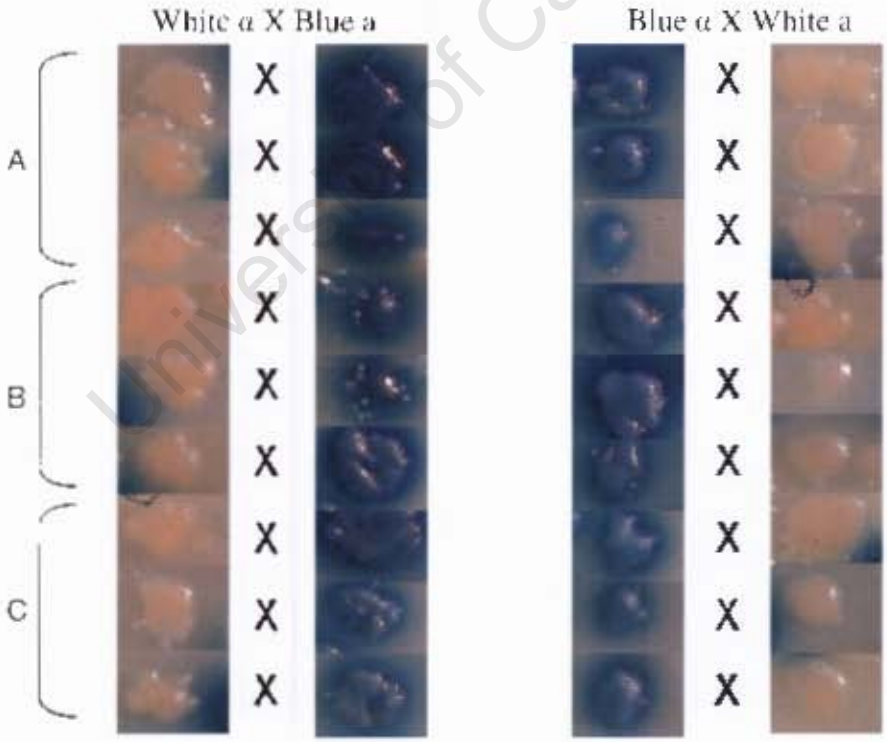

Figure 3.7. White α-type colonies were mated to blue a-type colonies, and blue α-type colonies were mated to white a-type colonies in the yeast mating experiment. (A) α-type colonies transformed with the pG1-NMGR^{526} construct and pL2/GZ were mated to a-type colonies transformed with the pYES2-NMGR^{526} construct and pL2/GZ, in triplicate. Similarly, α and a-type colonies transformed with the corresponding human (B) and rat (C) NFoxG1:GR^{526} constructs and pL2/GZ were mated, in triplicate.

Following yeast mating, diploid cells were selected for on triple dropout media. Two diploid cells for each mating were plated on X-gal supplemented media, to determine the colour of the progeny, resulting in six plates per performed cross mating (matings performed in triplicate, and two diploid cells selected from each one). The diploid colonies that resulted from the mating of the yeast carrying the two NM:GR^{526} plasmids and pL2/GZ were white in colour, as expected (Table 3.3, Fig. 3.8). The diploid progeny from the human NFoxG1:GR^{526} matings were all white in colour, demonstrating that the inactive form of the GR^{526} protein, when fused to the human NFoxG1, is transmissible. The progeny from the rat NFoxG1:GR^{526} matings were predominantly white: five of the six matings produced all white colonies, while the two diploid cells selected from one mating (the third blue α-type colony crossed with a white a-type colony in Fig. 3.7) produced half blue and half white colonies (Table 3.3, Fig. 3.8).

Table 3.3. Each mating was performed in triplicate, and the colour of two diploid cells determined on X-gal media. The number of blue, white and mixed plates out of six, for each mating was recorded.

Yeast mating	No. of blue progeny	No. of white progeny	No. of mixed plates
NM white α x blue a	**0**	**6**	**0**
NM blue α x white a	**0**	**6**	**0**
Human NFoxG1 white α x blue a	**0**	**6**	**0**
Human NFoxG1 blue α x white a	**0**	**6**	**0**
Rat NFoxG1 white α x blue a	**0**	**6**	**0**
Rat NFoxG1 blue α x white a	**0**	**4**	**2**

Table notes: mixed plates were considered plates on which half the progeny were blue and half were white.

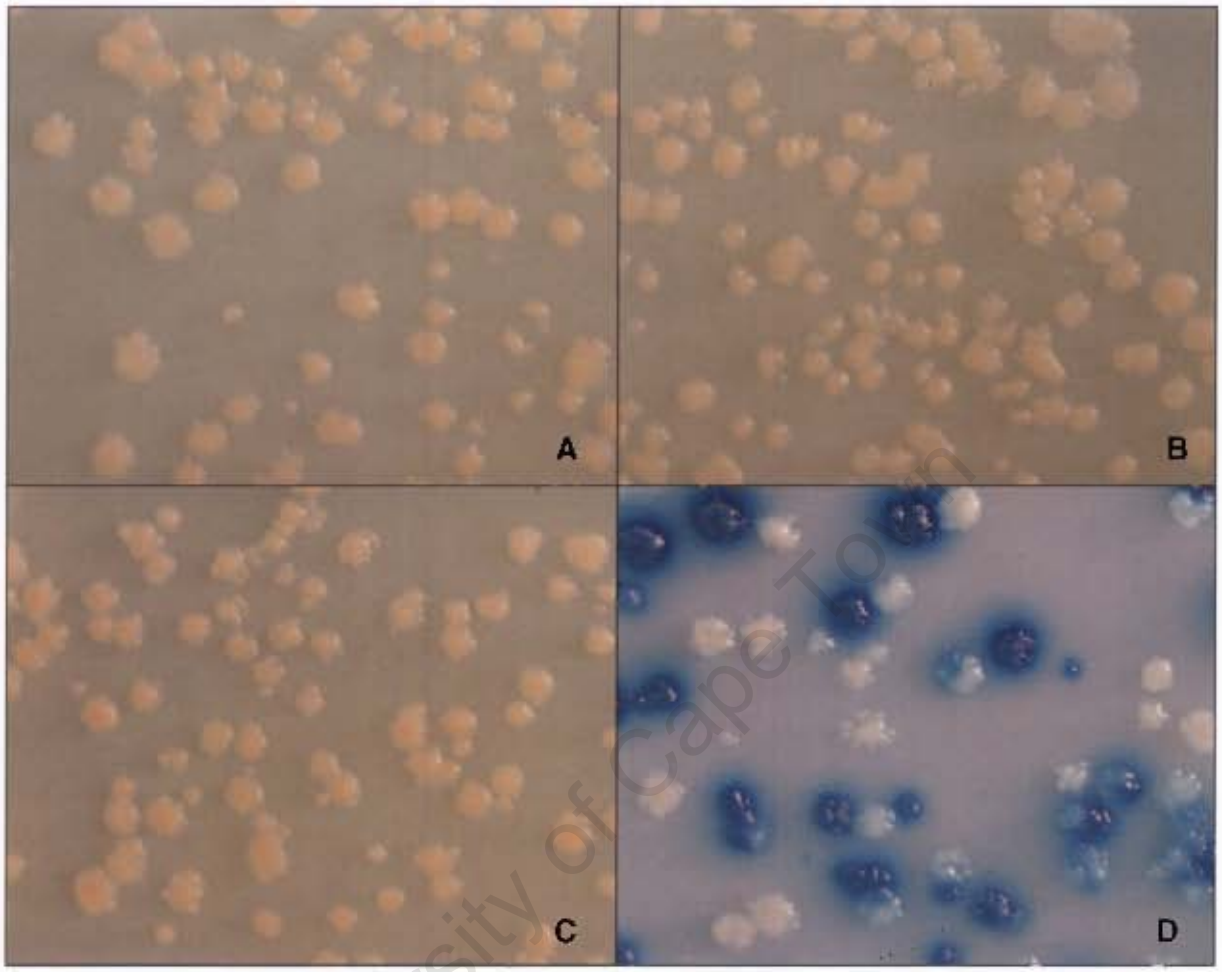

Figure 3.8. The inactive state of the NFoxG1:GR^{526} protein is infectious. The colour of the diploid progeny of the yeast matings was determined by growth on X-gal supplemented media. (A) The progeny of the NM:GR^{526} matings were all white. (B) The progeny from the human NFoxG1:GR^{526} matings were all white, demonstrating the inactive form of the protein is transmissible. The progeny from five of the rat NFoxG1:GR^{526} matings were white (C), while the last of the matings resulted in 50 % blue and 50 % white colonies, when plated on X-gal media. The differences in the background media colour were not due to differences in media composition.

3.4. Discussion

In this chapter, the physical properties of the inactive state of the GR^{526} protein, seen in the β-galactosidase assay in Chapter 2, were investigated. It was found that the white colonies seen in the assay were not due to reduced expression of the GR^{526} protein, or due to mutation. The inactive form of the protein was found to have a different sedimentation rate, when compared

to the active form, providing further evidence for the formation of aggregates, initially seen in the GFP assay (Chapter 2). Infectivity of the amyloid forms of the NFoxG1:GR^{526} constructs were also investigated via yeast mating, it was shown that the inactive, aggregated state of the protein was transmissible to uninfected cells, akin to prion proteins.

It was initially hypothesized that the white colonies seen in the β-galactosidase assay could be a consequence of one of three distinct mechanisms, namely the reduced expression of the GR^{526} protein, a mutation in the GR^{526} protein which had occurred in the process of transformation and growth of the cells, or alternatively a consequence of a conformational switch and formation of amyloid fibres typical of prion proteins. These alternatives were investigated.

The possibility that reduced levels of the GR^{526} protein could account for the inability of the protein to active the β-galactosidase reporter was ruled out by western blot analysis, performed with a GR specific antibody. The analysis showed that the protein was expressed in blue colonies transformed with the GR^{526} construct, pG1-GR^{526}, and was absent in untransformed cells. The GR^{526} protein was found to be expressed in comparable levels in white and blue colonies carrying the human and rat NFoxG1:GR^{526} constructs. Incubating the western blot membrane with a loading control antibody to GAPDH, revealed that the levels of GR^{526} protein within blue and white cells did not differ significantly (Fig. 3.2). The white colour of the colonies seen in the β-galactosidase assay was therefore not due to a lack of GR^{526} expression, but to some other mechanism of inactivation.

An alternative explanation could be that the white colonies were a consequence of a mutation in the NFoxG1:GR^{526} sequence. This was tested by growth of white colonies on GuHCl. Known prions can be cured by growth on GuHCl (Chernoff *et al.*, 2002), while proteins in which a mutation has occurred cannot. The white colonies transformed with the prion control NM:GR^{526} construct were found to be cured by growth on GuHCl supplemented media, as expected (Li and Lindquist, 2000). In Chapter 2, one white colony was identified from those transformed with the GR^{526}control plasmid, which provided a convenient positive mutation control. This colony was also subjected to growth on GuHCl and it was shown to be incurable, indicating that it resulted from a random mutation in the GR^{526} sequence and not from a prion-like mechanism (Fig. 3.3.i). The white cells transformed with the human construct pG1-hBF1GR^{526} and the rat construct pG1-rBF1GR^{526} were both found to be cured (Fig. 3.3.ii & iii). The progeny colonies were blue in colour, but the strain with the human NFoxG1 construct maintained a number of white colonies, giving them a mosaic appearance. This mosaic colony phenomenon was consistent with the instability of the human NFoxG1:GR^{526} protein conformation seen in the β-galactosidase assay (Chapter 2). The curing of the inactive state of the GR^{526} protein in the yeast transformed with the rat and human constructs suggests a prion-like mechanism, but does not provide definitive evidence.

Thirdly, white yeast colonies could have resulted from GR^{526} protein aggregation induced by the NFoxG1 domain. This was partially tested in Chapter 2 by fusing the NFoxG1 domain to GFP and viewing aggregates with fluorescent microscopy. The presence of aggregates, a characteristic of prion-like mechanisms, was investigated by sucrose gradient fractionation. The sedimentation rates of the NFoxG1:GR^{526} proteins extracted from blue and white colonies were investigated, to determine whether there were physical differences between the

active and inactive states of the protein. Incubation of the western blot membranes with the control GAPDH antibody revealed that the protein sedimented to the fractions numbered three, four and five from the top of the gradients, and showed that fractionation through the sucrose gradients was similar in all experiments (Fig. 3.4.A). The GR^{526} proteins from blue colonies sedimented at the same rate as the GAPDH protein, with the majority of the protein present in the third, fourth and fifth fractions from the top of the gradient. GR^{526} proteins isolated from white colonies, however, sedimented to fractions six, seven and eight (Fig. 3.4.B). These results show that the inactive GR^{526} protein present in the white colonies is present in a denser and more aggregated form than the GR^{526} protein isolated from blue colonies, in which it is active. The results described in this chapter therefore provide evidence that the white colour of the colonies seen in the β-galactosidase assay in Chapter 2, are a result of a conformational change and high molecular weight aggregate formation.

Thus far I have shown that the N-terminal domains of the human and rat FoxG1 transcription factors share a number of traits with prion proteins. These include: conformational flexibility and tracts of amino acid residues, an ability to confer upon other proteins (GR^{526} and GFP) a reversible change in conformation from the soluble form to the insoluble, aggregated form, and the ability of the aggregated form to be cured by a protein denaturant. These traits suggest, but do not prove, a prion-like mechanism. As previously discussed, not all proteins capable of distinct conformational states are prions; prions (for example mammalian PrP^{sc} and *Aplysia* CPEB) are proteins capable of infectious amyloid formation, while other amyloid forming proteins exist, which are not infectious (for example those responsible for Alzheimer and Parkinson's disease) (Brandner *et al.*, 1996, Dobson, 2003, Prusiner, 1998).

Yeast prion states are able to produce non-pathogenic, heritable changes in phenotype, which are transmissible and infectious between mating cell types and show non-Mendelian patterns of inheritance (Chernoff *et al.*, 1995, Sondheimer *et al.*, 2001). Mammalian prion diseases which include Creutzfeldt-Jakob disease and bovine spongiform encephalopathy, are infectious diseases resulting in severe neurodegeneration (Prusiner, 1998). Mammalian neurodegenerative diseases resulting from protein amyloid formation include Alzheimer disease, which results from aggregation of the β-amyloid precursor protein (βAPP), and Parkinson's disease, resulting from the accumulation of Lewy bodies, aggregates of the α-Synuclein protein (Checler and Vincent, 2002, Taylor *et al.*, 2002). Alzheimer and Parkinson's disease, although similar to the prion neurodegenerative diseases in the accumulation of protein deposits in brain tissue, are not considered prion diseases, as the disease state is not infectious. Thus, in order to determine whether the N-terminal domains of FoxG1 orthologues are amyloid forming proteins or prion proteins, the transmissibility of the aggregated conformation was investigated through a yeast mating experiment.

In the yeast mating experiment the NM:GR^{526} fragment was used as a positive prion control. Previous research has revealed that the amyloid state of the NM:GR^{526} protein is transmissible between mating cell types, giving rise to diploid progeny that maintain the prion state of the protein (Li and Lindquist, 2000). Yeast mating of blue and white colonies carrying the pG1-NMGR^{526} constructs resulted in white colonies (Fig. 3.8.A). The mating of blue and white colonies derived from the cells transformed with the human NFoxG1:GR^{526} constructs, also resulted in white diploid progeny (Fig. 3.8.B). Five of the matings of blue and white yeast colonies carrying the rat NFoxG1:GR^{526} constructs resulted in white progeny, the remaining mating resulted in a mix of 50 % white and 50 % blue colonies (Fig. 3.8.C & D). Although all

known yeast prion states are non-Mendelian elements and are usually dominant, some have shown unusual segregation ratios. These range from 4:0 to 0:4 (prion state:soluble state) in the progeny, during yeast mating experiments. These ratios can be explained by the fact that some of the yeast may lose the prion state of the protein during meiosis. Another explanation for the 2:2 ratio seen in the one rat NFoxG1:GR^{526} mating is the possibility that one parent in the mating contained a mutation which prevented prion fibre propagation (Chernoff *et al.*, 2002).

These results demonstrate that the high molecular weight forms of the human and rat NFoxG1:GR^{526} proteins are able to act as prion-like transmissible proteins, able to self-proliferate and infect yeast mating pairs. Besides the *Aplysia* CPEB protein, this is the second neural protein to display the ability to change conformation and propagate the alternative form without obvious deleterious effects (Si *et al.*, 2003).

CHAPTER 4

Conclusions

The purpose of this study was to investigate the possible prion-like properties of the N-terminal domains of the winged-helix transcription factor FoxG1. Prion proteins, which are able to form self-proliferating, infectious amyloids, are responsible for neurodegenerative diseases in mammals, such as bovine spongiform encephalopathy, and non-Mendelian traits in yeast, for example the yeast prion states [*PSI*$^{+}$], [*Ure3*] and [*RNQ1*] (Chernoff *et al*., 1995, Prusiner, 1998, Sondheimer *et al.*, 2001, Wickner *et al.*, 1994). The amino acid sequences of these proteins are often glutamine rich and include oligopeptide repeat sequences (Derkatch *et al.*, 2004). The N-terminal domains of prion proteins are also dispensable for their function and often display conformational flexibility. Similar amyloid proteins exist which are responsible for neurodegenerative diseases in mammals, but are not considered prions, due to their non-infectious nature; these include those proteins responsible for Alzheimer and Parkinson's disease (Dobson, 2003).

The mammalian orthologues of the FoxG1 transcription factor were of particular interest due to the unusual composition of their N-terminal domains. The DNA-binding and C-terminal domains are highly conserved amongst vertebrates; the DNA-binding domains all contain the 100-amino acid region characteristic of the winged-helix family, while the C-terminal domains contain a conserved 211 amino acid domain (Bredenkamp *et al.*, 2006). The N-terminal domains have in common the first 30 amino acid residues, including a Casein kinase 1 phosphorylation site, after which the domain becomes significantly different amongst

vertebrates (Regad *et al.*, 2006). The N-terminal domains of the mammalian orthologues contain significant quantities of histidine, proline and glutamine amino acid residues, regions significantly reduced in lower vertebrates such as *Xenopus* and zebrafish. The human sequence contains the greatest number of these amino acid residues, with an insertion of a poly-proline tract of six residues, which is absent in the rat sequence. It was this expanded domain that led to the hypothesis that the N-terminal domain might act as a prion-like switch and regulate the protein in some manner.

In this study, I initially showed that the NFoxG1 domains of the human, rat and *Xenopus* orthologues displayed high levels of conformational flexibility, similar to the N-terminal domains of some of the known prions. It was evident that the level of flexibility in the domain increased with the number of histidine, glutamine and proline residues, with the human sequence displaying the highest level of sustained flexibility and the greatest number of these residues. The human and rat orthologues were chosen for further experimental work, to compare differences in their prion-like properties.

The human and rat NFoxG1 domains were found to be able to alter the conformation of other proteins, namely the glucocorticoid receptor and green fluorescent proteins. In the yeast β-galactosidase assay, the NFoxG1 domains were fused to the constitutively active GR^{526} protein, and the effect of the domain assayed via a GR^{526} regulated LacZ reporter construct. Both the human and rat NFoxG1 domains were able to alter the conformation of the GR^{526} protein, rendering it inactive and resulting in white yeast colonies. Further experimental work established that the white colonies seen in the β-galactosidase assay were a result of aggregate formation. It was initially hypothesized that the white colour of the colonies was a result of

one of three possibilities: the first was that the GR^{526} protein was expressed at lower levels in the white colonies when compared to blue, alternatively that the GR^{526} had become mutated in the white colonies, or thirdly that the NFoxG1 domain induced an alternative, aggregated conformation of the GR^{526} protein. Western blot analysis, growth on a protein denaturant and the investigation of the sedimentation rates of the GR^{526} proteins in blue and white colonies, combined with the earlier results of the GFP assay, provided evidence that the white colour of the colonies was a result of aggregate formation. With the use of a yeast mating experiment, the transmissible nature of the aggregates induced by the NFoxG1 domains was displayed.

In the β-galactosidase assay, the human NFoxG1:GR^{526} fusion protein was found to switch between the active and prion state of the protein at a significantly higher rate than the rat fusion protein, which was comparable to the N-terminal domain of the known yeast prion Sup35. Research on the Sup35 N-terminal domain has shown that the insertion of additional amino acid repeat sequences results in the conversion from the active to the inactive state of the protein at a significantly higher rate than the wildtype protein, due to different [PSI^+] strain formation (Liu and Lindquist, 1999). It is suggested that the instability of the human NFoxG1 domain was a result of the expanded proline domain absent in the rat sequence, resulting in differences between the human and rat NFoxG1 prion strains, which may differ in size and structure of the likely amyloid fibres (Tanaka *et al.*, 2004).

Although I have shown in these yeast assays that the NFoxG1 domains display prion characteristics, a number of questions remain regarding the biological importance of the N-terminal domain in regulating FoxG1 in neural progenitor cells. The FoxG1 transcription factor has been shown to act as a transcriptional activator and repressor, repressing proneural

genes by interacting with the Gro/TLE1 complex (Yao *et al.*, 2001) and activating transcription by binding to Smad proteins and Smad binding partners, disrupting the TGF-β pathway (Dou *et al.*, 2000, Rodriguez *et al.*, 2001). FoxG1 is also known to act in a dosage dependent manner, stimulating proliferation in high concentrations and differentiation in low concentrations (Bourguignon *et al.*, 1998). Bone morphogenic protein and fibroblast growth factor-8 are also believed to be regulated by FoxG1 (Hanashima *et al.*, 2002, Martynoga *et al.*, 2005). Understanding how the formation of prion amyloids applies to the complex interactions and pathways involved in repression and activation of transcription is an immense task, and the purpose of such a mechanism in early telencephalic development remains to be explored. The *Aplysia* CPEB protein has been shown to be more active in the prion conformation, than the soluble conformation, able to bind CPE containing RNA (Si *et al.*, 2003). Thus, it is possible that the prion form of FoxG1 may be active and confer an alternative role for FoxG1 in development, or may be inactive and a means for FoxG1 disruption.

Thus, future research should first investigate whether the aggregated or soluble state of FoxG1 is the active conformation of the protein. It is suggested, that in order to do so, the full length FoxG1 protein be fused to the GR^{526} protein, to confirm that it is able to confer the same conformational change seen in this study, and investigate the effects of the DNA-binding and the C-terminal domains on amyloid formation. It would be interesting to map the exact amino acid residues in the N-terminal domains required for prion aggregate formation, and determine whether the insertion of the six proline residues in the human sequence results in the instability seen in this study, by creating a mutant in which the insertion is deleted. It would also be interesting to determine whether there is a functional difference between the

human and rat transcription factors, and investigate whether the difference in prion strains has any connection to the vast difference in cerebral cortex size seen between the orthologues (Hill and Walsh, 2005). Perhaps the N-terminal domains of lower vertebrates can be similarly tested, to determine whether the mammalian orthologues are unique in their prion properties. The results generated by this study are very exciting, providing proof of a second neuronal protein, and the first mammalian protein, displaying non-deleterious prion properties.

CHAPTER 5

References

Alper, T., Cramp, W., Haig, D. & Clarke, M. (1967). Does the agent of scrapie replicate without nucleic acid? *Nature.* **214,** 764-766.

Ausubel, F., Brent, R., Kingston, R., Moore, D., Siedman, J., Smith, J. and Struhl, K. (2001). *Current Protocols in Molecular Biology.* John Wiley and Sons, Inc. Volumes 1-5.

Bourguignon, C., Li, J. & Papalopulu, N. (1998). XBF-1, a winged helix transcription factor with dual activity, has a role in positioning neurogenesis in *Xenopus* competent ectoderm. *Development.* **125**, 4889-4990.

Brandner, S., Isenmann, S., Raeber, A., Fischer, M., Sailer, A., Kobayashi, Y., Marino, S., Weissmann, C. & Aguzzi, A. (1996). Normal host prion protein necessary for scrapie-induced neurotoxicity. *Nature.* **379**, 339-343.

Bredenkamp, N., Illing, N. & Seioghe, C. (2006). Evolutionary analysis of the Forkhead transcription factor FoxG1 in vertebrates. *Development, Genes and Evolution.* Manuscript in press.

Breslauer, K., Frank, R., Blocker, H. & Marky, L. (1986). Predicting DNA duplex stability from the base sequence. *Proc. Natl. Acad. Sci. USA.* **83**, 3746-3750.

Caviness, V., Takahashi, T. & Nowakowski, R. (1995). Numbers, time and neocortical neurogenesis: a general development and evolutionary model. *Trends in neuroscience.* **18,** 379-383.

Chapman, M., Robinson, L., Pinkner, J., Roth, R., Heuser, J., Hammar, M., Normark, S. & Hultgren, S. (2002). Role of *Escherichia coli* curli operons in directing amyloid fiber formation. *Science.* **295,** 851-855.

Checler, F. & Vincent, B. (2002). Alzheimer's and prion diseases: distinct pathologies, common proteolytic denominators. *TRENDS in neurosciences.* **25**, 616-620.

Chernoff, Y., Lindquist, S., Ono, B., Inge-Vechtomov, S. & Liebman, S. (1995). Role of the chaperone protein Hsp104 in propagation of the yeast prion-like factor [*psi*$^+$]. *Science.* **268,** 880-884.

Chernoff, Y. O., Uptain, S. M. & Lindquist, S. L. (2002). Analysis of Prion Factors in Yeast. *Methods In Enzymology.* **351**, 499-538.

Chung, C. & Miller, R. (1988). A rapid and convenient method for the preparation and storage of competent bacterial cells. *Nucleic Acids Res.* **16**, 3580.

Clark, D. A., Mitra, P. P. & Wang, S. S.-H. (2001). Scalable architecture in mammalian brains. *Nature.* **411**, 189-193.

Clonetech (2001). *Yeast protocols handbook.*

Derkatch, I., Uptain, S., Outeiro, T., Krishnan, R., Lindquist, S. & Liebman, S. (2004). Effects of Q/N-rich, polyQ, and non-polyQ amyloids on the *de novo* formation of the [PSI$^+$] prion in yeast and aggregation of Sup35 *in vitro*. *Proc. Natl. Acad. Sci. USA.* **101**, 12934-12939.

Derynck, R. & Zhang, Y. (2003). Smad-dependent and Smad-independent pathways in the TGF-β family signaling. *Nature.* **425,** 577-584.

Dobson, C. (2003). Protein folding and misfolding. *Nature.* **426**, 884-890.

Dosztanyi, Z., Csizmok, V., Tompa, P. & Simon, I. (2005). The pairwise energy content estimated from amino acid composition discriminates between folded and intrinsically unstructured proteins. *Journal of Molecular Biology.* **347**, 827-839.

Dou, C., Lee, J., Liu, B., Liu, F., Massague, J., Xuan, S. & Lai, E. (2000). BF-1 interferes with transforming growth factor β signaling by associating with smad partners. *Molecular and Cellular Biology.* **20**, 6201-6211.

Dou, C., Li, S. & Lai, E. (1999). Dual role of Brain Factor-1 in regulating growth and patterning of the cerebral hemispheres. *Cerebral Cortex.* **9**, 543-550.

Fukuchi-Shimogori, T. & Grove, E. (2001). Neocortex patterning by the secreted signaling molecule FGF8. *Science.* **294**, 1071-1074.

Govaerts, C., Wille, H., Prusiner, S. & Cohen, F. (2004). Evidence for assembly of prions with left-handed β-helices into trimers. *Proc. Natl. Acad. Sci. USA.* **101**, 8342-8347.

Hanashima, C., Li, S. C., Shen, L., Lai, E. & Fishell, G. (2004). *Foxg1* Suppresses Early Cortical Cell Fate. *Science.* **303**, 56-59.

Hanashima, C., Shen, L., Li, S. & Lai, E. (2002). *Brain Factor-1* controls the proliferation and differentiation of neocortical progenitor cells through independent mechanisms. *The Journal of Neuroscience.* **22,** 6526-6536.

Hardcastle, Z. & Papalopulu, N. (2000). Distinct effects of *XBF-1* in regulating the cell cycle inhibitor $p27^{XIC1}$ and imparting a neural plate. *Development.* **127,** 1303-1314.

Hill, R. & Walsh, C. (2005). Molecular insights into human brain evolution. *Nature.* **437**, 64-67.

Kaestner, K., Knöchel, W. & Martinez, D. (2000). Unified nomenclature for the winged helix/forkhead transcription factors. *Genes & Development* .**14**, 142-146.

Katoh, M. & Katoh, M. (2004). Human FOX gene family. *Int. J. Oncol.* **25**, 1495-1500.

Kimura, Y., Yahara, I. & Lindquist, S. (1995). Role of the protein chaperone YDJ1 in establishing Hsp90-mediated signal transduction pathways. *Science.* **268**, 1362-1365.

King, C. & Diaz-Avalos, R. (2004). Protein-only transmission of three yeast prion strains. *Nature*. **428**, 319-323.

Krishnan, R. & Lindquist, S. (2005). Structural insights into a yeast prion illuminate nucleation and strain diversity. *Nature*. **435**, 765-772.

Lai, E., Clark, K. L., Burley, S. K. & Darnell, J. E. (1993). Hepatocyte nuclear factor 3/fork head or "winged helix" proteins: A family of transcription factors of diverse function. *Proc. Natl. Acad. Sci. USA*. **90**, 10421-10423.

Lai, E., Prezioso, V., Tao, W., Chen, W. & Darnell, J. (1991). Hepatocyte nuclear factor 3 alpha belongs to a gene family in mammals that is homologous to the Drosophila homeotic gene fork head. *Genes Dev*. **5,** 416-427.

Lee, S., Danielian, P., Fritzsch, B. & McMahon, A. (1997). Evidence that FGF8 signaling from the midbrain-hindbrain junction regulates growth and polarity in the developing midbrain. *Development*. **124**, 959-969.

Legname, G., Baskakov, I., Nguyen, H., Riesner, D., Cohen, F., DeArmond, S. & Prusiner, S. (2004). Synthetic mammalian prions. *Science*. **305,** 673-676.

Li, J., Chang, H., Lai, E., Parker, E. & Vogt, P. (1995). The oncogene *qin* codes for a transcriptional repressor. *Cancer research*. **55**, 5540-5544.

Li, W., Cogswell, C. & LoTurco, J. (1998). Neuronal differentiation of precursors in the neocortical ventricular zone is triggered by BMP. *The Journal of Neuroscience*. **18**, 8853-8862.

Li, L. & Lindquist, S. (2000). Creating a Protein-Based Element of Inheritance. *Science*. **287**, 661-664.

Li, J., Thurm, H., Chang, H., Iacovoni, J. & Vogt, P. (1997). Oncogenic transformation induced by the Qin protein is correlated with transcriptional repression. *Proc. Natl. Acad. Sci.* **94**, 10885-10888.

Li, J. & Vogt, P. (1993). the retroviral oncogene *qin* belongs to the transcription factor family that includes the homeotic gene fork head. *Proc. Natl. Acad. Sci.* **90**, 4490-4494.

Lindquist, S. (1997). Mad Cows Meet Psi-chotic Yeast: The Expansion of the Prion Hypothesis. *Cell*. **89**, 495-498.

Liu, J. & Lindquist, S. (1999). Oligopeptide-repeat expansions modulate 'protein-only' inheritance in yeast. *Nature*. **400**, 573-576.

Marçal, N., Patel, H., Dong, Z., Belanger-Jasmin, S., Hoffman, B., Helgason, C., Dang, J. & Stifani, S. (2005). Antagonistic effects of Grg6 and Groucho/TLE on the transcription repression activity of Brain Factor-1/FoxG1 and cortical neuron differentiation. *Molecular and Cellular Biology*. **25,** 10916-10929.

Martynoga, B., Morrison, H., Price, D. & Mason, J. (2005). FoxG1 is required for specification of the ventral telencephalon and region-specific regulation of dorsal telencephalic precursor proliferation and apoptosis. *Developmental Biology*. **283**, 113-127.

Molnar, Z., Metin, C., Stoykova, A., Tarabykin, V., Price, D., Francis, F., Meyer, G., Dehay, C. & Kennedy, H. (2006). Comparative aspects of cerebral cortical development. *European Journal of Neuroscience*. **23,** 921-934.

Moriyama, H., Edskes, H. K. & Wickner, R. B. (2000). [URE3] prion propagation in Saccharomyces cerevisiae: requirement for chaperone Hsp104 and curing by overexpressed chaperone Ydj1. *Mol. Cell. Biol.* **20**, 8916-8922.

Murphy, D., Wiese, S., Burfeind, P., Schmundt, D., Mattei, M., Schulz-Schaeffer, W. & Thies, U. (1994). Human brain factor 1, a new member of the fork head gene family. *Genomics.* **21**, 551-557.

Muzio, L. & Mallamaci, A. (2005). *Foxg1* confines cajal-retzius neuronogenesis and hippocampal morphogenesis to the dorsomedial pallium. *The Journal of Neuroscience*. **25,** 4435-4441.

Pelton, R., Saxena, B., Jones, M., Moses, H. & Gold, L. (1991). Immunohistochemical localisation of TGFβ1, TGFβ2, and TGFβ3 in the mouse embryo: expression patterns suggest multiple roles during embryonic development. *The Journal of Cell Biology*. **115**, 1091-1105.

Peretz, D., Supattapone, S., Giles, K., Vergara, J., Freyman, Y., Lessard, P., Safar, J., Glidden, D., McCulloch, C., Nguyen, H., Scott, M., DeArmond, S. & Prusiner, S. (2006). Inactivation of prions by acidic sodium dodecyl sulfate. *Journal of Virology*. **80**, 322-331.

Patino, M. M., Liu, J.-J., Glover, J. R. & Lindquist, S. (1996). Support for the Prion Hypothesis for Inheritance of a Phenotypic Trait in Yeast. *Science*. **273**, 622-626.

Pratt, T., Tian, N., Simpson, T., Mason, J. & Price, D. (2004). The winged helix transcription factor Foxg1 facilitates retinal ganglion cell axon crossing of the ventral midline in the mouse. *Development.* **131**, 3773-3784.

Prusiner, S. B. (1982). Novel proteinaceous infectious particles cause scrapie. *Science*. **216,** 136-144.

Prusiner, S. B. (1991). Molecular biology of prion diseases. *Science*. **252**, 1515-1522.

Prusiner, S.B. (1998). Prions. *Proc. Natl. Acad. Sci. USA*. **95**, 13363-13383.

Rakic, P. (1995). A small step for the cell, a giant leap for mankind: a hypothesis of neocortical expansion during evolution. *TINS*. **18**, 383-388.

Regad, T., Roth, M., Bredenkamp, N., Illing, N. & Papalopulu, N. (2006). The neural progenitor specifying activity of Forkhead transcription factor FoxG1 is antagonistically regulated by CKI and FGF. *Nature*. Manuscript under review.

Rodriguez, C., Huang, L., Son, J., McKee, A., Xiao, Z. & Lodish, H. (2001). Functional cloning of the proto-oncogene Brain Factor-1 (BF-1) as a smad-binding antagonist of transforming growth factor-β signaling. *The Journal of Biological Chemistry*. **276**, 30224-30230.

Saa, P., Castilla, J. & Soto, C. (2006) Ultra-efficient replication of infectious prions by automated protein misfolding cyclic amplification. *J Biol Chem*. **281,** 35245-35252.

Scheibel, T., Bloom, J. & Lindquist, S. (2004). The elongation of yeast prion fibers involves separable steps of association and conversion. *Proc. Natl. Acad. Sci. USA*. **101**, 2287-2292.

Seoane, J., Le, H. V., Shen, L., Anderson, S. & Massagué, J. (2004). Integration of smad and forkhead pathways in the control of neuroepithelial and glioblastoma cell proliferation. *Cell*. **117,** 211-223.

Shorter, J. & Lindquist, S. Prions as adaptive conduits of memory and inheritance. *Nature reviews*. **6,** 435-450.

Si, K., Lindquist, S. & Kandel, E. R. (2003). A Neuronal Isoform of the *Alypsia* CPEB Has Prion-Like Properties. *Cell.* **115**, 879-891.

Sondheimer, N., Lopez, N., Craig, E. & Lindquist, S. (2001). The role of Sis1 in the maintenance of the [*RNQ*$^{+}$] prion. *EMBO.* **20**, 2435-2442.

Steele, A., Emsley, J., Ozdinler, P., Lindquist, S. & Macklis, J. (2006). Prion protein (PrP^{c}) positively regulates neural precursor proliferation during development and adult mammalian neurogenesis. *Proc. Natl. Acad. Sci. USA.* **103**, 3416-3421.

Sultan, F. (2002). Analysis of mammalian brain architecture. *Nature.* **415**, 133-134.

Tanaka, M., Chien, P., Naber, N., Cooke, R. & Weissman, J. (2004). Conformational variations in an infectious protein determine prion strain differences. *Nature.* **428**, 323-327.

Tao, W. & Lai, E. (1992). Telencephalon-Restricted Expression of BF-1, a New Member of the HNF-3/*fork head* Gene Family, in the Developing Rat Brain. *Neuron.* **8**, 957-955.

Taylor, J., Hardy, J. & Fischbeck, K. (2002). Toxic proteins in neurodegenerative disease. *Science.* **296**, 1991-1995.

Ter-Avanesyan, M., Dagkesamanskaya, A., Kushnirov, V. & Smirnov, V. (1994). The *SUP35* omnipotent suppressor gene is involved in the maitenance of the non-mendelian determinant [*psi*+] in the yeast *Saccharomyces cerevisiae. Genetics.* **157.** 671-676.

Toresson, H., Martinez-Barbera, J. P., Bardsley, A., Caubit, X. & Krauss, S. (1998). Conservation of BF-1 expression in amphioxus and zebrafish suggests evolutionary ancestry of anterior cell types that contribute to the vertebrate telencephalon. *Development Genes and Evolution.* **208,** 431-439.

Tremblay, P., Ball, H., Kaneko, K., Groth, D., Hedge, R., Cohen, F., DeArmond, S., Prusiner, S. & Safar, J. (2004). Mutant PrP^{sc} conformers induced by a synthetic peptide and several prion strains. *Journal of Virology*. **78**, 2088-2099.

Weigel, D., Jűrgens, G., Kűttner, F., Seifert, E. & Jäckle, H. (1989). The homeotic gene *fork head* encodes a nuclear protein and is expressed in the terminal regions of the Drosophila embryo. *Cell*. **57**, 645-658.

Wickner, R. (1994). [URE3] as an altered *URE2* protein: evidence for a prion analog in *Saccharomyces cerevisiae*. *Science*. **264**, 566-569.

Xuan, S., Baptista, C. A., Balas, G., Tao, W., Soares, V. C. & Lai, E. (1995). Winged Helix Transcription Factor BF-1 Is Essential for the Development of the Cerebral Hemispheres. *Neuron*. **14,** 1141-1152.

Yao, J., Lai, E. & Stifani, S. (2001). The winged-helix protein Brain Factor-1 interacts with Groucho and Hes proteins to repress transcription. *Molecular and Cellular Biology*. **21**, 1962-1972.

Yao, J., Liu, Y., Lo, R., Tretjakoff, I., Peterson, A. & Stifani, S. (2000). Disrupted development of the cerebral hemispheres in transgenic mice expressing the mammalian Groucho homologue Transducin-like-Enhancer of split 1 in postmitotic neurons. *Mechanisms of Development*. **93**, 105-115.

Supplementary data

Figure S1. The sequence of the human FoxG1 N-terminal domain fused in frame to GR, in the construct pG1-hBFIGR[526]. No frameshift or other mutations have occurred. Primers sites are in italics, FoxG1 specific primers are green, restriction enzyme sites are in red, the GR specific primer is blue and the GR sequence is underlined.

```
1          GGATCCTCGATGCTGGACATGGGAGATAGCAAAGAGGTGAAAATGATCCCCAAGTCCTCG
1           G  S  S  M  L  D  M  G  D  R  K  E  V  K  M  I  P  K  S  S

61         TTCAGCATCAACAGCCTGGTGCCCGAGGCGGTCCAGAACGACAACCACCACGCGAGCCAC
21          F  S  I  N  S  L  V  P  E  A  V  Q  N  D  N  H  H  A  S  H

121        GGCCACCACAACAGCCACCACCCCCAGCACCACCACCACCACCACCACCATCACCACCAC
41          G  H  H  N  S  H  H  P  Q  H  H  H  H  H  H  H  H  H  H

181        CCGCCGCCGCCCCCCCCCCGCAACCGCCGCCGCCGCCGCAGCAGCAGCAGCCGCCGCCGCCG
61          P  P  P  P  A  P  Q  P  P  P  P  P  Q  Q  Q  Q  P  P  P  P

241        CCGCCCCCGGCACCGCAGCCCCCCCAGACGCCGGGCGCCCCCGGCCGCCGACGACGACAAG
81          P  P  P  A  P  Q  P  P  Q  T  R  G  A  P  A  A  D  D  D  K

301        GGCCCCCAGCAGCTGCTGCTCCCGCCGCCGCCACCGCCACCACCGCCCCCCCCCCCTGCAC
101         G  P  Q  Q  L  L  L  P  P  P  P  P  P  P  P  A  A  A  L  D

361        GGGGCTAAAGCGGACGGGCTGGGCGGCAAGGGCGAGCCGGGCGGCGGGGCCGGGGGAGCTG
121         G  A  K  A  D  G  L  G  G  K  G  E  P  G  G  G  P  G  E  L

421        GCGCCCGTCGGGCCGGACGAGAAGGAGAAGGGCGCCCGCCGCCCGGCGGCAGGAGAAGAAG
141         A  P  V  G  P  D  E  K  E  K  G  A  G  A  G  G  E  E  K  K

481        GCGGCGGGCGAGGGGGCGCAAGGACGGGTATCCGCGGATGGACTCCAAAGAATCCTTAGCT
161         G  A  G  E  G  G  K  D  G  Y  P  R  M  D  S  K  E  S  L  A

541        CCCCCTGGTAGAGACGAAGTCCCTGGCAGTTTGCTTGGCCAAGGGAGGGGGAGCGTAATG
181         P  P  G  R  D  E  V  P  G  S  L  L  G  Q  G  R  G  S  V  M

601        GACTTTTATAAAAGCCTGAGGGGAGGAGCTACAGTCAAGGTTTCTGCATCTTCGCCCTCA
201         D  F  Y  K  S  L  R  G  G  A  T  V  K  V  S  A  S  S  P  S

661        GTGGCTGCTGCTTCTCAGGCAGATTCCAAGCAGCAGAGGATTCTCCTTGATTTCTCGAAA
221         V  A  A  A  S  Q  A  D  S  K  Q  Q  R  I  L  L  D  F  S  K

721        GGCTCCACAAGCAATGTG
241         G  S  T  S  N  V
```

Figure S2. The sequence of the rat FoxG1 N-terminal domain fused in frame to GR, in the construct pG1-rBFIGR[526]. No frameshift or other mutations have occurred. Primers sites are in italics, FoxG1 specific primers are green, restriction enzyme sites are in red, the GR specific primer is blue and the GR sequence is underlined.

```
1       GGATCCTCGATGCCTGGACATGGCAGATACGAAAGAGGTCAAAATCATCCCCAAGTCCTCG
1        G  S  S  M  L  D  M  G  D  R  K  E  V  K  M  I  P  K  S  S

61      TTCAGCATCAACAGCCTGGTCCCTGAGGCCGTCCAGAACGACAACCACCACGCGAGCCAC
21       F  S  I  N  S  L  V  P  E  A  V  Q  N  D  N  H  H  A  S  H

121     GGTCACCACAACAGCCACCACCCCCAGCATCACCATCATCATCACCACCACCACCACCCG
41       G  H  H  N  S  H  H  P  Q  H  H  H  H  H  H  H  H  H  H  P

181     CCGCCGCCCGCGCCTCAGCCGCCGCCACCGCCGCCCCAGCAGCAGCAGCCGCCCCCG
61       P  P  P  A  P  Q  P  P  P  P  P  P  Q  Q  Q  Q  Q  P  P  P

241     GCCCCGCAGCCCCCGCAGGCGCGCGGCGCCCCAGCAGCGGACGACGACAAGGCCCCCAG
81       A  P  Q  P  P  Q  A  R  G  A  P  A  A  D  D  D  K  G  P  Q

301     CCGCTTCTGCTCCCGCCGTCCGCCGCCCTGGACGGGGCCAAGGCTGACGCACTTGGAGCC
101      P  L  L  L  P  P  S  A  A  L  D  G  A  K  A  D  A  L  G  A

361     AAAGGCGAGCCAGGCGGCGGGCCTGCCGAGCTGGCGCCCGTCGGGCCCGACGAGAAGGAG
121      K  G  E  P  G  G  G  P  A  E  L  A  P  V  G  P  D  E  K  E

421     AAGGGCGCGGGCGCTGGGGGAGGAGAAGAAGGGGGCGGGCGAGGGCGGCAAGGACGGC
141      K  G  A  G  A  G  G  E  E  K  K  G  A  G  E  G  G  K  D  G

481     TATCCGCGGATGGACTCCAAAGAATCCTTAGCTCCCCCTGGTAGAGACGAAGTCCCTGGC
161      Y  P  R  M  D  S  K  E  S  L  A  P  P  G  R  D  E  V  P  G

541     AGTTTGCTTGGCCAAGGGAGGGGGAGCGTAATGGACTTTTATAAAAGCCTGAGGGGAGGA
181      S  L  L  G  Q  G  R  G  S  V  M  D  F  Y  K  S  L  R  G  G

601     GCTACAGTCAAGGTTTCTGCATCTTCGCCCTCAGTGGCTGCTGCTTCTCAGGCAGATTCC
201      A  T  V  K  V  S  A  S  S  P  S  V  A  A  A  S  Q  A  D  S

661     AAGCAGCAGAGGATTCTCCTTGATTTCTCGAAAGCCTCCACAAGCAATCTG
221      K  Q  Q  R  I  L  L  D  F  S  K  G  S  T  S  N  V
```

Figure S3. The sequence of the human FoxG1 N-terminal domain fused in frame to GFP, in the construct p2μ-hBF1GFP. No frameshift or other mutations have occurred. Primers sites are in italics, FoxG1 specific primers are green, restriction enzyme sites are in red, the GFP specific primer is blue and the GFP sequence is underlined.

```
1          GGATCCTCGATGCTGGACATGGGAGATAGGAAAGAGGTGAAAATGATCCCCAAGTCCTCG
1           G  S  S  M  L  D  M  G  D  R  K  E  V  K  M  I  P  K  S  S

61         TTCAGCATCAACAGCCTGGTGCCCGAGGCGGTCCAGAACGACAACCACCACGCGAGCCAC
21          F  S  I  N  S  L  V  P  E  A  V  Q  N  D  N  H  H  A  S  H

121        GGCCACCACAACAGCCACCACCCCCAGCACCACCACCACCACCACCACCATCACCACCAC
41          G  H  H  N  S  H  H  P  Q  H  H  H  H  H  H  H  H  H  H  H

181        CCGCCGCCGCCGCCGCCGCAACCGCCGCCGCCGCCGCAGCAGCAGCAGCCGCCGCCGCCG
61          P  P  P  P  A  P  Q  P  P  P  P  P  Q  Q  Q  Q  P  P  P  P

241        CCGCCCCCGGCACCGCAGCCCCCCCAGACGCGGGGCGCCCCGCCGCCGACGACGACAAG
81          P  P  P  A  P  Q  P  P  Q  T  R  G  A  P  A  A  D  D  D  K

301        GGCCCCCAGCAGCTGCTGCTCCCGCCGCCGCCACCGCCACCACCGGCCGCCGCCCTGGAC
101         G  P  Q  Q  L  L  L  P  P  P  P  P  P  P  P  A  A  A  L  D

361        CCGCCTAAACGCGCACCGGCTGGGCGGCAAGGGCGAGCCGGGCGCGCGGCCCGGGGGAGCTG
121         G  A  K  A  D  G  L  G  G  K  G  E  P  G  G  G  P  G  E  L

421        GCGCCCGTCGGGCCGGACGAGAAGGAGAAGGGCGCCGGCGCCCGGGGGGCAGCAGAAGAAG
141         A  P  V  G  P  D  E  K  E  K  G  A  G  A  G  G  E  E  K  K

481        GGGGCGGGCGAGGGCGGCAAGGACGGGTATGGATCCCATATGAGTAAAGGAGAAGAACTT
161         G  A  G  E  G  G  K  D  G  Y  G  S  H  M  S  K  G  E  E  L
```

Figure S4. The sequence of the rat FoxG1 N-terminal domain fused in frame to GFP, in the construct p2μ-rBF1GFP. No frameshift or other mutations have occurred. Primers sites are in italics, FoxG1 specific primers are green, restriction enzyme sites are in red, the GFP specific primer is blue and the GFP sequence is underlined.

```
1          GGATCCTCGAGGCTGGACATGGGAGATAGGAAAGAGGTGAAAATGATTCCCAAGTCCTCG
1           G   S   S   M   L   D   M   G   D   R   K   E   V   K   M   I   P   K   S   S

61         TTCAGCATCAACAGCCTGGTCCCTGAGGCCGTCCAGAACGACAACCACCACGCGAGCCAC
21          F   S   I   N   S   L   V   P   E   A   V   Q   N   D   N   H   H   A   S   H

121        CGTCACCACAACAGCCACCACCCCCAGCATCACCATCATCATCACCACCAGCACCACCCCG
41          G   H   H   N   S   H   H   P   Q   H   H   H   H   H   H   H   H   H   P

181        CCGCCGCCCGCGCCTCAGCCGCCGCCACCGCCGCCCCAGCAGCAGCAGCCGCCCCCG
61          P   P   P   A   P   Q   P   P   P   P   P   P   Q   Q   Q   Q   Q   P   P   P

241        GCCCCGCAGCCCCCGCAGGCGCGCGGCGCCCCAGCAGCGGACGACGACAAGGGCCCCCAG
81          A   P   Q   P   P   Q   A   R   G   A   P   A   A   D   D   D   K   G   P   Q

301        CCGCTTCTGCTCCCGCCGTCCGCCGCCCTGGACGGGGCCAAGGCTGACGCACTTGGAGCC
101         P   L   L   L   P   P   S   A   A   L   D   G   A   K   A   D   A   L   G   A

361        AAAGGCGAGCCAGGCGGCGGGCCTGCGGAGCTGGCGCCCGTCGGCCCGGACGAGAAGGAG
121         K   G   E   P   G   G   G   P   A   E   L   A   P   V   G   P   D   E   K   E

421        AAGGGCGCGGGGCGCTGGGGGGGAGGAGAAGAAGGGGGCGGGCGAGGGCGGCTAGGACGGG
141         K   G   A   G   A   G   G   E   E   K   K   G   A   G   P   G   G   K   D   G

481        TATGGATCCCATATGAGTAAAGGAGAAGAACTT
161         Y   G   S   H   M   S   K   G   E   E   L
```

Declaration

I know that plagiarism is wrong. Plagiarism is to use another's work and pretend that it is one's own. Each contribution to, and quotation in this research report from other peoples' work has been attributed, and has been cited and referenced.

This report is my own work and has not previously been submitted at any other university for another degree.

I have not allowed, nor will allow, anyone to copy my work with the intention of passing it off as his or her own work.

Signature Signed by candidate Date 2 June 2007

Jessica Learmont